AD-A181 310 CREEP IN PRESTRESSED CONCRETE PILES: A COMPARISON OF THE DIRECT SOLUTION (U) ARMY MILITARY PERSONNEL CENTER ALEXANDRIA VA S K HIRATA MAY 87 1/2

UNCLASSIFIED F/G 11/2 NL

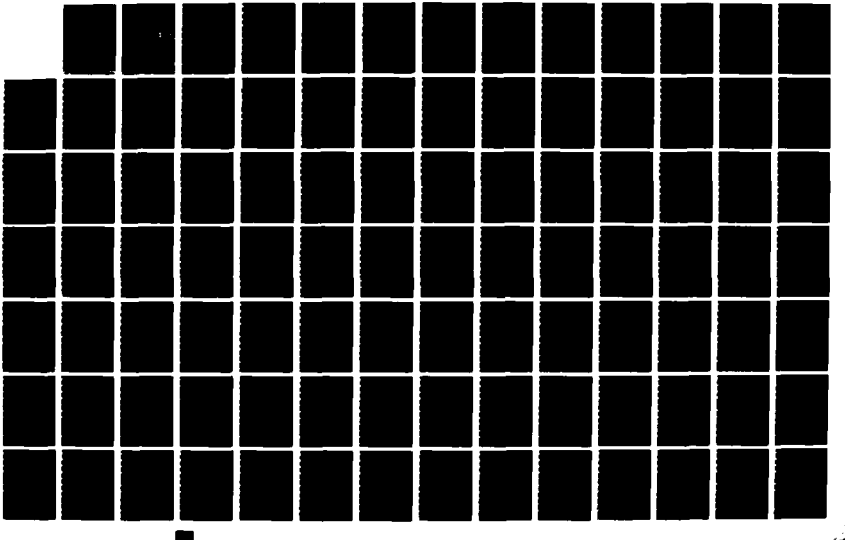

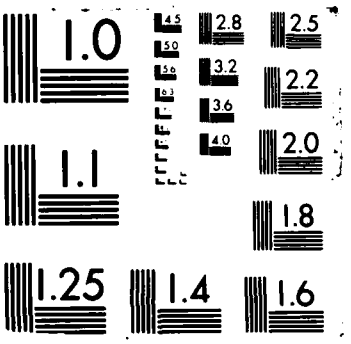
1.0
1.1
1.25
1.4
1.6
1.8
2.0
2.2
2.5
2.8
3.2
3.6
4.0
4.5
5.0
5.6
6.3

(2)

CREEP IN PRESTRESSED CONCRETE PILES

A Comparison of the Direct Solution Method, the Incremental Time Step Method, and the Curve Fitted Equation Method of Calculating Time Dependent Losses in Hawaiian Aggregate Prestressed Concrete Piles

CPT Stacey K. Hirata
HQDA, MILPERCEN (DAPC-OPA-E)
200 Stovall Street
Alexandria, Virginia 22332

May 1987

Approved for public release; distribution is unlimited

A thesis submitted to the Graduate Division of the University of Hawaii at Manoa in partial fulfillment of the requirements for the degree of

Master of Science
in
Civil Engineering

SECURITY CLASSIFICATION OF THIS PAGE *(When Data Entered)*

REPORT DOCUMENTATION PAGE

READ INSTRUCTIONS BEFORE COMPLETING FORM

1. REPORT NUMBER	2. GOVT ACCESSION NO.
3. RECIPIENT'S CATALOG NUMBER	A181 310
4. TITLE *(and Subtitle)*	CREEP IN PRESTRESSED CONCRETE PILES: A Comparison of the Direct Solution Method, the Incremental Time Step Method, and the Curve Fitted Equation Method of Calculating Time Dependent Losses in Hawaiian Aggregate Prestressed Concrete Piles
5. TYPE OF REPORT & PERIOD COVERED	Final Report May 1987
6. PERFORMING ORG. REPORT NUMBER	
7. AUTHOR(s)	CPT Stacey K. Hirata
8. CONTRACT OR GRANT NUMBER(s)	
9. PERFORMING ORGANIZATION NAME AND ADDRESS	Student, HQDA, MILPERCEN (DAPC-OPA-E), 200 Stovall Street, Alexandria, Virginia 22332
10. PROGRAM ELEMENT, PROJECT, TASK AREA & WORK UNIT NUMBERS	
11. CONTROLLING OFFICE NAME AND ADDRESS	HQDA, MILPERCEN, ATTN: DAPC-OPA-E, 200 Stovall Street, Alexandria, Virginia 22332
12. REPORT DATE	May 1987
13. NUMBER OF PAGES	135
14. MONITORING AGENCY NAME & ADDRESS *(if different from Controlling Office)*	
15. SECURITY CLASS. *(of this report)*	
15a. DECLASSIFICATION/DOWNGRADING SCHEDULE	

16. DISTRIBUTION STATEMENT *(of this Report)*

Approved for public release; distribution unlimited.

17. DISTRIBUTION STATEMENT *(of the abstract entered in Block 20, if different from Report)*

18. SUPPLEMENTARY NOTES

A thesis submitted to the Graduate Division of the University of Hawaii at Manoa in partial fulfillment of the requirements for the degree of Master of Science in Civil Engineering.

19. KEY WORDS *(Continue on reverse side if necessary and identify by block number)*

concrete time dependent losses, creep strain, shrinkage strain

20. ABSTRACT *(Continue on reverse side if necessary and identify by block number)*

Three methods to calculate creep strains were examined and their results were compared against the strains observed in 55 foot long, 16.5 inch octagonol, prestressed concrete piles.

The direct solution method involved the straight forward application of the creep strain equation. The incremental time step method used the creep strain equation and accounted for the stress reduction in the prestressing steel over each time interval. The curve fitted equation method involved

DD FORM 1 JAN 73 1473 EDITION OF 1 NOV 65 IS OBSOLETE

SECURITY CLASSIFICATION OF THIS PAGE *(When Data Entered)*

Block 20 continued

curve fitting the observed creep strain to the hyperbolic, exponential, and power equation forms by the method of least squares.

Two different creep and shrinkage equation sets were used in the direct solution and incremental time step methods. The American Concrete Institute's recommended equations with correction factors were used as one set. The other set consisted of empirically derived equations of the hyperbolic form which resulted from a companion creep study involving standard test cylinders.

The direct solution method using the local test cylinder's empirically derived creep and shrinkage equations produced reasonably accurate predictions of strain for the cost.

CREEP IN PRESTRESSED CONCRETE PILES

A Comparison of the
Direct Solution Method, the
Incremental Time Step Method, and the
Curve Fitted Equation Method of
Calculating Time Dependent Losses in
Hawaiian Aggregate Prestressed Concrete Piles

A THESIS SUBMITTED TO THE GRADUATE DIVISION OF THE
UNIVERSITY OF HAWAII AT MANOA
IN PARTIAL FULFILLMENT OF THE REQUIREMENTS
FOR THE DEGREE OF

MASTER OF SCIENCE
IN
CIVIL ENGINEERING

MAY 1987

By

Stacey Katsuto Hirata

Thesis Committee:

Harold S. Hamada, Chairman
Tetsuichi Mitsuda
C. S. Papacostas

We certify that we have read this thesis and that, in our opinion, it is satisfactory in scope and quality as a thesis for the degree of Master of Science in Civil Engineering.

THESIS COMMITTEE

Harold S Hamed
Chairman

L. Fritsche

C Papacostas

ABSTRACT

Three methods to calculate creep strains were examined and their results were compared against the strains observed in 55 foot long, 16.5 inch octagonol, prestressed concrete piles.

The direct solution method involved the straight forward application of the creep strain equation. The incremental time step method used the creep strain equation and accounted for the stress reduction in the prestressing steel over each time interval. The curve fitted equation method involved curve fitting the observed creep strain to the hyperbolic, exponential, and power equation forms by the method of least squares.

Two different creep and shrinkage equation sets were used in the direct solution and incremental time step methods. The American Concrete Institute's recommended equations with correction factors were used as one set. The other set consisted of empirically derived equations of the hyperbolic form which resulted from a companion creep study involving standard test cylinders.

The direct solution method using the local test cylinder's empirically derived creep and shrinkage equations produced reasonably accurate predictions of strain for the cost.

TABLE OF CONTENTS

Page

ABSTRACT iii

LIST OF TABLES vi

LIST OF ILLUSTRATIONS ix

LIST OF SYMBOLS xiv

CHAPTER I INTRODUCTION 1

CHAPTER II LITERATURE REVIEW 5

The Creep Phenomenon and Shrinkage 5
Factors Affecting Creep 7

CHAPTER III PRESTRESSED CONCRETE PILE DESCRIPTION 13

Pile Dimensions 13
Concrete Constituents and Characteristics ... 13
Reinforcing Steel 14
Pile Casting and Loading 15
Strain Measurement Results 16

CHAPTER IV METHODS OF CALCULATING CREEP AND SHRINKAGE IN PRESTRESSED CONCRETE 18

Direct Solution Method 18
Incremental Time Step Method 29
Curve Fitting 35

CHAPTER V METHOD OF ANALYSIS OF THE COMPARISONS 38

Curve Fitting 38
Standard Error of the Estimate 39

CHAPTER VI RESULTS 41

Direct Solution Method - ACI vs Cylinder Equations 41
The Direct Solution vs the Incremental Time Step Method 45
Curve Fitted Equation 54

Page

CHAPTER VII CONCLUSIONS 62

CHAPTER VIII RECOMMENDATIONS 66

APPENDICES:

A TABLES 67

B ILLUSTRATIONS 91

LIST OF REFERENCES 134

LIST OF TABLES

Table		Page
1	Quantity of Constituents per Cubic Yard of Concrete	68
2	Chemical Composition of the Cement	68
3	Summary of Casting, Curing and Loading of the Cylinders	69
4	Summary of Casting, Curing and Loading of the Piles	70
5	Creep Strain Data Set Information	71
6	Comparison of Standard Error of the Estimate, ACI Equation versus Cylinder Equation, Data Points Prior to Loading, Point 1	72
7	Comparison of Standard Error of the Estimate, ACI Equation versus Cylinder Equation, Data Points Prior to Loading, Point 3	73
8	Comparison of Standard Error of the Estimate, ACI Equation versus Cylinder Equation, Data Points Prior to Loading, Point 2	74
9	Comparison, ACI Equations, Direct Solution Method vs Incremental Time Step Method, Points 1 and 3	75
10	Comparison of Standard Error of the Estimate, ACI Equations, Incremental Time Step vs Direct Solution, Data Points Prior to Loading, Point 1	76
11	Comparison of Standard Error of the Estimate, ACI Equations, Incremental Time Step vs Direct Solution, Data Points Prior to Loading, Point 3	77

Table		Page
12	Comparison, ACI Equations, Direct Solution Method vs Incremental Time Step Method, Point 2	78
13	Comparison of Standard Error of the Estimate, ACI Equations, Incremental Time Step vs Direct Solution, Data Points Prior to Loading, Point 2	79
14	Comparison, Cylinder Equations, Direct Solution Method vs Incremental Time Step Method, Points 1 and 3 .	80
15	Comparison of Standard Error of the Estimate, Cylinder Equations, Incremental Time Step vs Direct Solution, Data Points Prior to Loading, Point 1	81
16	Comparison of Standard Error of the Estimate, Cylinder Equations, Incremental Time Step vs Direct Solution, Data Points Prior to Loading, Point 3	82
17	Comparison, Cylinder Equations, Direct Solution Method vs Incremental Time Step Method, Point 2	83
18	Comparison of Standard Error of the Estimate, Cylinder Equations, Incremental Time Step vs Direct Solution, Data Points Prior to Loading, Point 2	84
19	Exponential Equation Curve Fitting Parameters	85
20	Power Equation Curve Fitting Parameters	85
21	Hyperbolic Equation Curve Fitting Parameters	86
22	Comparison of the Correlation Coefficient, Points 1 and 3	87
23	Comparison of the Correlation Coefficient, Point 2	87

Table		Page
24	Comparison of Standard Error of the Estimate, Curve Fitted Equations, Data Points Prior to Loading, Point 1	88
25	Comparison of Standard Error of the Estimate, Curve Fitted Equations, Data Points Prior to Loading, Point 3	89
26	Comparison of Standard Error of the Estimate, Curve Fitted Equations, Data Points Prior to Loading, Point 2	90

LIST OF ILLUSTRATIONS

Figure		Page
1	Total Strain versus Age of Pile Pile 1 Points 1 and 3	92
2	Total Strain versus Age of Pile Pile 2 Points 1 and 3	93
3	Total Strain versus Age of Pile Pile 3 Points 1 and 3	94
4	Total Strain versus Age of Pile Pile 4 Points 1 and 3	95
5	Total Strain versus Age of Pile Pile 5 Points 1 and 3	96
6	Total Strain versus Age of Pile Pile 6 Points 1 and 3	97
7	Total Strain versus Age of Pile Pile 7 Points 1 and 3	98
8	Total Strain versus Age of Pile Pile 8 Points 1 and 3	99
9	Total Strain versus Age of Pile Pile 9 Points 1 and 3	100
10	Total Strain versus Age of Pile Pile 1 Point 2	101
11	Total Strain versus Age of Pile Pile 2 Point 2	102
12	Total Strain versus Age of Pile Pile 3 Point 2	103
13	Total Strain versus Age of Pile Pile 4 Point 2	104
14	Total Strain versus Age of Pile Pile 5 Point 2	105
15	Total Strain versus Age of Pile Pile 6 Point 2	106

Figure		Page
16	Total Strain versus Age of Pile Pile 7 Point 2	107
17	Total Strain versus Age of Pile Pile 8 Point 2	108
18	Total Strain versus Age of Pile Pile 9 Point 2	109
19	Comparison of Total Strain, Direct Solution Method Using the ACI Equations and Cylinder Equations Against Pile 8 Points 1 and 3 Observed Data	110
20	Overlay of Total Strains, Direct Solution Method Using the ACI Equations and Cylinder Equations for Points 1 and 3	111
21	Comparison of Total Strains of Points 1 and 3 Prior to Loading, All Piles, Direct Solution Method Using ACI Equations and Cylinder Equations	112
22	Comparison of Total Strain, Direct Solution Method Using the ACI Equations and Cylinder Equations Against Pile 8 Point 2 Observed Data	113
23	Overlay of Total Strains, Direct Solution Method Using the ACI Equations and Cylinder Equations for Point 2	114
24	Comparison of Total Strains of Point 2 Prior to Loading, All Piles, Direct Solution Method Using ACI Equations and Cylinder Equations	115
25	Comparison of Total Strain, Cylinder Equations, Incremental Time Step Method versus Direct Solution Method Against Pile 8 Points 1 and 3 Observed Data	116

Figure		Page
26	Overlay of Total Strain, Cylinder Equations, Incremental Time Step Method versus Direct Solution Method for Points 1 and 3	117
27	Comparison of Total Strains of Points 1 and 3 Prior to Loading, All Piles, Cylinder Equations, Incremental Time Step Method versus Direct Solution Method	118
28	Comparison of Total Strain, Cylinder Equations, Incremental Time Step Method versus Direct Solution Method Against Pile 8 Point 2 Observed Data	119
29	Overlay of Total Strain, Cylinder Equations, Incremental Time Step Method versus Direct Solution Method for Point 2	120
30	Comparison of Total Strains of Point 2 Prior to Loading, All Piles, Cylinder Equations, Incremental Time Step Method versus Direct Solution Method	121
31	Comparison of Total Strain, Curve Fitted Equations Against Pile 8 Points 1 and 3	122
32	Comparison of Total Strain, Curve Fitted Equations Against Pile 8 Point 2	123
33	Comparison of Total Strain versus Calculated Curve Using Creep Power Equation, Cylinder Shrinkage Equation, and Observed Initial Elastic Strain Pile 1 Points 1 and 3	124
34	Comparison of Total Strain versus Calculated Curve Using Creep Power Equation, Cylinder Shrinkage Equation, and Observed Initial Elastic Strain Pile 2 Points 1 and 3	125

Figure		Page
35	Comparison of Total Strain versus Calculated Curve Using Creep Power Equation, Cylinder Shrinkage Equation, and Observed Initial Elastic Strain Piles 3 and 4 Points 1 and 3	126
36	Comparison of Total Strain versus Calculated Curve Using Creep Power Equation, Cylinder Shrinkage Equation, and Observed Initial Elastic Strain Piles 5 and 9 Points 1 and 3	127
37	Comparison of Total Strain versus Calculated Curve Using Creep Power Equation, Cylinder Shrinkage Equation, and Observed Initial Elastic Strain Piles 6 and 7 Points 1 and 3	128
38	Comparison of Total Strain versus Calculated Curve Using Creep Power Equation, Cylinder Shrinkage Equation, and Observed Initial Elastic Strain Pile 1 Point 2	129
39	Comparison of Total Strain versus Calculated Curve Using Creep Power Equation, Cylinder Shrinkage Equation, and Observed Initial Elastic Strain Pile 2 Point 2	130
40	Comparison of Total Strain versus Calculated Curve Using Creep Power Equation, Cylinder Shrinkage Equation, and Observed Initial Elastic Strain Piles 3 and 4 Point 2	131
41	Comparison of Total Strain versus Calculated Curve Using Creep Power Equation, Cylinder Shrinkage Equation, and Observed Initial Elastic Strain Piles 5 and 9 Point 2	132

Figure Page

42 Comparison of Total Strain versus Calculated Curve Using Creep Power Equation, Cylinder Shrinkage Equation, and Observed Initial Elastic Strain Piles 6 and 7 Point 2 133

LIST OF SYMBOLS

A_c	cross sectional area of the concrete
A_p	cross sectional area of the prestressing steel
C	y axis intercept of the straight line
c	distance between the member centroidal axis and the face
cc	cement content in pounds per cubic yard of concrete
$CF_{cp,c}$	creep correction factor for cement content
$CF_{cp,cc}$	creep correction factor for concrete composition
$CF_{cp,fa}$	creep correction factor for percentage of fine aggregate
$CF_{cp,h}$	creep correction factor for relative humidity
$CF_{cp,la}$	creep correction factor for loading age
$CF_{cp,s}$	creep correction factor for slump
$CF_{cp,vs}$	creep correction factor for member volume to surface ratio
$CF_{sh,c}$	shrinkage correction factor for cement content
$CF_{sh,cc}$	shrinkage correction factor for concrete composition
$CF_{sh,fa}$	shrinkage correction factor for percentage of fine aggregate
$CF_{sh,h}$	shrinkage correction factor for relative humidity
$CF_{sh,s}$	shrinkage correction factor for slump
$CF_{sh,vs}$	shrinkage correction factor for member volume to surface ratio

C_t	creep coefficient at time "t"
C_u	ultimate creep coefficient
De_c	change in concrete strain over the time interval
De_{sh}	change of shrinkage strain during the time interval
Df_c	change in concrete stress over the time interval
Df_p	total loss of steel stress over the time interval
D gr e_{cp}	gross creep strain for the time interval
d_t	creep strain per unit stress at time "t"
d_{t1}	creep strain per unit stress at time "t1"
d_{t2}	creep strain per unit stress at time "t2"
Dx	difference between the observed "X" variable and the mean of all "X"s
Dy	difference between the observed "Y" variable and the mean of all "Y"s
e	distance between the prestressing steel and the member centroidal axis
E_c	modulus of elasticity of the concrete
$e_{cp,t}$	creep strain at time "t" in days since casting the concrete
e_i	initial elastic strain
E_p	elastic modulus of the prestressing steel
E_s	modulus of elasticity of the reinforcing steel
$e_{sh,t}$	shrinkage strain at time "t"

$e_{sh,u}$	ultimate shrinkage strain
$f_{c,t1}$	concrete stress at the start of the interval, time "t1"
$f_{c,t2}$	concrete stress at the end of the interval, time "t2"
f_p	stress in the steel at time "t"
f_{pi}	initial stress in the steel
f_{py}	yield stress of the steel
H	relative humidity in percent
m	slope of the line
N	number of observations
n	modular ratio
net De_{cp}	net creep strain increment over the time interval
OBS	measured strain observed in the experiment
PRED	calculated strain predicted by one of the three methods at the same time of the corresponding observed data point
R	correlation coefficient
r	radius of gyration
S	sample standard deviation
s	slump in inches
SQRT	the function "square root of"
STER	standard error of the estimate
SUM	the function "summation of"
t	age of the concrete in days
t_{1a}	concrete age at loading in days
t_r	time pretensioned steel was released in days

vs	volume to surface area ratio of the member in inches
X	independent variable
Y	dependent variable
%fa	the ratio by weight of the fine aggregate to the total aggregate expressed as a percentage

CHAPTER I

INTRODUCTION

In the 1930's and 1940's, a medium to compact coral/sand fill was dredged from the ocean and hydraulically placed to reclaim land from Keehi Lagoon on Oahu, Hawaii. This surface fill was eight to fifteen feet thick and beneath this fill layer existed a very deep, very soft and underconsolidated soil.

In the 1980's, the Keehi Highway Interchange of the H-1 Interstate in Hawaii was to be constructed on a pile foundation in this subsiding ground. [1] The State of Hawaii Department of Transportation Highways Division commissioned a consultant to determine the magnitude of the long term downdrag that the pile foundation would experience. The description and results of the consultants field testing project can be found in Downdrag, Negative Skin Friction and Bitumen Coatings on Prestressed Concrete Piles by Frank M. Clemente, Jr. [1]

In order to precisely isolate the magnitude of the downdrag values measured in Clemente's field testing project, two related research studies were also sponsored by the Highways Division and conducted in the Civil Engineering Department of the University of Hawaii at Manoa. Creep and Shrinkage of Hawaiian Aggregate

Concrete by Keith K. Kalani and Harold S. Hamada [2] examined the creep and shrinkage of six inch diameter by twelve inch test cylinders composed of the concrete mix used for the foundation piles. Creep in Prestress Concrete Piles by David J. Mukai and Harold S. Hamada [3] examined the creep and shrinkage of fifty five feet long prestressed concrete piles composed of the same concrete mix as the test cylinders, and cast at the same dimension and prestressed with the same load as the piles used on the project.

Increased accuracy in predicting creep strains in a member is directly proportional to the expense of specimen testing. Creep strains can be calculated using the American Concrete Institute (ACI) Committee 209 equations requiring minimal field measurements and at minimal cost. At the expense of observing test cylinders of the local concrete design mix, a creep equation can be derived which provides a more accurate creep strain prediction. A greater accuracy in predicting creep strains can be attained at a greater expense by testing the actual member.

The research of Kalani and Hamada [2] and Mukai and Hamada [3] provides an opportunity to compare predicted strains using the ACI equations, equations based on test cylinders [2], and equations based on the actual member [3].

Chapter II contains a discussion of the concrete creep phenomenon and shrinkage. A physical description of the prestressed concrete piles, the concrete mix design, and the observed total strain by Mukai and Hamada [2] with additional data recorded by the author are contained in Chapter III.

Chapter IV discusses the direct solution method, the incremental time step method, and the member observed strain curve fitted method of calculating creep and shrinkage strains in prestressed concrete. The direct solution method applies either the ACI equations or the equations based on test cylinders to calculate the strains. The incremental time step method utilizes the direct solution method equations and reduces the applied stress by the relaxation of the prestressing steel through each time interval. The member observed strain curve fitted method is based on equations derived from the observed data on the actual members.

The objectives of this thesis are as follows:

1) to compare the direct solution method using the ACI Committee 209 equations for creep and shrinkage strains with the incremental time step method using the ACI equations.

2) to compare the direct solution method using the equations based on the test cylinder results with the incremental time step method using the test

cylinder equations.

3) to evaluate and select an equation of the hyperbolic, power, or exponential form that best describes the observed creep strain and steel relaxation in the actual member.

4) to determine the accuracy of the direct solution ACI, the ACI with incremental time step, the direct solution test cylinder, the test cylinder with incremental time step, and the actual member equations in predicting the observed strains.

The method of analyzing and comparing the calculation methods is discussed in Chapter V. The results of the comparisons are presented in Chapter VI. Conclusions and Recommendations are contained in Chapters VII and VIII respectively.

CHAPTER II

LITERATURE REVIEW

The Creep Phenomenon and Shrinkage

In 1678, Robert Hooke discovered that the load applied to a material was proportional to the deflection. Thomas Young in 1807, suggested that within the elastic limit, the ratio of the unit stress to the corresponding strain is constant. Thus for a constant unit stress below the elastic limit there is a constant unit strain or a corresponding initial elastic deformation which is independent of time.

Investigators examining deformations in concrete members discovered that the deformations did not remain constant with time. From the initial elastic deformation under constant load or constant stress, the deformation continually increased with time. This increasing deformation was a result of creep and shrinkage strains.

Creep is the increase in strain over time due to an applied constant stress. Shrinkage is the increase in strain over time due to moisture withdrawal in the absence of an applied load. [4] Thus the total strain of a concrete member is a result of the initial elastic strain due to the applied load, creep strain due to the

sustained applied load and shrinkage strain due to moisture withdrawal from the member.

A number of theories have been proposed in an attempt to explain the mechanisms of the creep phenomenon. Each theory explains a number of observations and support some experimental results. But of these theories, none is capable of accounting for all the observed facts. Creep is probably the result of a combination of two or more of the following mechanisms:

a) viscous flow theory: hydrated cement paste is viscous under load and flows around the aggregate.

b) crystalline flow (plastic) theory: aggregate and hardened cement paste flow in the nature of slipping along planes within the crystal lattice.

c) closing of internal voids: internal voids within the member collapse.

d) seepage theory: the flow of water out of the cement gel due to external loading and drying.

e) mechanism of action of admixtures: admixtures affect surface forces between the water and the cement gel. [4]

A more detailed discussion of these and other less accepted theories which attempt to explain the creep phenomenon is addressed by Neville [4]. Mukai and Hamada [3] also provide an excellent summary of these mechanisms.

Factors Affecting Creep

Factors affecting the magnitude of creep are:

a) constituents - such as the compostion of the cement, the admixtures, and the size, grading, and mineral content of the aggregate.

b) water-cement ratio.

c) curing method.

d) age at loading.

e) temperature.

f) humidity.

g) member volume to surface ratio.

h) stress-strength ratio.

Constituents

Numerous studies have shown that different types of cements, admixtures and aggregate have produced different magnitudes of creep. These differences of creep measurements are due to the variations within each constituent's physical and chemical properties.

Neville [4] presented some typical data for creep of concretes made with different cements and all other conditions being constant. The American Society for Testing Materials (ASTM) classified Type I cement consistently exhibited more creep than ASTM classified Type III cement. The Type III cement exhibited more

creep than the high alumina cement. Neville [4] generalizes this relationship by stating that creep is inversely proportional to the rapidity of the hardening of the cement used. The high alumina cement hardens the quickest followed by the Type III and the Type I. Supporting this generalization, is the fact that the high alumina cement hardens the quickest and produces the least creep. The Type I cement is the slowest of the three to harden and it produces the highest creep.

Admixtures influence the physical and chemical composition of the concrete mix differently, thus their influence on creep cannot be generalized. Studies have shown an increase in creep when comparing concrete with and without water-reducing admixtures with concrete. Some concretes exhibit reduced creep with other admixtures but this behavior is perhaps the exception rather than the norm.

The size, grading, and mineral content of the aggregate present variations in chemical and physical properties which produce different magnitudes of creep. Creep has been observed in the parent rock of aggregate at very high stresses. But the magnitude of the creep is very small when compared to the creep in concrete and the stresses that the aggregate experiences in concrete do not attain the high levels of stress which produced the

creep in the parent rock. Thus the aggregates in the concrete do not creep.

The aggregate's modulus of elasticity, absorption, and shape and grading affect creep. The greater the aggregate modulus of elasticity, the lesser the creep in the concrete. The higher aggregate modulus of elasticity, the greater the restraint offered by the aggregate. The aggregate restrains more of the applied stress resulting in less stress being imposed on the cement paste. Creep strain is proportional to stress, thus the less stress on the cement paste produces less creep.

Absorption of water by the aggregate affects the creep of the concrete. Greater absorption by the aggregate occurs at the expense of water movement from the cement paste which leads to more creep.

The influence of the shape and grading of the aggregate on creep is unproven as of yet. However, it is postulated that the shape and grading of the aggregate influences the strength of the bond between the aggregate and the cement paste. Creep resulting from microcracking and the slipping of the cement paste is directly related to the strength of the bond between the aggregate and the paste.

Each of the different types of cements, admixtures, and aggregates affect creep differently.

Similarly, various mix compositions consisting of different quantities of the constituents affect the magnitude of creep.

Water-Cement Ratio

The quantity of water as a component in the mix composition also affects creep. The water-cement ratio measures the amount of water within the mix. The lower the water-cement ratio, the greater the strength of the concrete and the smaller the creep.

Curing Method

Extensive data on the influence of curing on creep obtained by Hanson [5] indicates that accelerated curing methods reduce creep. Steam cured concrete creeps less than moist cured concrete.

Age at Loading

The older the concrete is at loading, the greater its strength. Creep is inversely proportional to strength. Thus with two identical concrete specimens loaded with the same stress but at different ages, the specimen with the greater age at loading will creep less than the other.

Temperature

Creep strains increase for increasing temperatures to a maximum temperature of about 160°F. [4] Observations by Marechal [6] indicate that at temperatures greater then 122°F, creep decreases with increasing temperatures and attains a minimum at about 221°F. At temperatures from 221°F to 752°F, creep again increases with increasing temperature.

Humidity

Humidity influences the volume proportions of hydrate, absorbed and capillary water, and the rate at which moisture diffuses in the concrete and evaporates to the atmosphere. [7] Creep strains increase for decreasing relative humidity.

Member Volume to Surface Ratio

Hanson and Mattock (1966) confirmed what Ross had suggested (1944) that the volume to surface ratio was a suitable parameter for estimating the influence of size and shape of a member on shrinkage and creep deformations. [8] The higher the volume to surface ratio, the smaller the relative surface area and the less moisture loss at the surface thus the smaller creep.

Stress-strength Ratio

The stress-strength ratio is the ratio of the applied load (stress) and the concrete strength at loading. Creep is proportional to the applied stress and inversely proportional to the strength of the concrete at loading. Thus, creep increases with an increase in the stress-strength ratios.

There is substantial evidence which establishes a linear relationship between creep and the stress-strength ratio. This relationship is subjected to the following limitations:

a) members must be loaded sometime after 3 days.

b) the member must have no previous load history.

c) the stress-strength ratio must be no greater than 0.50.

CHAPTER III

PRESTRESSED CONCRETE PILE DESCRIPTION

Pile Dimensions

The prestressed concrete piles were 55 feet long. Their octagonal cross section had a depth of 16.5 inches with each side of the eight sides being 6.84 inches. A five inch diameter hole in the center of the octagonal cross section traversed the entire length of the pile.

The cross sectional area of the concrete was 205.9 square inches. The moment of inertia was 4,028 $inches^4$. [3]

Concrete Constituents and Characteristics

Concrete Constituents

The materials consisted of Type II Portland Cement, limestone sand from Waimanalo, Hawaii, #3 coarse and #4 fine basalt aggregate from Makakilo, Hawaii, and sikament. Sikament is a superplasticizing admixture which provides high slump action with minimal water. The lower water-cement ratio produces concrete with a higher early strength.

The amount of each constituent in one cubic yard

of concrete is given in Table 1. The concrete had a water-cement ratio of 0.3, a sand to cement ratio of 0.87, and a coarse aggregate to cement ratio of 2.2.

The Type II Portland Cement conformed with ASTM specification C-150-84, Federal specification SS-C-1960/3B and American Association of State Highway Transportation Officials (AASHTO) specification M-85-80. Table 2 identifies the percentage of the four major compounds of the cement.

Concrete Characteristics

The slump of the concrete was typically six inches and the concrete weight at casting was 157.9 pounds per cubic foot.

Strength tests on standard 6 inch by 12 inch concrete cylinders revealed a 28 day, moist cured strength of 7,446 psi. Strength for one day and 28 day, steam cured cylinders were 4,100 psi and 5,823 psi respectively.

Reinforcing Steel

The first 13 feet of both ends of the 55 foot piles were reinforced with eight #9 rebars which amounts to eight square inches of reinforcing steel. In addition to the reinforcing steel, six 0.6 inch diameter, 270 ksi

prestressing strands ran the entire length of the pile.

Pile Casting and Loading

Pile Casting

The piles were cast in two phases: five on May 30, 1984 (Piles 1 to 5) and four on September 4, 1984 (Piles 6 to 9). The individual phases were cast in one continuous line and steam cured.

Six inch diameter concrete cylinders were obtained from the same batches used to cast the piles. Information on creep and shrinkage in these cylinders and others cast with the same mix design can be found in Kalani and Hamada [2]. Frames 2, 4 and 8 contain cylinders cast on May 30, 1984 and moist cured. Frames 1, 3, 5, 6, 7 and 9 were cast with the same mix design on August 9, 1984 and steam cured. Frame 10 was cast with the same mix design on June 12, 1985 and moist cured. A summary of the cylinders date of casting, applied stress, age at loading, and method of curing can be found in Table 3.

Pile Loading

The nine piles were loaded with three different loads and four different ages of loading. Table 4 provides a summary of the piles date of casting, applied

stress, age at loading, and method of curing.

Pile 8 was not loaded and it provided measurements of shrinkage strains, creep strains due to the prestressing load, and environmental affects on these strains for the experiment.

Additional information on the method of experimentation, the loading system, the measuring system and experimental procedures can be found in Mukai and Hamada [3].

Strain Measurement Results

Each pile had six measurement points. Points 1 and 3 consisting of two measurement points each, recorded strains of the first 13 feet on each end of the pile. The measurements of Points 1 and 3 reflect strains of prestressed reinforced concrete. Point 2 consisted of two measurement points in the middle, unreinforced section of the 55 foot pile.

The measurement technique established by Mukai and Hamada [3] was continued during the additional year of data gathering. Information on the measurement system and technique utilized can be found in Mukai and Hamada [3].

Figures 1 to 9 depict the total strain versus the age of the pile for Piles 1 to 9, Points 1 and 3.

Figures 10 to 18 depict the total strain versus the age of the pile for Piles 1 to 9, Point 2.

The instantaneous increase in strain at 30 days for Piles 1, 6 and 7, at 72 days for Pile 2, and at about 120 days for Piles 3, 4, 5 and 9 reflects the initial elastic strain due to loading. Pile 8 was not loaded and thus does not exhibit any initial elastic strain.

CHAPTER IV

METHODS OF CALCULATING CREEP AND SHRINKAGE IN PRESTRESSED CONCRETE

Direct Solution Method

The direct solution method uses two distinct equations to calculate creep and shrinkage strains, respectively. These creep and shrinkage equations produce strains for a specific age of the concrete at standard conditions. Standard conditions are defined as a four inch slump, 40% relative humidity, a member volume to surface area ratio of 1.5 inches^3/inches^2, and an age of concrete at loading of seven days for moist cured and one to three days for steam cured members. [9] Empirically derived correction factors adjust the calculated creep and shrinkage strains for concrete stored in other than standard conditions.

Creep Strains

Creep strain is equal to the product of the initial elastic strain and a creep coefficient.

$$e_{cp,t} = e_i \, C_t \qquad \text{Eq 4.1}$$

where $e_{cp,t}$ = creep strain at time "t" in days since casting the concrete

e_i = initial elastic strain

C_t = creep coefficient at time "t". [10]

The model to calculate the creep coefficient which was proposed by Branson and adopted by the ACI Committee 209 is:

$$C_t = \frac{t^{0.6}}{10 + t^{0.6}} C_u \qquad \text{Eq 4.2}$$

where t = age of the concrete in days

C_u = ultimate creep coefficient. [10]

The ultimate creep coefficient is empirically derived. Where specific data for local aggregates are not available, Branson recommends use of a value for C_u equal to 2.35. [10]

Kalani and Hamada [2] empirically derived the following equation for the creep coefficient for the concrete mix used in the prestressed piles and stored at 75% relative humidity as:

$$C_t = \frac{t^{0.5}}{23 + t^{0.5}} C_u \qquad \text{Eq 4.3}$$

The ultimate creep coefficient was determined to be equal to 2.311.

Creep Correction Factor for Concrete Composition

The creep correction factor for concrete composition is the product of the creep correction

factors for slump, percent of fine aggregate, and cement content.

$$CF_{cp,cc} = CF_{cp,s}\ CF_{cp,fa}\ CF_{cp,c} \qquad \text{Eq 4.4}$$

where $CF_{cp,cc}$ = creep correction factor for concrete composition

$CF_{cp,s}$ = creep correction factor for slump

$CF_{cp,fa}$ = creep correction factor for percentage of fine aggregate

$CF_{cp,c}$ = creep correction factor for cement content. [10]

The creep correction factor for slump is:

$$CF_{cp,s} = 0.82 + 0.067\ s \qquad \text{Eq 4.5}$$

where s = slump in inches. [10]

A typical slump of six inches was observed in the concrete for the piles thus the creep correction factor for slump is equal to 1.222.

The creep correction factor for the percentage of fine aggregate is:

$$CF_{cp,fa} = 0.88 + 0.0024\ \%fa \qquad \text{Eq 4.6}$$

where %fa = the ratio by weight of the fine aggregate to the total aggregate expressed as a percentage. [10]

From Table 1, the ratio by weight of fine aggregate to total aggregate is 1405. to 3203. or 43.865%. Thus the creep correction factor for the percentage of fine aggregate of the piles concrete is equal to 0.985.

Cement content has a negligible effect on the creep coefficient. [10] Thus the creep correction factor for cement content ($CF_{cp,c}$) is equal to 1.0.

Using Equation 4.4 yields the correction factor for the composition of the concrete used in the pile equal to 1.204. This factor of 1.204 will only be used with the ACI Equation (Equation 4.2). Equation 4.3 proposed by Kalani and Hamada [2] was empirically derived with the corrections for the concrete composition included in the general expression.

Creep Correction Factor for Relative Humidity

The creep correction factor for relative humidity is:

$$CF_{cp,h} = 1.27 - 0.0067\ H \qquad \text{Eq 4.7}$$

where $CF_{cp,h}$ = creep correction factor for relative humidity

H = relative humidity in percent. [10]

The relative humidity of the experiment location was assumed to be a constant 75% which produces a creep correction factor for relative humidity equal to 0.768.

Creep Correction Factor for Member Volume to Surface Ratio

The correction factor which accounts for the influence of size and shape of a member on creep is:

$$CF_{cp,vs} = \frac{2}{3}(1 + 1.13 \exp(-0.54\ vs)) \qquad \text{Eq 4.8}$$

where $CF_{cp,vs}$ = creep correction factor for member volume to surface ratio

vs = volume to surface area ratio of the member in inches. [10]

The concrete pile has a volume to surface area ratio of 2.92 inches. Thus the creep correction factor for the member volume to surface ratio is 0.822.

Creep Correction Factor for Loading Age

The creep correction factor for loading age is dependent upon the curing method used on the concrete. For moist cured concrete loaded after seven days, the creep correction factor is:

$$CF_{cp,la} = 1.25\ t_{la}^{-0.118} \qquad \text{Eq 4.9}$$

where $CF_{cp,la}$ = creep correction factor for loading age

t_{la} = concrete age at loading in days. [10]

For steam cured concrete loaded later then one to three days, the creep correction factor is:

$$CF_{cp,la} = 1.13\ t_{la}^{-0.094}\ [10] \qquad \text{Eq 4.10}$$

From Table 4, the concrete piles were steam cured and loaded at 30, 72, 120, and 121 days. Using Equation 4.10, the creep correction factors for age of loading are

0.821, 0.756, 0.721, and 0.720, respectively.

Shrinkage Strains

Shrinkage strain is calculated using ACI Committee 209 equation for moist cured concrete loaded after seven days which is:

$$e_{sh,t} = \frac{t}{35 + t} e_{sh,u} \qquad \text{Eq 4.11}$$

where $e_{sh,t}$ = shrinkage strain at time "t"

$e_{sh,u}$ = ultimate shrinkage strain. [10]

For steam cured concrete loaded after one to three days, the general equation for shrinkage strain is:

$$e_{sh,t} = \frac{t}{55 + t} e_{sh,u} \text{ [10]} \qquad \text{Eq 4.12}$$

Where specific data for local aggregates are not available, the ACI recommends use of a value for $e_{sh,u}$ equal to 780×10^{-6} inch/inch. [10]

Kalani and Hamada [2] empirically derived the following equations for shrinkage strain. For moist cured concrete loaded after seven days and stored at a relative humidity of 75%, the general equation is:

$$e_{sh,t} = \frac{t}{31 + t} e_{sh,u} \qquad \text{Eq 4.13}$$

The ultimate shrinkage strain for the moist cured concrete was determined to be 472.6×10^{-6} inch/inch. [2]

For steam cured concrete loaded after one to three days and stored at 75% humidity, the general equation is:

$$e_{sh,t} = \frac{t}{65 + t} e_{sh,u} \qquad \text{Eq 4.14}$$

The ultimate shrinkage strain for the steam cured concrete was determined to be 389.1×10^{-6} inch/inch. [2]

Shrinkage Correction Factor for Concrete Composition

The shrinkage correction factor for concrete composition is the product of the shrinkage correction factors for slump, percent of fine aggregate, and cement content.

$$CF_{sh,cc} = CF_{sh,s}\ CF_{sh,fa}\ CF_{sh,c} \qquad \text{Eq 4.15}$$

where $CF_{sh,cc}$ = shrinkage correction factor for concrete composition

$CF_{sh,s}$ = shrinkage correction factor for slump

$CF_{sh,fa}$ = shrinkage correction factor for percentage of fine aggregate

$CF_{sh,c}$ = shrinkage correction factor for cement content. [10]

The shrinkage correction factor for slump is:

$$CF_{sh,s} = 0.89 + 0.041\ s \quad [10] \qquad \text{Eq 4.16}$$

For a six inch slump, the shrinkage correction factor is equal to 1.136.

The shrinkage correction factor for the percentage of fine aggregate less than or equal to 50% is:

$$CF_{sh,fa} = 0.30 + 0.014\ \%fa\ [10] \qquad \text{Eq 4.17}$$

For the percentage of fine aggregate greater than 50%, the shrinkage correction factor is:

$$CF_{sh,fa} = 0.90 + 0.002\ \%fa\ [10] \qquad \text{Eq 4.18}$$

The shrinkage correction factor for percent of fine aggregate for a 43.865% using Equation 4.17 is equal to 0.914.

The shrinkage correction factor for cement content is:

$$CF_{sh,c} = 0.75 + 0.00036\ cc \qquad \text{Eq 4.19}$$

where cc = cement content in pounds per cubic yard of concrete. [10]

From Table 1, 808 pounds of cement was used per cubic yard of concrete which yields a shrinkage correction factor for cement equal to 1.041.

Using Equation 4.15 yields the shrinkage correction factor for the composition of the concrete used in the pile equal to 1.081. This factor of 1.081 will only be used with the ACI Equations (Equation 4.11 or 4.12). Equations 4.13 and 4.14 proposed by Kalani and Hamada were empirically derived with the correction for the concrete composition included in the general expression.

Shrinkage Correction Factor for Relative Humidity

The shrinkage correction factor for relative humidity between 40% and 80%, inclusive is:

$$CF_{sh,h} = 1.40 - 0.010\ H \qquad \text{Eq 4.20}$$

where $CF_{sh,h}$ = shrinkage correction factor for relative humidity. [10]

For humidity greater then 80% and less than or equal to 100%, the shrinkage correction factor is:

$$CF_{sh,h} = 3.00 - 0.030\ H \quad [10] \qquad \text{Eq 4.21}$$

For the constant relative humidity of 75%, Equation 4.20 yields a shrinkage correction factor for relative humidity equal to 0.650.

Shrinkage Correction Factor for Member Volume to Surface Ratio

The correction factor which accounts for the influence of size and shape of a member on shrinkage is:

$$CF_{sh,vs} = 1.2 \exp(-0.12\ vs) \qquad \text{Eq 4.22}$$

where $CF_{sh,vs}$ = shrinkage correction factor for member volume to surface ratio. [10]

The shrinkage correction factor for the pile volume to surface ratio of 2.92 inches is equal to 0.938.

Summary of the Direct Solution Method Using the ACI Equations

Equations 4.1 and 4.2 provide the general expression for creep strain calculations. The ultimate creep coefficient of 2.35 must be corrected for the pile concrete composition by multiplying it by a correction factor of 1.204. The ultimate creep coefficient must further be multiplied by correction factors of 0.822 for the pile volume to surface ratio and either 0.821, 0.756, 0.721, or 0.720 for the particular age of loading of 30, 72, 120, or 121 days respectively. Dependent upon the method of reducing the pile creep strain data, the ultimate creep coefficient may be further multipied by a correction factor of 0.768 for relative humidity.

Equation 4.12 provides the general equation for shrinkage strain calculations for steam cured concrete. The ultimate shrinkage strain of 780×10^{-6} inch/inch must be corrected for the pile concrete composition by multiplying it by a correction factor of 1.081. The ultimate shrinkage strain must further be multiplied by correction factors of 0.650 for relative humidity and 0.938 for the pile volume to surface ratio.

The sum of the initial elastic strain and creep and shrinkage strains derived for a particular time and applying the appropriate correction factors provides the total strain for that particular age of the concrete.

Summary of the Direct Solution Method Using the Cylinder Equations

Equation 4.3 provides the creep strain equation empirically derived from the cylinder data by Kalani and Hamada. [2] The ultimate creep coefficient of 2.311 must be corrected for the member volume to surface ratio by multiplying it by 0.822. The ultimate creep coefficient must further be multiplied by either 0.821, 0.756, 0.721, or 0.720 to correct for the particular age of loading of 30, 72, 120, or 121 days respectively. Since the cylinder creep equation is derived for a relative humidity of 75%, any adjustment for relative humidity must be made by calculating the correction factor using Equation 4.7, dividing it by 0.768 and multiplying the resultant ratio to the ultimate creep coefficient.

Equation 4.14 provides the steam cured concrete shrinkage strain equation empirically derived from the cylinder data. The ultimate shrinkage strain of 389.1 x 10^{-6} inch/inch must be adjusted for the relative humidity and the the pile volume to surface ratio. Since the cylinder shrinkage equation is derived for a relative humidity of 75%, any adjustment for relative humidity must be made by calculating the correction factor using Equation 4.20 or 4.21, dividing it by 0.650 and multiplying the resultant ratio to the ultimate shrinkage strain. The ultimate shrinkage strain must also be

multiplied by 0.938 to correct for the pile volume to surface ratio.

The sum of the initial elastic strain and creep and shrinkage strains derived for a particular time and applying the appropriate correction factors provides the total strain for that particular age of the concrete.

Incremental Time Step Method

The incremental time step method of calculating total strain accounts for the time dependent loss of stress in the prestressing steel. A precise determination of stress losses in prestressed concrete members is a complicated problem because the rate of loss due to one factor, such as relaxation of the prestressing steel, is altered by changes in stress due to other factors, such as creep and shrinkage of the concrete. Rate of creep in turn is altered by the change in stress. [11]

The incremental time step method produces an accurate estimate of time dependent losses of stress by accounting for the influence of time and the interdependence of these losses. Creep and shrinkage of concrete and steel relaxation are presented as functions of time. By calculating losses over short time intervals in which the dependent variables are assumed constant, it

is possible to estimate the interdependence of these effects. [11] The smaller the time interval, the more accurate the estimate of each separate time dependent loss and the smaller the relative impact of their interdependence.

For each time step, time dependent parameters for creep, shrinkage, and steel relaxation losses are calculated. The time dependent parameter for creep is the unit creep strain.

$$d_t = \frac{C_t}{E_c} \qquad \text{Eq 4.23}$$

where d_t = creep strain per unit stress at time t

E_c = modulus of elasticity of the concrete. [9]

The creep coefficient (C_t) is calculated by using either Equation 4.2 or 4.3. It is noted that all applicable correction factors for concrete composition, relative humidity, member volume to surface ratio, and age of loading should be incorporated in the creep coefficient used in Equation 4.23.

The time dependent parameter for shrinkage is the shrinkage strain calculated using either Equation 4.11, 4.12, 4.13, or 4.14. All applicable correction factors for concrete composition, relative humidity, and member volume to surface ratio should be incorporated into the calculated shrinkage strain.

The time dependent parameter for the relaxation of the steel is the loss ratio. The loss of stress in steel due to relaxation is given by the equation:

$$\frac{f_p}{f_{pi}} = 1 - \left(\frac{\log(24\ (t - t_r))}{10}\right)\left(\frac{f_{pi}}{f_{py}} - 0.55\right) \qquad \text{Eq 4.24}$$

where f_p = stress in the steel at time t

f_{pi} = initial stress in the steel

t_r = time pretensioned steel was released in days

f_{py} = yield stress of the steel. [9]

The loss ratio for the steel relaxation is calculated as:

$$\text{loss ratio} = 1 - \frac{f_p}{f_{pi}} \qquad [9] \quad \text{Eq 4.25}$$

For each time interval, the prestress loss due to creep and shrinkage of the concrete and the steel relaxation is accounted for in calculating the total strain.

The gross creep strain for the time interval at the level of the prestressing steel is:

$$D\ gr\ e_{cp} = f_{c,t1}\ (d_{t2} - d_{t1}) \qquad \text{Eq 4.26}$$

where $D\ gr\ e_{cp}$ = gross creep strain for the time interval

$f_{c,t1}$ = concrete stress at the start of the interval, time t1

d_{t2} = creep strain per unit stress at time t2

d_{t1} = creep strain per unit stress at time t1. [9]

The sum of the gross creep strain for the time interval and the change of shrinkage strain during the interval yields the total strain of the concrete at the level of the prestressing steel. Since the strain of the concrete is equal to the strain of the steel, the loss of steel stress due to creep and shrinkage is equal to the sum of the strain multiplied by the elastic modulus of the steel. The total loss of steel stress is the sum of the creep and shrinkage contributions and the loss of stress due to the relaxation of the steel itself.

$$Df_p = (D\ gr\ e_{cp} + De_{sh})\ E_p + (\text{loss ratio})\ f_{pi} \qquad \text{Eq 4.27}$$

where Df_p = total loss of steel stress over the time interval

De_{sh} = change of shrinkage strain during the time interval

E_p = elastic modulus of the prestressing steel. [9]

The corresponding change in concrete stress is:

$$Df_c = \frac{Df_p\ A_p}{A_c}\left(1 \pm \frac{e\ c}{r^2}\right) \qquad \text{Eq 4.28}$$

where Df_c = change in concrete stress over the time interval

A_p = cross sectional area of the prestressing steel

A_c = cross sectional area of the concrete

e = distance between the prestressing steel and the member centroidal axis

c = distance between the member centroidal axis and the face

r = radius of gyration. [9]

In cases where the concrete member is reinforced with steel rebars, the area of the concrete should be adjusted by substituting the transformed area of the member in place for the A_c term.

For the concrete piles, the distance between the prestressing steel and the member centroid is assumed to be zero due to the symmetric placement of the steel around the concrete centroid. Thus equation 4.28 reduces to:

$$Df_c = \frac{Df_p \, A_p}{A_c} \qquad \text{Eq 4.29}$$

The stress in the concrete at the end of the time interval, time "t2" is calculated as:

$$f_{c,t2} = f_{c,t1} - Df_c \qquad \text{Eq 4.30}$$

where $f_{c,t2}$ = stress in the concrete at the end of the interval, time t2.

The change in concrete strain is:

$$De_c = \frac{Df_c}{E_c} \qquad \text{Eq 4.31}$$

where De_c = change in concrete strain over the time interval. [9]

Accounting for the interdependence of the applied stress on creep strain, the net creep strain increment over the time interval is:

$$\text{net } De_{cp} = D \text{ gr } e_{cp} - De_c \qquad \text{Eq 4.32}$$

where net De_{cp} = net creep strain increment over the time interval. [9]

The total strain in the concrete to time "t2" can now be calculated as the sum of the initial elastic, creep, and shrinkage strains. To account for the decreasing stress due to creep, shrinkage, and steel relaxation, the initial elastic strain is calculated for each time interval as:

$$e_i = \frac{f_{c,t2}}{E_c} \qquad \text{Eq 4.33}$$

The sum of the net creep strain increments of Equation 4.32 from time equal zero to time "t2" produces the total creep strain to time "t2". The shrinkage strain is calculated using either Equation 4.11, 4.12, 4.13, or 4.14 with the applicable correction factors.

Subsequent total strain calculations can be achieved by renaming all time "t2" values as the new time "t1" and recalculating new values for the new time "t2". Due to the repetitive nature of the iterative calculations, the incremental time step method of calculating total strain is conducive to computer application.

Curve Fitting

Curve fitting is a means of selecting a curve through the creep strain data. The resultant equation accounts for the interdependence of creep and shrinkage in the concrete and the relaxation of the prestressing steel on the imposed stress. The creep correction factor for concrete composition is also incorporated in the resultant equation.

The creep correction factors for relative humidity, member volume to surface ratio, and age of loading can be extracted from the resultant equation. This final expression can be applied to other prestressed members at different conditions of environment and loading but composed of the same concrete constituents.

The International Mathematical and Statistical Language (IMSL) routine RLONE performs a simple linear regression analysis using the method of least squares in fitting a straight line through given data. RLONE was employed in fitting exponential, power, and hyperbolic equations to the available prestressed concrete pile creep strain data.

Equations of the exponential, power, and hyperbolic form are first transformed to a linear format.

$$Y = m\,X + C \qquad \text{Eq 4.34}$$

where Y = dependent variable (creep strain)

m = slope of the line (unknown parameter)

X = independent variable (time).

C = y axis intercept of the straight line (unknown parameter)

The data of time and/or creep strain are correspondingly transformed and the IMSL routine RLONE fits the straight line using linear regression. The unknown parameters m and C are determined and retransformed to yield the parameters of the initial equation form.

The exponential equation of the form:

$$t = A\, e^{(B\, e_{cp,t})} \qquad \text{Eq 4.35}$$

where $e_{cp,t}$ = creep strain at time "t"

is transformed to the linear form:

$$\ln t = B\, e_{cp,t} + \ln A \qquad \text{Eq 4.36}$$

where Y = ln t

m = B

X = $e_{cp,t}$

C = ln A

The power equation of the form:

$$e_{cp,t} = A\, t^{B} \qquad \text{Eq 4.37}$$

is transformed to the linear form:

$$\ln e_{cp,t} = B \ln t + \ln A \qquad \text{Eq 4.38}$$

where $Y = \ln e_{cp,t}$

$m = B$

$X = \ln t$

$C = \ln A$

The hyperbolic equation of the form:

$$e_{cp,t} = \frac{t}{A + B\,t} \qquad \text{Eq 4.39}$$

is transformed to the linear form:

$$\frac{t}{e_{cp,t}} = B\,t + A \qquad \text{Eq 4.40}$$

where $Y = \dfrac{t}{e_{cp,t}}$

$m = B$

$X = t$

$C = A$

CHAPTER V

METHOD OF ANALYSIS OF THE COMPARISONS

Curve Fitting

The correlation coefficient will be used to compare and select one of the three equation forms as that which best describes the observed creep strain data. The coefficient provides an estimation of the linear correlation between two variables "X" and "Y". The correlation coefficient is defined as:

$$R = \frac{\text{SUM } (Dx)(Dy)}{\text{SQRT } ((\text{SUM } Dx^2)(\text{SUM } Dy^2))} \qquad \text{Eq 5.1}$$

where R = correlation coefficient

SUM = the function "summation of"

Dx = difference between the observed "X" variable and the mean of all "X"s

Dy = difference between the observed "Y" variable and the mean of all "Y"s

SQRT = the function "square root of". [12]

Possible correlation coefficients range in value from negative one to positive one. In applying this statistic to the relationship between creep strain and time, one expects the coefficient to range in value from

zero to positive one since the strain is increasing with increasing time. The higher the coefficient, the greater the correlation between variable "X" and "Y".

Table 5 identifies the number of creep data points per data set through which the simple linear regression will be performed. Similar points of Piles 3 and 4, Piles 5 and 9, and Piles 6 and 7 have been consolidated since these piles were loaded at the same age of the pile and at the same stresses. Note the number of data points less than or equal to zero. These negative strain points result after the shrinkage strains of Pile 8 and the measured initial elastic strains due to the load are separated from the total measured strains.

The comparison of correlation coefficients for the equations fitted through these consolidated data sets will determine which of the three equation forms best describes the observed creep strains.

Standard Error of the Estimate

In comparing the outcome of the direct solution method and the incremental time step method using the ACI equations and the cylinder equations and the curve fitted equation, the standard error of the estimate will be calculated as:

$$STER = \frac{S}{SQRT(N-1)} \qquad \text{Eq 5.2}$$

where STER = standard error of the estimate

S = sample standard deviation

where:

$$S = SQRT\left(\frac{SUM\ (OBS - PRED)^2}{N-1}\right) \qquad \text{Eq 5.3}$$

where OBS = measured strain observed in the experiment

PRED = calculated strain predicted by one of the three methods at the same time of the corresponding observed data point

N = number of observations.
[13]

In comparing two different calculation methods against the observed data points, the method producing the smaller standard error of the estimate better predicts the observed strain.

CHAPTER VI

RESULTS

Direct Solution Method - ACI vs Cylinder Equations

To illustrate that increased accuracy in predicting total strain in a member is directly related to the expense of specimen testing, the least costly application of the direct solution method using the ACI equations is compared with the more costly application of the direct solution method using the cylinder equations.

Points 1 and 3 (Reinforced Concrete) Prior to Loading

Total strain calculated using the direct solution method with the ACI equations for creep and shrinkage strains were compared with the total strains calculated using the direct solution method with the cylinder equations for creep and shrinkage strains. The general conditions for the comparison were a load stress of one ksi, 75% relative humidity and a concrete pile with a volume to surface ratio of 2.92 inches. The ACI equations were further corrected by a correction factor for concrete composition of 1.204 for creep strains and 1.081 for shrinkage strains. The transformed area technique was used to account for the reinforcing steel

in the concrete in these sections.

Figure 19 compares the total strain calculated with the direct solution method with the ACI equations and the cylinder equations against the observed strain in Pile 8 Points 1 and 3. Although neither the ACI equations nor the cylinder equations predict strains overlapping the observed values, Figure 19 clearly shows that the cylinder equations better predicts the observed strains of Pile 8 Points 1 and 3.

Figure 20 is designed to be reproduced as an acetate overlay. The total strain and age of pile scales of Figure 20 are the same as in Figures 1 through 9. Thus by using the overlay of Figure 20, one can visually compare the observed total strains of Figures 1 through 9 against the predicted total strain. Note that the conditions for calculating the predicted total strains only apply to the observed strains prior to loading the member. Accordingly, any comparison between the predicted overlay and the observed total strains should be restricted to the strain values prior to loading.

Graphically plotting on one chart all observed total strains for all piles, Points 1 and 3 prior to loading results in an unreadable mess. A representative sample of these points were plotted in Figure 21 and compared against the predicted total strains from the direct solution method using the ACI equations and the

cylinder equations. The number symbols of Figure 21 correspond to the pile numbers. Piles 8 and 9 represent the lower total strain readings and Piles 3 and 6 represent the upper total strain readings for Points 1 and 3. The remaining Piles numbered 1, 2, 4, 5, and 7 are nestled between these limits. The predicted total strains calculated from the cylinder equations correspond with the upper range and Pile 3 observations. Clearly from Figure 21, the cylinder equations better predict the total strains than the ACI equations.

In Figure 21, one notes that the general shape of the predicted curves at the age of the piles greater than 120 days do not correspond with the observed data of Pile 8. the slope of the curves tend to decrease over time while the observed data tends to maintain a constant rise. The curves decreasing slope is attributed to the hyperbolic forms of both the shrinkage and creep strain equations. This observation supports the suggestion that perhaps other alternative equation forms could better represent this constant slope of increasing strain over time.

Tables 6 and 7 provide the standard error calculations for the direct solution method using the ACI equations and cylinder equations for Point 1 and Point 3 respectively. Comparisons between the ACI equations and cylinder equations should be restricted to the same pile

and point. As would be expected from the plots of Figures 19 and 21, the cylinder equations produced the lower standard error for all comparisons of Tables 6 and 7. Clearly the cylinder equations best predicts the observed data for Points 1 and 3.

Point 2 (Unreinforced Concrete) Prior to Loading

The general conditions for the comparison were the same as described for Points 1 and 3. The transformed area technique was not required since the Point 2 sections consisted of unreinforced concrete.

Figure 22 compares the total strain calculated with the direct solution method with the ACI equations and the cylinder equations against the observed strain in Pile 8 Point 2. The cylinder equations closely resemble the observed total strains.

Figure 23, if reproduced as an acetate overlay, may be used for visual comparisons of the direct solution method using the ACI equations and cylinder equations against the observed total strain prior to loading plotted on Figures 10 through 18.

A representative sample of Point 2 observed data for all piles were plotted in Figure 24 and compared against the direct solution method using the ACI equations and the cylinder equations. The number symbols in the figure correspond to the pile numbers. Since Pile

8 was never loaded, it has the oldest age of pile observed total strains. The cylinder equations curve is well within the upper range of Pile 3 and lower range of Pile 9 while the ACI equations curve is well above the observed data. Clearly the cylinder equations best predicts the observed total strains.

In Figure 24, as was noted in the discussion of Figure 21, the general shape of the predicted curves at the age greater than 120 days do not correspond with the observed data of Pile 8. As discussed in the prior section, this observation supports the suggestion that perhaps other alternative equation forms could better represent shrinkage and creep strains.

Table 8 provides the standard error calculations for the direct solution method using the ACI equations and cylinder equations for Point 2. In comparing the standard error of the ACI equations against the standard error of the cylinder equations for each respective pile, one clearly sees that the cylinder equations produced the lower standard error in all nine cases.

The Direct Solution vs the Incremental Time Step Method

ACI Equations - Points 1 and 3 Prior to Loading

Total strains calculated using the ACI equations and the direct solution method were compared with total

strains calculated using the same ACI equations in the incremental time step method. The general conditions of the comparison were a load stress of one ksi, 75% relative humidity and a concrete pile with a volume to surface ratio of 2.92 inches. The ACI equations were further corrected by a correction factor for concrete composition of 1.204 for creep strains and 1.081 for shrinkage strains. The transformed area technique was used to account for the reinforcing steel in the concrete in these sections. An incremental time step of one day was used.

Table 9 compares these two methods at 30 day intervals. As expected, the incremental time step method produced lower total strains than the direct solution method. The lower strains were a result of the decreasing applied stress on the concrete due to the interrelationship of the time dependent strains and the relaxation of the prestressing steel.

The difference between these two methods was 15.61 micro inch/inch at 30 days which increased to 17.27 micro inch/inch at 90 days and then decreased steadily to 10.42 micro inch/inch at 720 days. The 10.42 micro inch/inch difference at 720 days represents a 1.2 percent reduction of strain calculated by the incremental time step method from the direct solution method.

One would expect the difference in strains between

these methods to increase over time at a decreasing rate. Both the creep and shrinkage strain equations achieve half their ultimate values within the first 47 and 55 days respectively. The rate of increase in strain then decreases with the remaining half of the ultimate values being attained over a greater period of time. The observed trend of an increase in the difference to 90 days then a steady decrease is due to the affect of the transformed area technique in acounting for the reinforcing steel in the section.

The modular ratio "n" accounts for the reinforcing steel by increasing the concrete cross sectional area by "n" times the area of steel. "n" is defined as:

$$n = \frac{E_s}{E_c} (1 + C_t) \qquad \text{Eq 6.1}$$

where n = modular ratio

E_s = modulus of elasticity of the reinforcing steel

The transformed concrete area increase over time is directly related to the rate of creep. During the first 90 days, the transformed area increases and the applied stress decreases at different rates due to the affect of shrinkage on the later. This results in the observed increase in the difference between the direct solution method and incremental time step method.

The decrease in the differences of strains

calculated by both methods which follows after 90 days is due to the decreased affect of shrinkage strains on the applied stress. Half of the ultimate shrinkage strain is attained in the first 55 days.

Figures 19 through 21 can be used to compare the direct solution method and the incremental time step method. A curve 10 to 15 micro inch/inch below the solid ACI equations direct solution line would depict the predicted total strain due to the ACI equations incremental time step method.

Tables 10 and 11 confirm the visual comparison of the above figures. The standard error of the estimates in all eighteen comparisons were lower in the incremental time step method.

ACI Equations - Point 2 Prior to Loading

The general conditions for the comparison were the same as described for Points 1 and 3 of this section. The transformed area technique was not required since the Point 2 sections consisted of unreinforced concrete.

Table 12 compares the direct solution method and the incremental time step method at 30 day intervals. The incremental time step method produced lower total strains as expected.

The difference between these two methods was 65.98 micro inch/inch at 30 days which increased to 153.66

micro inch/inch at 720 days. The differences change greatly in the first 90 days as explained by both the creep and shrinkage component of the total strain attaining half their ultimate values during this time. The change in the differences gradually become smaller over time as illustrated in the 0.78 micro inch/inch change between 690 and 720 days. The 153.66 micro inch/inch difference at 720 days represents a 13.6 percent reduction of strain calculated by the incremental time step method from the direct solution method.

Figures 22 through 24 can be used to compare the direct solution method and the incremental time step method. A curve 65.98 micro inch/inch at 30 days and 153.66 micro inch/inch at 720 days below the solid ACI equations direct solution line would depict the predicted total strain due to the ACI equations incremental time step method. The incremental time step curve would lie very close to Piles 3 and 4 and could serve as the upper limit of total strain expected.

Table 13 confirms the visual comparison of the above figures. The standard error of the estimates in all nine comparisons were lower in the incremental time step method.

Cylinder Equations - Points 1 and 3 Prior to Loading

Total strains calculated using the cylinder equations in the direct solution method were compared with total strains calculated using the same cylinder equations in the incremental time step method. The general conditions of the comparison were a load stress of one ksi, 75% relative humidity and a concrete pile with a volume to surface ratio of 2.92 inches. The transformed area technique was used to account for the reinforcing steel in the concrete in these sections. An incremental time step of one day was used.

Table 14 compares these two methods at 30 day intervals. As expected, the incremental time step method produced a smaller total strain than the direct solution method as a result of a decreasing applied stress.

The difference between these two methods was 24.28 micro inch/inch at 30 days which increased to 35.86 micro inch/inch at 270 days and then decreased steadily to 33.46 micro inch/inch at 720 days. The 33.46 micro inch/inch difference at 720 days represents a 4.8 percent reduction of strain calculated by the incremental time step method from the direct solution method.

The increasing then decreasing strain differences are due to the affect of the transformed area technique. This affect was explained in the ACI equations section for Points 1 and 3. From Equation 4.3, half the ultimate

creep strain is attained within the first 530 days. Half the ultimate shrinkage strain is attained at 65 days.

The ACI equations maximum difference occured at about 90 days as compared to 270 days for the cylinder equations. The later cylinder equation maximum difference can be attributed to the creep coefficient equation where half the ultimate is attained at 47 days for the ACI and 530 days for the cylinder equation.

Figure 25 compares the total strain calculated using the cylinder equations with the direct solution method and incremental time step method against the observed strain in Pile 8 Points 1 and 3. As expected, the incremental time step method produced a smaller total strain than the direct solution method as a result of a decreasing applied stress.

Figure 26 if reproduced as an acetate overlay, may be used to visually compare these two methods of calculation against the observed total strains prior to loading on Figures 1 through 9.

A representative sample of Points 1 and 3 observed data prior to loading for all piles was plotted in Figure 27 and compared against the two calculation methods. From the figure, it seems that the incremental time step method is the better method.

As was noted in the discussion of Figures 21 and 24, the general shape of the predicted curves at the age

greater than 120 days do not correspond with the observed data of Pile 8 as seen in Figure 27. As cited in these prior discussions, this observation supports the suggestion that other alternative equation forms, other than the hyperbolic form, could better represent shrinkage and creep strains.

Tables 15 and 16 provide the standard error calculations for the incremental time step method and the direct solution method for Point 1 and Point 3 respectively. These tables confirm the visual comparison of Figure 27. The standard errors favor the incremental time step method in seventeen of the eighteen comparisons. Clearly the incremental time step method is the better method.

Point 2 Prior to Loading

The general conditions for the comparison were the same as described for Points 1 and 3 of this section. The transformed area technique was not required since the Point 2 sections consisted of unreinforced concrete.

Table 17 compares these two methods at 30 day intervals. The incremental time step method produced lower total strains as expected.

The difference between the two methods was 44.80 micro inch/inch at 30 days which increased to 115.66 micro inch/inch at 720 days. The 115.66 micro inch/inch

represents a 13.3 percent reduction of strain calculated by the incremental time step method from the direct solution method.

Figure 28 compares the total strain calculated using the cylinder equations with the direct solution method and incremental time step method against the observed strain in Pile 8 Point 2. The decreasing stress accounted for in the incremental time step calculation produced lower strains than the direct solution method calculated strains.

Figure 29, if reproduced as an acetate overlay, may be used to visually compare these two methods of calculation against the observed total strains prior to loading on Figures 10 through 18.

A representative sample of Point 2 observed data prior to loading for all piles was plotted in Figure 30 and compared against the two calculation methods. Both calculation method curves are within the array of observed data. It appears that the direct solution method curve best represents the mean of the observed data while the incremental time step curve is somewhat lower.

As was noted in the discussion of Figures 21, 24, and 27, the general shape of the predicted curves at the age greater than 120 days do not correspond with the observed data of Pile 8 as seen in Figure 30. As cited

in these prior discussions, this observation supports the suggestion that other alternative equation forms, other than the hyperbolic form, could better represent shrinkage and creep strains.

Table 18 provides the standard error calculations for the incremental time step method and the direct solution method using the cylinder equations for creep and shrinkage strains. The direct solution method produced the lower standard error in five of the nine comparisons.

Curve Fitted Equation

Exponential Equation

Table 19 identifies the A and B parameters determined by IMSL's subroutine RLONE for the exponential equation (Equation 4.35). The data points were not corrected for humidity, age of loading nor volume to surface ratio.

The conspicuously different parameter values for Pile 2 were due to the affect of the negative strain values in the data set. Negative strain values were attained as a result of separating the total strain readings from the observed initial elastic strain and Pile 8's shrinkage strains. Table 5 identifies the number of negative strain values per data set. A

comparison of the number of negative strain values with the total number of data points in the corresponding set provides some idea as to the relative impact of these negative values on the resultant parameters A and B.

From Equation 4.36, the exponential equation may be rewritten as:

$$e_{cp,t} = \frac{1}{B} (\ln t - \ln A)\, e_i \qquad \text{Eq 6.1}$$

Eliminating all data sets with negative strain values from consideration and taking the average of the remaining parameters produce a natural logarithm of the parameter A equal to -1.002 for Points 1 and 3 and -1.416 for Point 2.

The parameter 1/B must be adjusted to some standard before an average can be taken. Adjusting for age of loading and volume to surface ratio with the appropriate creep strain correction factors previously identified provides a parameter which applies to the standard cylinders stored at 75% relative humidity. A value for 1/B of 0.0781 for Points 1 and 3 and 0.123 for Point 2 result.

Thus for Points 1 and 3, Equation 6.1 can be written as:

$$e_{cp,t} = 0.0781\ (\ln t + 1.002)\, e_i \qquad \text{Eq 6.2}$$

and for Point 2, Equation 6.1 is:

$$e_{cp,t} = 0.123\ (\ln t + 1.416)\, e_i \qquad \text{Eq 6.3}$$

Power Equation

Table 20 identifies the A and B parameters for the power equation (Equation 4.37). The missing parameters for Piles 1, 2, and 3 and 4, Points 1 and 3 and Pile 2 Point 2 are a result of the negative creep strain values within the data set. Negative strain values could not be transformed to the linearizing coordinate system since it required a natural logarithm operation to be performed (Equation 4.38). Elimination of the negative strain valued data points would create a biased curve, thus no parameters were sought for these data sets.

The parameter A must be adjusted to the standard described in the previous section before an average can be taken. After applying the adjustments a value for A of 0.0388 for Points 1 and 3 and 0.0691 for Point 2 result.

The average value for B is 0.487 for Points 1 and 3 and 0.464 for Point 2.

Thus for Points 1 and 3, Equation 4.37 can be rewritten as:

$$e_{cp,t} = 0.0388\ t^{0.487}\ e_i \qquad \text{Eq 6.4}$$

and for Point 2, Equation 4.37 is:

$$e_{cp,t} = 0.0691\ t^{0.464}\ e_i \qquad \text{Eq 6.5}$$

Hyperbolic Equation

Table 21 identifies the A and B parameters for the hyperbolic equation form (Equation 4.39). Equation 4.39 can be rewritten as:

$$e_{cp,t} = \frac{1}{B} \left(\frac{t}{A/B + t} \right) e_i \qquad \text{Eq 6.6}$$

Thus the 1/B parameter must be adjusted to the standard condition to obtain the general hyperbolic equation.

Eliminating all data sets with negative strain values from consideration and adjusting the 1/B parameter to standard conditions yields a 1/B value of 0.690 for Points 1 and 3 and 0.973 for Point 2.

The average value for A/B is 50.830 for Points 1 and 3 and 43.121 for Point 2.

Thus for Points 1 and 3, Equation 6.6 yields:

$$e_{cp,t} = 0.690 \left(\frac{t}{50.830 + t} \right) e_i \qquad \text{Eq 6.7}$$

and for Point 2, Equation 6.6 is:

$$e_{cp,t} = 0.973 \left(\frac{t}{43.121 + t} \right) e_i \qquad \text{Eq 6.8}$$

Comparison of the Correlation Coefficient

It was determined in Chapter V that the comparison of correlation coefficients for each of the three equation forms per data set would determine which equation best describes the observed creep strains. The

closer the value of the correlation coefficients is to one, the greater the linear relationship between the variables.

Table 22 contain the correlation coefficients for Points 1 and 3 data sets and Table 23 contain the coefficients for Point 2 data sets. Three Points 1 and 3 data sets in Table 22 and one Point 2 data set in Table 23 were not fitted to the power equation form due to the negative creep strain values in the set. Therefore these data sets do not have correlation coefficients listed.

If one excludes from consideration those data sets with negative creep strain values, one notes that the hyperbolic equation form exhibits the greatest linear correlation characteristics of the three equations. The hyperbolic equation form had the higher coefficient in both of the two comparisons of Table 22. Both of these coefficients were over 0.90. In Table 23, the hyperbolic equation form had the higher coefficient in all four of the comparisons. Three of the four coefficients were well over 0.90.

Points 1 and 3 Prior to Loading

The general conditions for the comparison were a load stress of one ksi, 75% relative humidity and a concrete pile with a volume to surface ratio of 2.92 inches. The exponential equation (Equation 6.2), power

equation (Equation 6.4), and hyperbolic equation (Equation 6.7) need not be adjusted for concrete composition since the equations were derived from data of this particular design mix. The effect of the reinforcing steel is also accounted for in these equations thus the transformed area technique need not be applied. The effect of the time dependent losses of applied stress due to the creep and shrinkage of the concrete and steel relaxation need not be accounted for as in the incremental time step method since these losses were reflected in the data through which the curves were fitted.

Tables 24 and 25 provide the standard errors for each of the three equations for Point 1 and Point 3 respectively. The power equation produced the lower standard error in twelve of the eighteen comparisons. The exponential equation had the lower standard error in the remaining six comparisons. These comparisons seem to contradict the conclusions attained from the comparison of correlation coefficients of Table 22.

Figure 31 compares the predicted total strain as calculated by the three curve fitted equations against Pile 8 Points 1 and 3. Clearly the power equation in Figure 31 best represents the general shape of the increasing total strain at ages greater than 120 days. It would seem that the power equation best represents the

observed data in this case.

The contradiction between the correlation coefficient and the standard errors is due to the nature of the observed data. The frequency of recorded observations for ages less than 150 days was once every one to seven days. The frequency of recorded observations after 150 days was once every thirty to sixty days. The greater frequency of observations in the early ages of the pile tends to minimize the mean of the time and strain variables which affects the outcome of the correlation coefficient of Equation 5.1. Thus the hyperbolic and exponential equation forms were favored with the higher coefficients due to the early age shape of these equation forms. Visual observations of Figures 21, 24, 27, and 30 noted that at later ages of the pile, the general shape of the hyperbolic equation form of the cylinder equations did not describe the observed data. Thus the nature of the data weights the early observations and results in a correlation coefficient which favors the hyperbolic equation form while the standard error of the estimate and the visual comparison of Figure 31 favors the power equation.

Point 2 Prior to Loading

The general conditions for the comparison were the same as described for Points 1 and 3 of this section.

The exponential equation (Equation 6.3), power equation (Equation 6.5), and hyperbolic equation (Equation 6.8) need not be corrected for concrete composition and the effects of the time dependent losses.

Table 26 provides the standard errors for each of the three equations for Point 2. The power equation produced the lower standard error in four of the nine comparisons. The exponential equation was better in three of the nine comparisons and the hyperbolic equation was best in the remaining two.

Figure 32 compares the predicted total strain as calculated by the three curve fitted equations against Pile 8 Point 2. Clearly from the figure, the power equation best predicts the observed data and this is confirmed by the standard error comparison of Table 25. As was the case in Points 1 and 3, note that the general shape of the increasing total strain is best represented by the power equation.

The contradiction between the visual comparison of Figure 32 and the correlation coefficient of Table 23 are a result of the nature of the data. The ramifications of the nature of the data were discussed in the previous section on Points 1 and 3.

CHAPTER VII

CONCLUSIONS

The comparison of the ACI equations and the cylinder equations using the direct solution method amplifies the need to conduct creep and shrinkage testing on local concrete mixes to ascertain their parameters and equation forms. The ACI equations with all of the correction factors for the local conditions over estimated the observed total strain. The cylinder equations which did not require correction for local conditions provided a more realistic estimate of the measured total strain.

For the reinforced concrete section, the incremental time step method using the ACI equations reduced the total strain by 15.61 micro inch/inch at 30 days and 10.42 micro inch/inch at 720 days from those strains calculated using the ACI equations with the direct solution method. The 10.42 micro inch/inch at 720 days represented a 1.2 percent reduction of strain. Compared to the observed strains, this percent reduction proved insignificant. Irrespective of the reduction of strain, neither method was able to approximate the observed strain.

For the unreinforced concrete section, the

incremental time step method using the ACI equations reduced the total strain by 65.98 micro inch/inch at 30 days and 153.66 micro inch/inch at 720 days from those strains calculated using the ACI equations with the direct solution method. The 153.66 micro inch/inch at 720 days represented a 13.6 percent reduction of strain. With the reduction, the incremental time step method using the ACI equations approximated the upper limit of observed total strain values.

The incremental time step method using the cylinder equations for the reinforced concrete sections reduced the total strain by 24.28 micro inch/inch at 30 days and 33.46 micro inch/inch at 720 days. The 33.46 micro inch/inch represented a 4.8 percent reduction of strain. The reduction improved the estimate of the observed total strain. But in general, the estimate remained higher than the observed strain.

In both the ACI and cylinder equations the reinforced concrete estimate remained higher than the observed data. This was due in part to the shrinkage strain equation which did not vary between reinforced and unreinforced sections. The transformed area technique could have also contributed to the over estimate of strain by not adequately accounting for the affect of the reinforcing steel.

The incremental time step method using the

cylinder equations for the unreinforced concrete sections reduced the total strain by 44.80 micro inch/inch at 30 days and 115.66 micro inch/inch at 720 days. The 115.66 micro inch/inch represented a 13.3 percent reduction of strain. With the reduction, the predicted strain values approximated the lower bound of observed strain data. It would seem that the incremental time step method over compensated for the stress reduction and thus provided lower than realistic estimates of the measured total strain in this case.

In the curve fitting of the hyperbolic, exponential, and power equation forms to the observed creep strain data, the comparison of the correlation coefficients suggested that the hyperbolic equation form best predicted the observed data. However, a visual comparison suggested that the general shape of the power equation better predicted strains at ages greater than 120 days. This observation was reinforced by the lower standard error of the estimate for the power equation. This contradiction between the correlation coefficient and the standard errors is due to the nature of the data. The data weights the early observations since about half of the data was recorded in the first 150 days and the remainder was recorded over the last 570 days. The weighted data produced the higher correlation coefficient for the hyperbolic equation form even though

the power equation better represented the observed creep strain data.

The curve fitted power equation coupled with the cylinder shrinkage equation and applicable correction factors, described the general shape of the observed strain in the prestressed piles at ages greater than 120 days. Figures 33 to 42 provides this comparison and supports the conclusion that the power equation form was the best of the three equation forms considered.

As expected, the curve fitted equations of the observed creep strains of the actual member produced accurate predictions of the strain but this method incurs the greatest cost. Creep and shrinkage equations derived from test cylinders better predicted the strains than the general ACI equations as previously discussed. The equations empirically derived from the test cylinders using the direct solution method are probably the most cost effective method in obtaining reasonably accurate results.

CHAPTER VIII

RECOMMENDATIONS

Creep and shrinkage testing on local concrete mixes must be conducted whenever the mix design or material source changes.

The methodology of this testing must insure a constant time interval such that the data is not biased.

The transformed area technique as a method to account for reinforcing steel in concrete needs to be reevaluated with respect to creep and shrinkage strains. Unreinforced concrete and reinforced concrete do not shrink at the same rate yet the transformed area technique uses one shrinkage equation to describe both the unreinforced and reinforced concrete sections.

Local testing on reinforced concrete cylinders must be undertaken to determine the effect of the number and cross sectional area of steel on shrinkage and creep strains. The transformed area technique and its effectiveness to predict the observed strains must be evaluated using these test results.

Local testing on prestressed steel should be conducted to verify the accuracy of the steel relaxation equation.

APPENDIX A

TABLES

TABLE 1

Quantity of Constituents per Cubic Yard of Concrete

Constituents	Quantity
Cement	808 pounds
#3 Coarse Aggregate	1798 pounds
#4 Fine Aggregate	704 pounds
Sand	701 pounds
Water	236 pounds
Sikament	128 fluid ounces

TABLE 2

Chemical Composition of the Cement

Compound	Percent
Tricalcium Silicate	53.0
Dicalcium Silicate	16.0
Tetracalcium Aluminoferrite	9.0
Tricalcium Aluminate	6.0
subtotal	84.0
Other Compounds (lesser quantities)	16.0
total	100.0

TABLE 3

Summary of Casting, Curing and Loading of the Cylinders

Frame	Date of Casting	Applied Stress (ksi)	Age at Loading (days)	Method of Curing
1	August 9, 1984	0.0	0	Steam
2	May 30, 1984	2.0	120	Moist
3	August 9, 1984	1.0	1	Steam
4	May 30, 1984	1.0	30	Moist
5	August 9, 1984	3.0	120	Steam
6	August 9, 1984	3.0	120	Steam
7	August 9, 1984	3.0	30	Steam
8	May 30, 1984	3.0	120	Moist
9	August 9, 1984	0.0	0	Steam
10	June 12, 1985	0.0	0	Moist

TABLE 4

Summary of Casting, Curing and Loading of the Piles

Pile	Date of Casting	Applied Stress (ksi)	Age at Loading (days)	Method of Curing
1	May 30, 1984	0.8	30	Steam
2	May 30, 1984	1.0	72	Steam
3	May 30, 1984	1.0	120	Steam
4	May 30, 1984	1.0	121	Steam
5	May 30, 1984	1.9	121	Steam
6	September 4, 1984	1.9	30	Steam
7	September 4, 1984	1.9	30	Steam
8	September 4, 1984	0.0	0	Steam
9	September 4, 1984	1.9	120	Steam

TABLE 5

Creep Strain Data Set Information

Pile	Points	Total Number of Data Points	Number of Points with Strains Less Than Zero
1	1 & 3	210	2
1	2	105	0
2	1 & 3	124	39
2	2	62	18
3 & 4	1 & 3	240	20
3 & 4	2	120	0
5 & 9	1 & 3	236	0
5 & 9	2	118	0
6 & 7	1 & 3	248	0
6 & 7	2	124	0

TABLE 6

Comparison of Standard Error of the Estimate
ACI Equation vs Cylinder Equation
Observed Data Points Prior to Loading

Point 1

Pile	ACI Equation Standard Error (Micro in/in)	Cylinder Equation Standard Error (Micro in/in)	Number of Data Points
1	43.13	29.91	40
2	24.70	11.12	50
3	21.37	7.93	53
4	19.29	6.45	60
5	22.28	7.46	64
6	23.03	9.28	19
7	32.51	12.73	19
8	43.81	23.24	69
9	54.15	29.54	25

TABLE 7

Comparison of Standard Error of the Estimate
ACI Equation vs Cylinder Equation
Observed Data Points Prior to Loading

Point 3

Pile	ACI Equation Standard Error (Micro in/in)	Cylinder Equation Standard Error (Micro in/in)	Number of Data Points
1	36.49	23.89	40
2	19.76	6.06	50
3	17.69	5.02	53
4	25.97	10.84	60
5	25.29	10.29	63
6	30.93	12.44	19
7	41.46	18.74	19
8	42.98	22.49	69
9	54.83	30.12	25

TABLE 8

Comparison of Standard Error of the Estimate
ACI Equation vs Cylinder Equation
Observed Data Points Prior to Loading

Point 2

Pile	ACI Equation Standard Error (Micro in/in)	Cylinder Equation Standard Error (Micro in/in)	Number of Data Points
1	28.32	12.48	40
2	26.29	7.90	50
3	12.94	11.47	53
4	15.25	9.20	60
5	23.04	4.65	64
6	54.01	23.44	19
7	30.33	17.65	19
8	30.57	5.72	69
9	42.58	16.74	25

TABLE 9

Comparison
ACI Equations
Direct Solution Method vs Incremental Time Step Method
Points 1 and 3

Age of Concrete (days)	Direct Solution Method (10^{-6} in/in)	Incremental Time Step Method (10^{-6} in/in)	Difference (10^{-6} in/in)
30	519.12	503.51	15.61
60	624.66	607.47	17.19
90	685.37	668.10	17.27
120	725.32	708.39	16.93
150	753.76	737.32	16.44
180	775.13	759.20	15.93
210	791.81	776.40	15.41
240	805.23	790.30	14.93
270	816.28	801.80	14.48
300	825.54	811.49	14.05
330	833.44	819.78	13.66
360	840.25	826.96	13.39
390	846.19	833.24	12.95
420	851.43	838.79	12.64
450	856.08	843.73	12.35
480	860.24	848.16	12.08
510	863.99	852.17	11.82
540	867.38	855.80	11.58
570	870.47	859.11	11.36
600	873.30	862.15	11.15
630	875.90	864.94	10.96
660	878.29	867.52	10.77
690	880.50	869.91	10.59
720	882.56	872.14	10.42

TABLE 10

Comparison of Standard Error of the Estimate
ACI Equations
Incremental Time Step vs Direct Solution
Observed Data Points Prior to Loading

Point 1

Pile	Incremental Time Step Standard Error (Micro in/in)	Direct Solution Standard Error (Micro in/in)	Number of Data Points
1	41.03	43.13	40
2	22.66	24.70	50
3	19.40	21.37	53
4	17.47	19.29	60
5	20.37	22.28	64
6	19.48	23.03	19
7	28.94	32.51	19
8	42.04	43.81	69
9	50.79	54.15	25

AD-A181 310 CREEP IN PRESTRESSED CONCRETE PILES: A COMPARISON OF 2/2
THE DIRECT SOLUTION (U) ARMY MILITARY PERSONNEL CENTER
ALEXANDRIA VA S K HIRATA MAY 87

UNCLASSIFIED F/G 11/2 NL

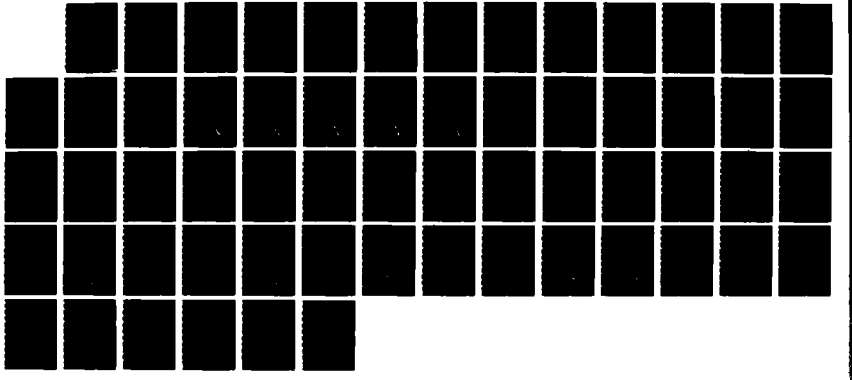

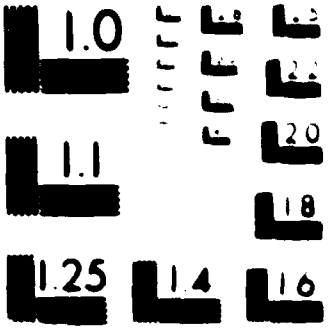
1.0
1.1
1.25
1.4
1.6
2.0
1.8

TABLE 11

Comparison of Standard Error of the Estimate
ACI Equations
Incremental Time Step vs Direct Solution
Observed Data Points Prior to Loading

Point 3

Pile	Incremental Time Step Standard Error (Micro in/in)	Direct Solution Standard Error (Micro in/in)	Number of Data Points
1	34.88	36.49	40
2	17.73	19.76	50
3	15.71	17.69	53
4	24.03	25.97	60
5	23.36	25.29	63
6	27.30	30.93	19
7	37.62	41.46	19
8	41.20	42.98	69
9	51.47	54.83	25

TABLE 12

Comparison
ACI Equations
Direct Solution Method vs Incremental Time Step Method
Point 2

Age of Concrete (days)	Direct Solution Method (10^{-6} in/in)	Incremental Time Step Method (10^{-6} in/in)	Difference (10^{-6} in/in)
30	662.83	596.85	65.98
60	792.98	705.04	87.94
90	868.74	767.73	101.01
120	919.29	809.31	109.98
150	955.80	839.15	116.65
180	983.59	861.72	121.87
210	1005.57	879.46	126.11
240	1023.45	893.81	129.64
270	1038.32	905.69	132.63
300	1050.93	915.70	135.23
330	1061.77	924.26	137.51
360	1071.21	931.68	139.53
390	1079.51	938.18	141.33
420	1086.89	943.92	142.97
450	1093.48	949.04	144.44
480	1099.43	953.63	145.80
510	1104.82	957.78	147.04
540	1109.74	961.54	148.20
570	1114.24	964.97	149.27
600	1118.38	968.12	150.26
630	1122.20	971.02	151.18
660	1125.75	973.69	152.06
690	1129.05	976.17	152.88
720	1132.13	978.47	153.66

TABLE 13

Comparison of Standard Error of the Estimate
ACI Equations
Incremental Time Step vs Direct Solution
Observed Data Points Prior to Loading

Point 2

Pile	Incremental Time Step Standard Error (Micro in/in)	Direct Solution Standard Error (Micro in/in)	Number of Data Points
1	21.75	28.32	40
2	18.65	26.29	50
3	6.60	12.94	53
4	7.31	15.25	60
5	14.65	23.04	64
6	41.37	54.01	19
7	20.67	30.33	19
8	17.30	30.57	69
9	29.91	42.58	25

TABLE 14

Comparison
Cylinder Equations
Direct Solution Method vs Incremental Time Step Method
Points 1 and 3

Age of Concrete (days)	Direct Solution Method (10^{-6} in/in)	Incremental Time Step Method (10^{-6} in/in)	Difference (10^{-6} in/in)
30	390.81	366.53	24.28
60	464.93	435.14	29.79
90	511.03	478.52	32.51
120	543.03	509.03	34.00
150	566.82	531.94	34.88
180	585.34	549.95	35.39
210	600.27	564.58	35.69
240	612.61	576.79	35.82
270	623.03	587.17	35.86
300	631.98	596.15	35.83
330	639.78	604.02	35.76
360	646.64	611.00	35.64
390	652.75	617.25	35.50
420	658.23	622.88	35.35
450	663.18	628.01	35.17
480	667.69	632.69	35.00
510	671.81	637.00	34.81
540	675.60	640.98	34.62
570	679.10	644.67	34.43
600	682.35	648.11	34.24
630	685.37	651.33	34.04
660	688.19	654.34	33.85
690	690.84	657.18	33.66
720	693.32	659.86	33.46

TABLE 15

Comparison of Standard Error of the Estimate
Cylinder Equations
Incremental Time Step vs Direct Solution
Observed Data Points Prior to Loading

Point 1

Pile	Incremental Time Step Standard Error (Micro in/in)	Direct Solution Standard Error (Micro in/in)	Number of Data Points
1	27.18	29.91	40
2	8.74	11.12	50
3	6.33	7.93	53
4	5.94	6.45	60
5	5.00	7.46	64
6	11.89	9.28	19
7	10.97	12.73	19
8	19.40	23.24	69
9	24.63	29.54	25

TABLE 16

Comparison of Standard Error of the Estimate
Cylinder Equations
Incremental Time Step vs Direct Solution
Observed Data Points Prior to Loading

Point 3

Pile	Incremental Time Step Standard Error (Micro in/in)	Direct Solution Standard Error (Micro in/in)	Number of Data Points
1	20.91	23.89	40
2	4.11	6.06	50
3	4.87	5.02	53
4	8.11	10.84	60
5	7.53	10.37	63
6	11.52	12.44	19
7	14.31	18.74	19
8	18.69	22.49	69
9	25.18	30.12	25

TABLE 17

Comparison
Cylinder Equations
Direct Solution Method vs Incremental Time Step Method
Point 2

Age of Concrete (days)	Direct Solution Method (10^{-6} in/in)	Incremental Time Step Method (10^{-6} in/in)	Difference (10^{-6} in/in)
30	487.64	442.84	44.80
60	573.48	514.48	59.00
90	627.99	559.90	68.09
120	666.70	591.98	74.72
150	696.10	616.19	79.91
180	719.46	635.31	84.15
210	738.65	650.93	87.72
240	754.82	664.00	90.82
270	768.70	675.16	93.54
300	780.81	684.85	95.96
330	791.52	693.38	98.14
360	801.08	700.95	100.13
390	809.70	707.75	101.95
420	817.54	713.91	103.63
450	824.70	719.51	105.19
480	831.29	724.65	106.64
510	837.38	729.38	108.00
540	843.04	733.76	109.28
570	848.32	737.83	110.49
600	853.26	741.63	111.63
630	857.90	745.19	112.71
660	862.27	748.53	113.74
690	866.40	751.68	114.72
720	870.31	754.65	115.66

TABLE 18

Comparison of Standard Error of the Estimate
Cylinder Equations
Incremental Time Step vs Direct Solution
Observed Data Points Prior to Loading

Point 2

Pile	Incremental Time Step Standard Error (Micro in/in)	Direct Solution Standard Error (Micro in/in)	Number of Data Points
1	9.81	12.48	40
2	5.30	7.90	50
3	16.59	11.47	53
4	14.48	9.20	60
5	6.27	4.65	64
6	16.20	23.44	19
7	22.65	17.65	19
8	10.81	5.72	69
9	16.50	16.74	25

TABLE 19

Exponential Equation Curve Fitting Parameters

$$t = Ae^{Be_{cp,t}}$$

Pile	Points 1 & 3		Point 2	
	Parameters		Parameters	
	A	B	A	B
1	1.03222	0.06457	0.79607	0.04080
2	132.75381	-0.27795	614.70264	-0.15630
3 & 4	0.02209	0.24448	0.02474	0.13309
5 & 9	0.50249	0.03558	0.46239	0.02111
6 & 7	0.26815	0.04374	0.38060	0.02250

TABLE 20

Power Equation Curve Fitting Parameters

$$e_{cp,t} = At^{B}$$

Pile	Points 1 & 3		Point 2	
	Parameters		Parameters	
	A	B	A	B
1	****	****	14.13398	0.44550
2	****	****	****	****
3 & 4	****	****	10.32157	0.36480
5 & 9	12.20617	0.51519	19.12013	0.53457
6 & 7	13.34700	0.45948	19.40129	0.50941

**** curve was not fitted to the available data therefore no parameters were determined.

TABLE 21

Hyperbolic Equation Curve Fitting Parameters

$$e_{cp,t} = \frac{t}{A + Bt}$$

Pile	Points 1 & 3		Point 2	
	Parameters		Parameters	
	A	B	A	B
1	0.44982	0.00865	0.26263	0.00532
2	-0.23273	0.01088	-5.62219	0.04375
3 & 4	0.62115	0.01338	0.60217	0.01536
5 & 9	0.16513	0.00470	0.08681	0.00286
6 & 7	0.32331	0.00486	0.14033	0.00262

TABLE 22

Comparison of the Correlation Coefficient

Points 1 and 3

Pile	Exponential Equation	Power Equation	Hyperbolic Equation
1	0.73	*****	0.56
2	-0.23	*****	0.09
3 & 4	0.35	*****	0.08
5 & 9	0.90	0.81	0.96
6 & 7	0.80	0.75	0.91

TABLE 23

Comparison of the Correlation Coefficient

Point 2

Pile	Exponential Equation	Power Equation	Hyperbolic Equation
1	0.87	0.79	0.95
2	-0.45	*****	0.27
3 & 4	0.57	0.64	0.65
5 & 9	0.88	0.79	0.95
6 & 7	0.93	0.76	0.97

***** Curve was not fitted to the available data therefore no correlation coefficient was determined.

TABLE 24

Comparison of Standard Error of the Estimate
Curve Fitted Equations
Observed Data Points Prior to Loading

Point 1

Pile	Exponental	Power	Hyperbolic	Number of Data Points
	Standard Error (Micro in/in)			
1	29.15	25.64	25.82	40
2	10.16	7.57	7.83	50
3	6.98	6.16	6.51	53
4	5.76	6.48	6.62	60
5	5.76	4.32	5.12	64
6	9.62	13.91	13.88	19
7	11.31	11.23	12.12	19
8	18.35	19.18	18.69	69
9	26.55	22.54	24.10	25

TABLE 25

Comparison of Standard Error of the Estimate
Curve Fitted Equations
Observed Data Points Prior to Loading

Point 3

Pile	Exponental	Power	Hyperbolic	Number of Data Points
	Standard Error (Micro in/in)			
1	22.82	19.40	19.48	39
2	5.05	3.83	4.20	50
3	4.72	5.61	5.43	53
4	9.12	7.12	8.03	60
5	8.60	6.36	7.33	63
6	11.31	12.18	12.85	19
7	16.73	12.46	13.61	19
8	17.78	18.38	18.08	69
9	27.09	23.08	24.70	25

TABLE 26

Comparison of Standard Error of the Estimate
Curve Fitted Equations
Observed Data Points Prior to Loading

Point 2

Pile	Exponental	Power	Hyperbolic	Number of Data Points
		Standard Error (Micro in/in)		
1	17.03	10.43	10.14	40
2	11.74	5.88	6.50	50
3	9.22	14.12	13.00	53
4	6.21	9.01	11.15	60
5	7.22	4.45	3.95	64
6	29.78	18.80	20.77	19
7	13.95	20.85	21.71	19
8	7.11	4.97	8.15	69
9	17.20	16.43	18.08	25

APPENDIX B

ILLUSTRATIONS

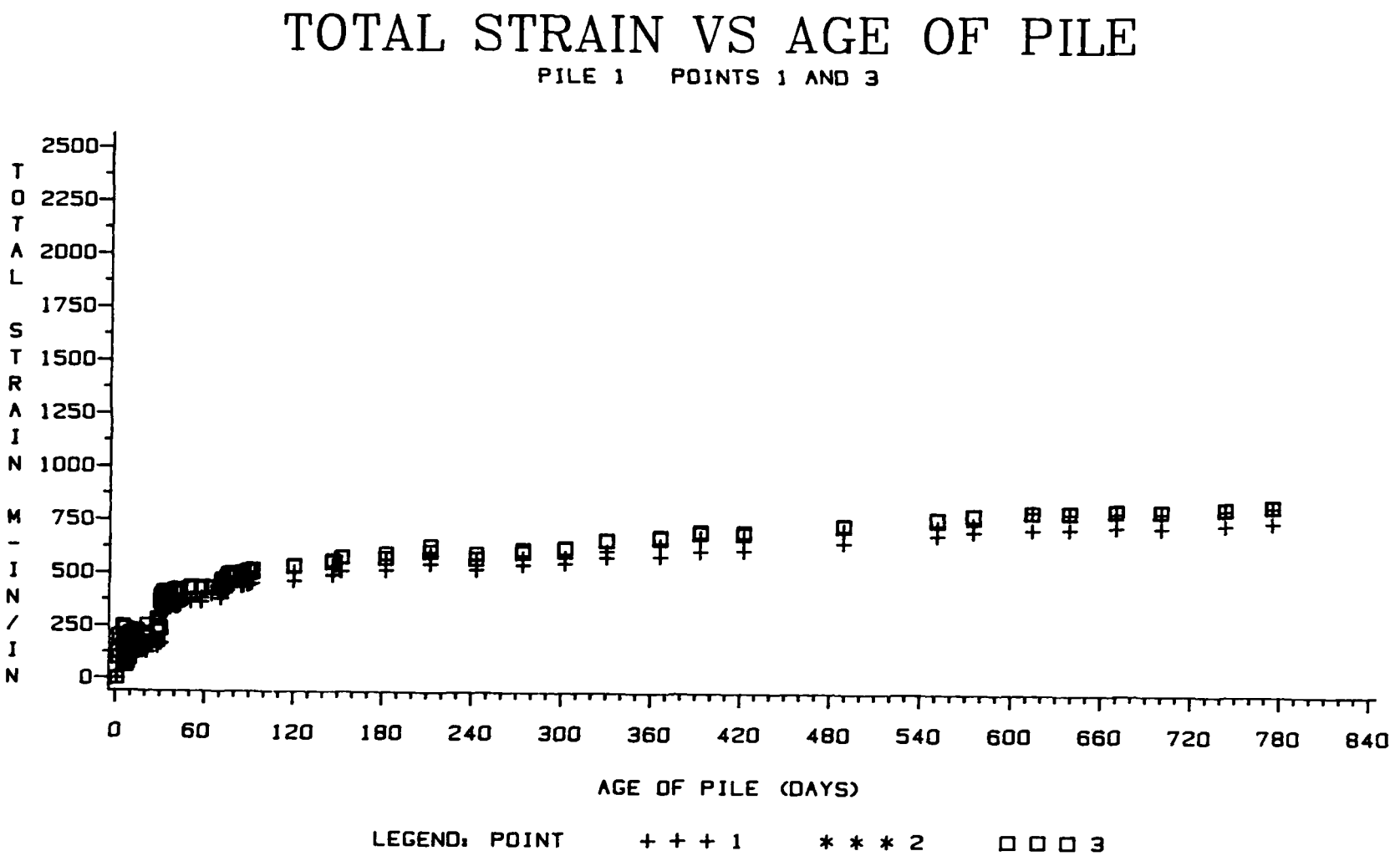

Figure 1 Total Strain versus Age of Pile Pile 1 Points 1 and 3

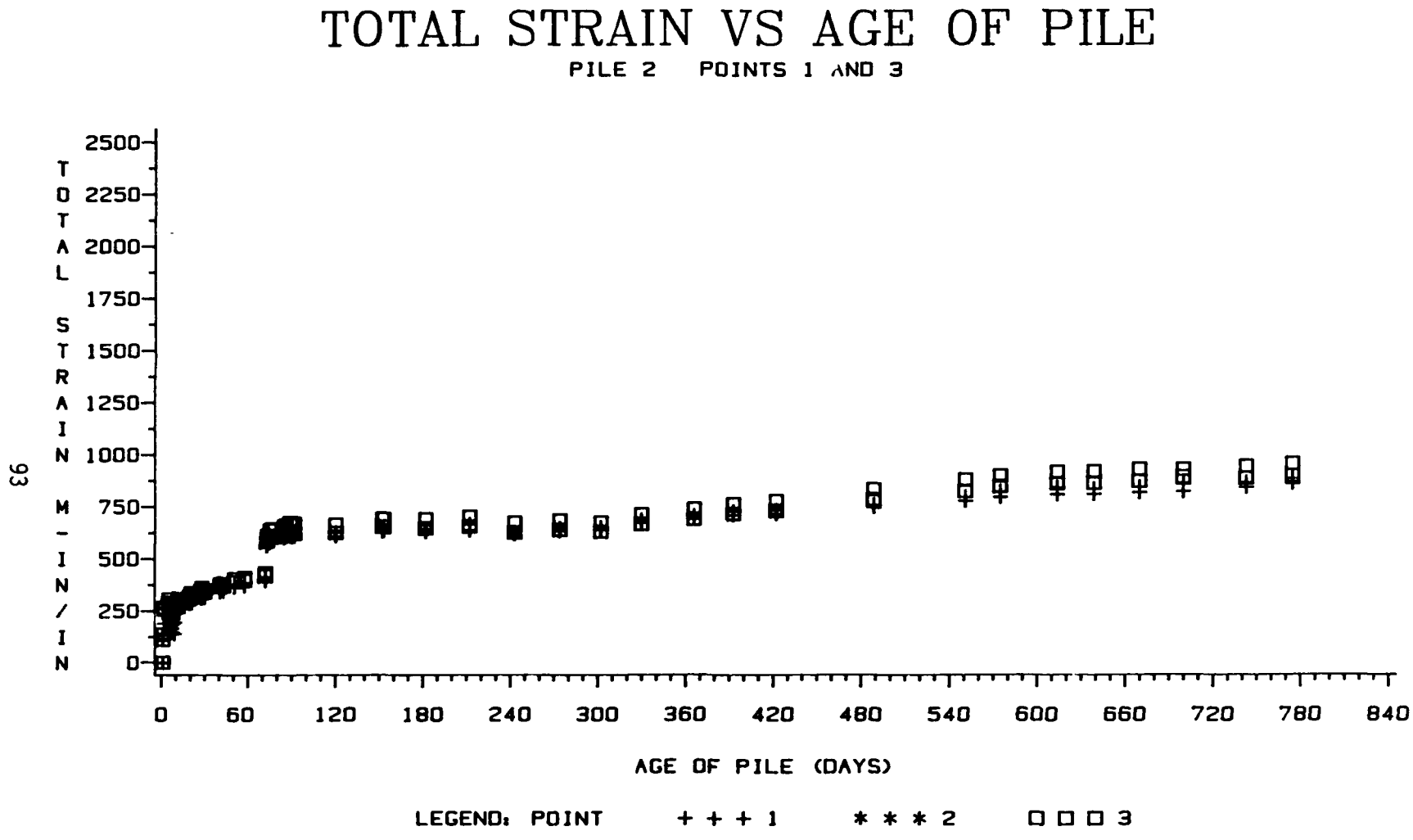

Figure 2 Total Strain versus Age of Pile Pile 2 Points 1 and 3

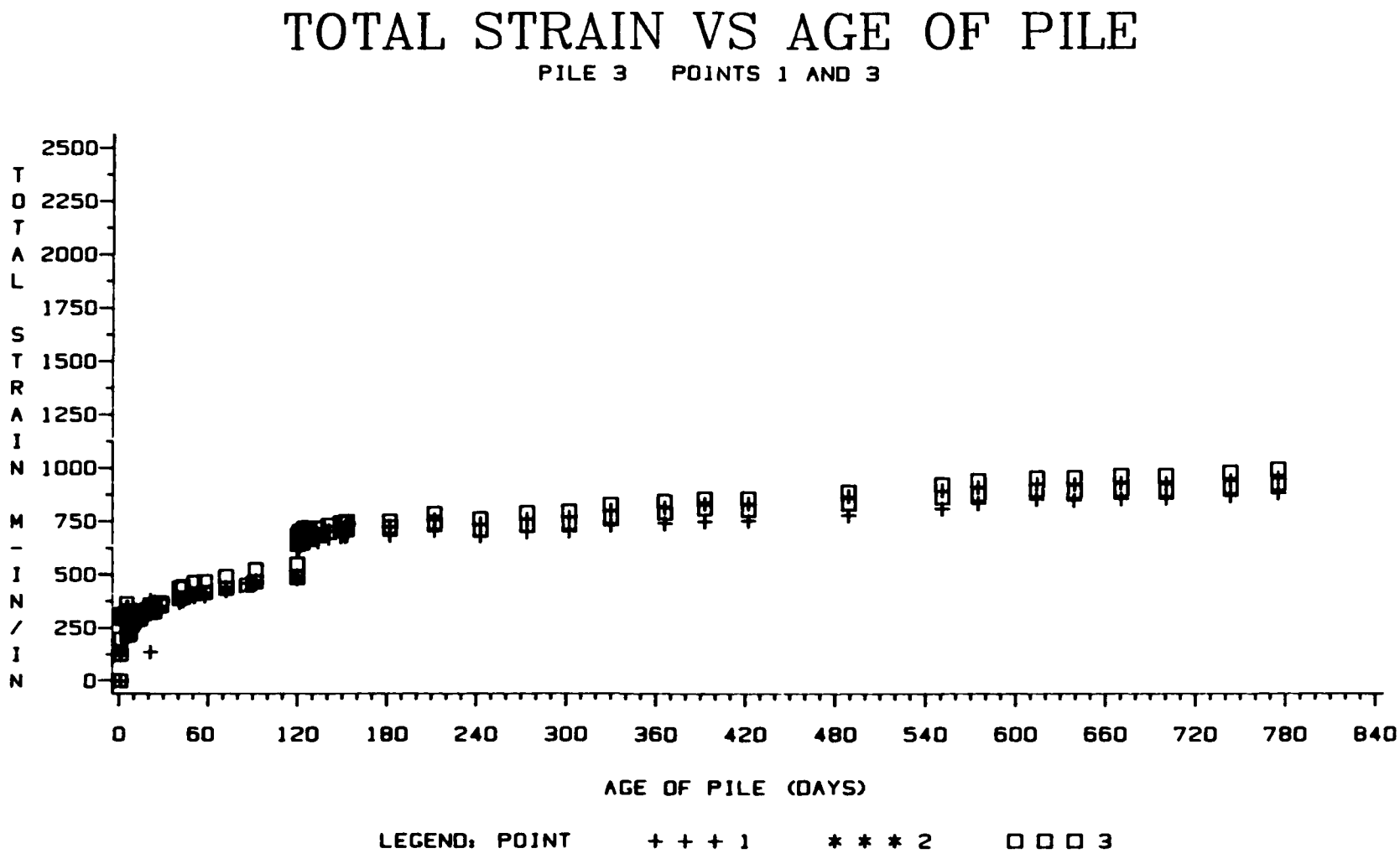

Figure 3 Total Strain versus Age of Pile Pile 3 Points 1 and 3

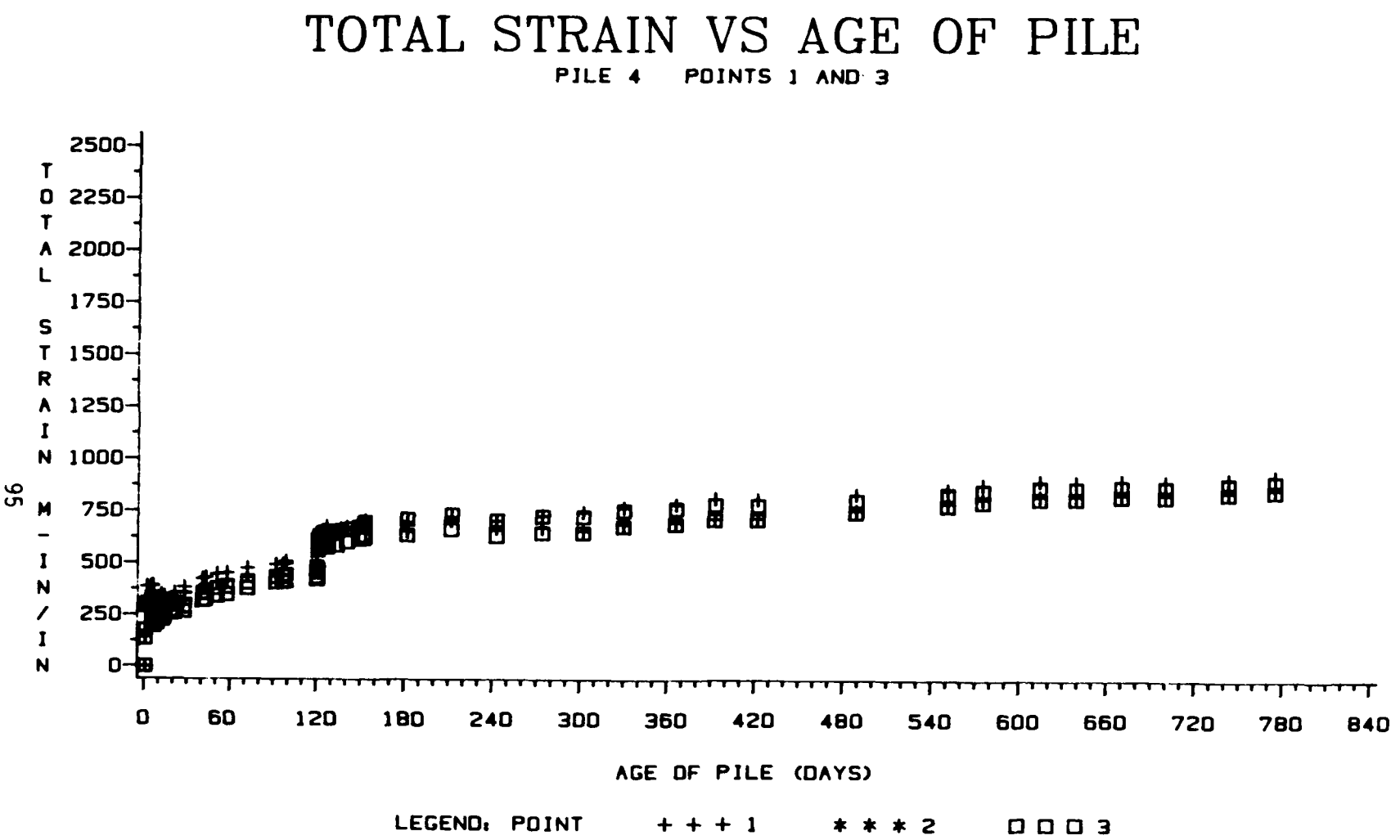

Figure 4 Total Strain versus Age of Pile Pile 4 Points 1 and 3

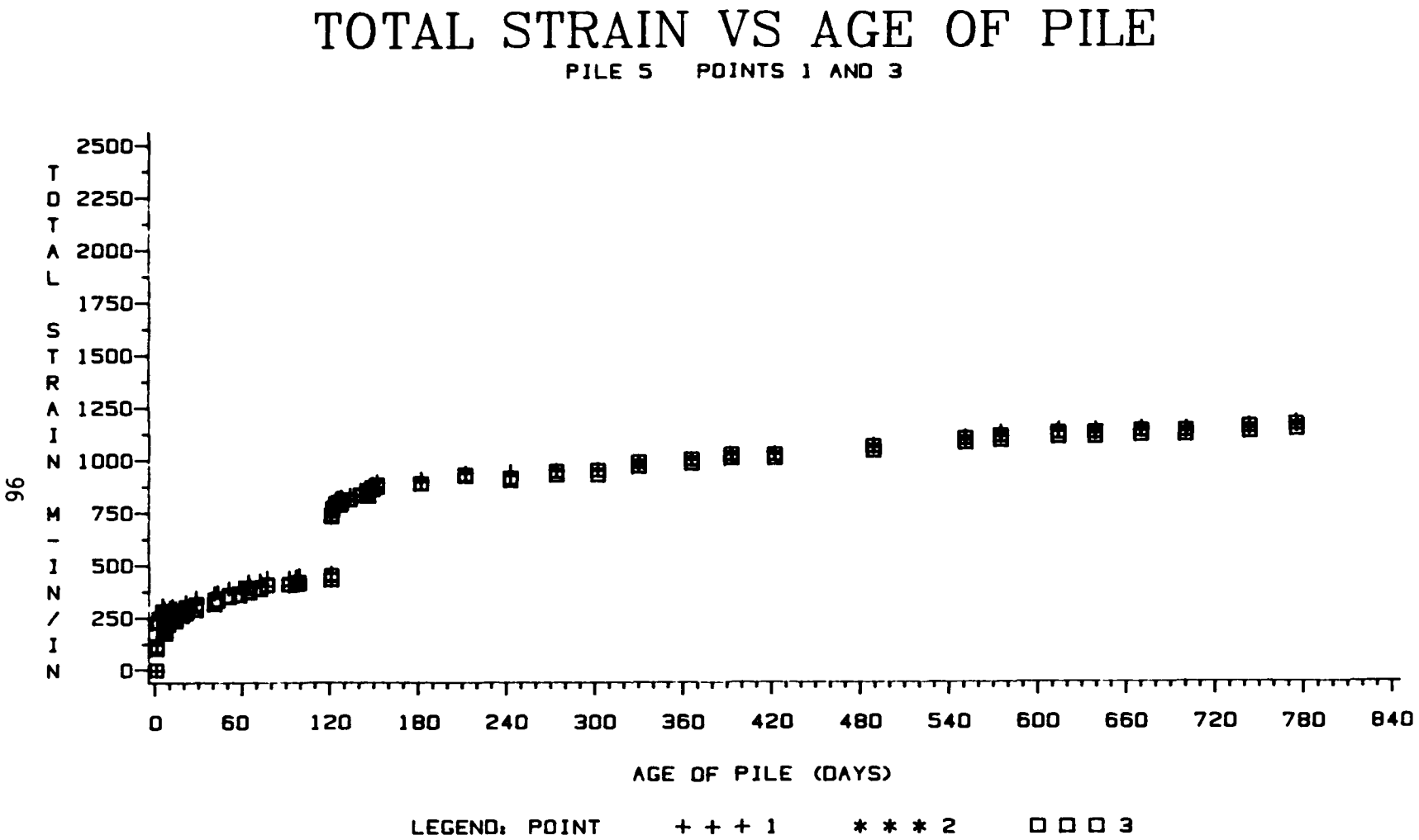

Figure 5 Total Strain versus Age of Pile Pile 5 Points 1 and 3

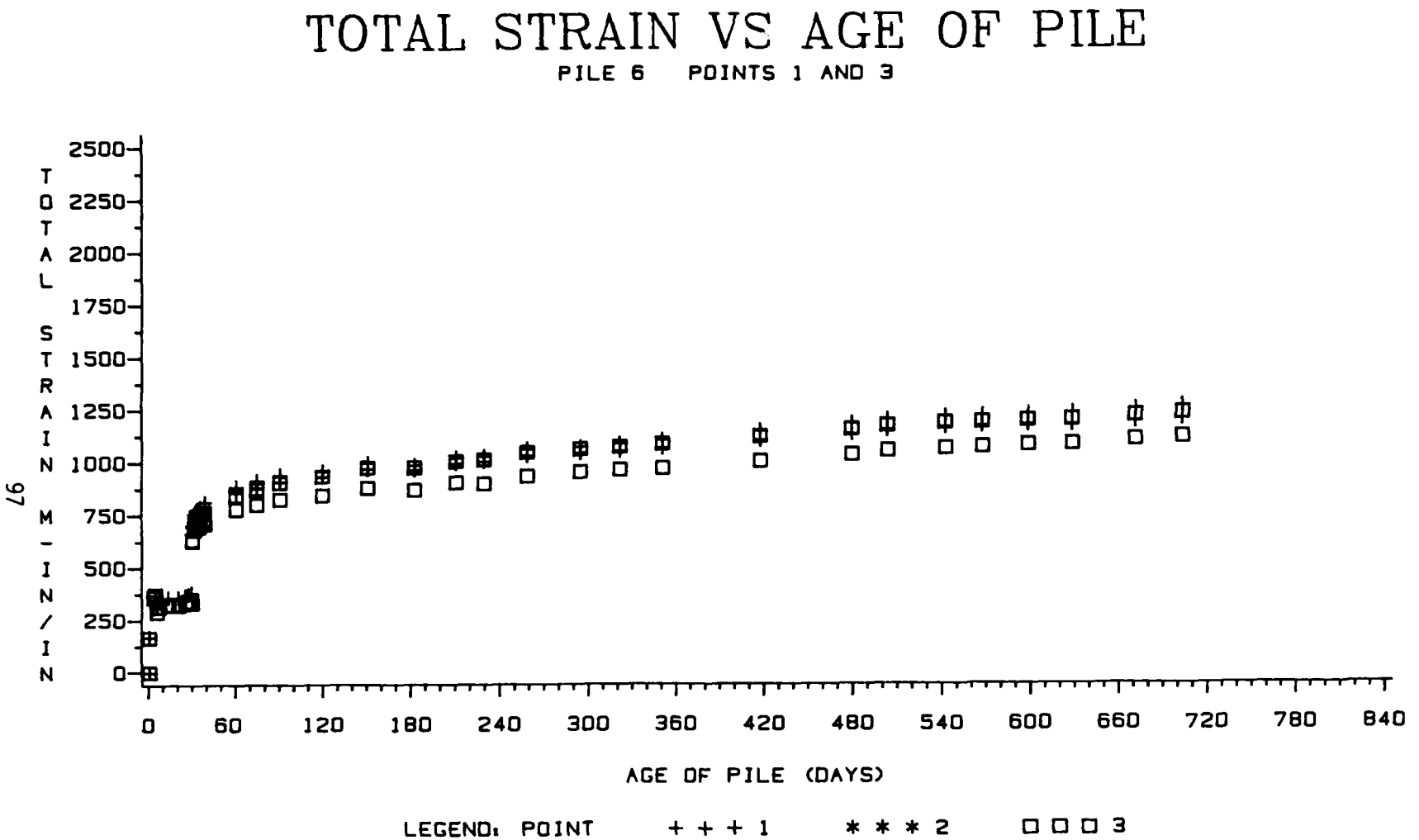

Figure 6 Total Strain versus Age of Pile Pile 6 Points 1 and 3

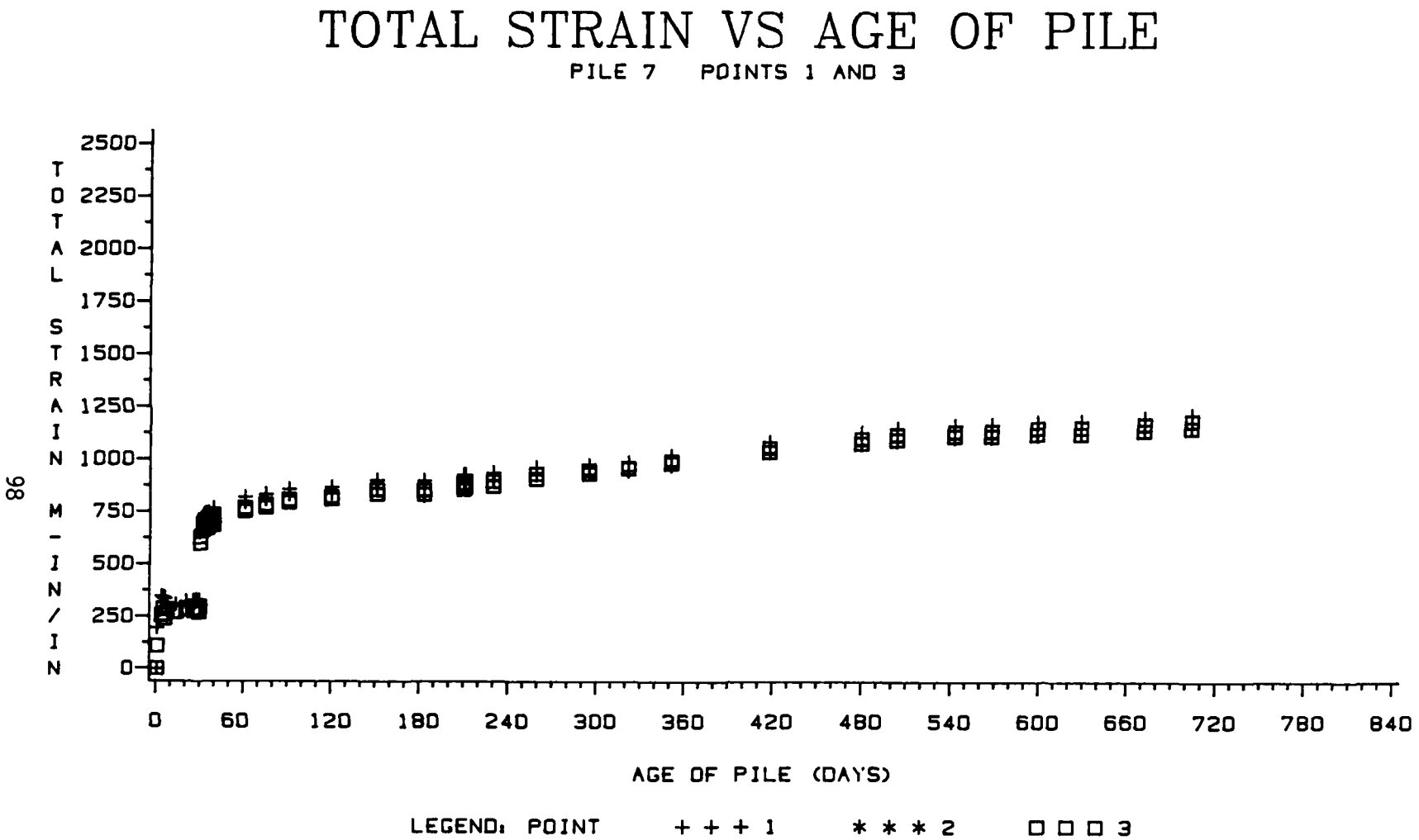

Figure 7 Total Strain versus Age of Pile Pile 7 Points 1 and 3

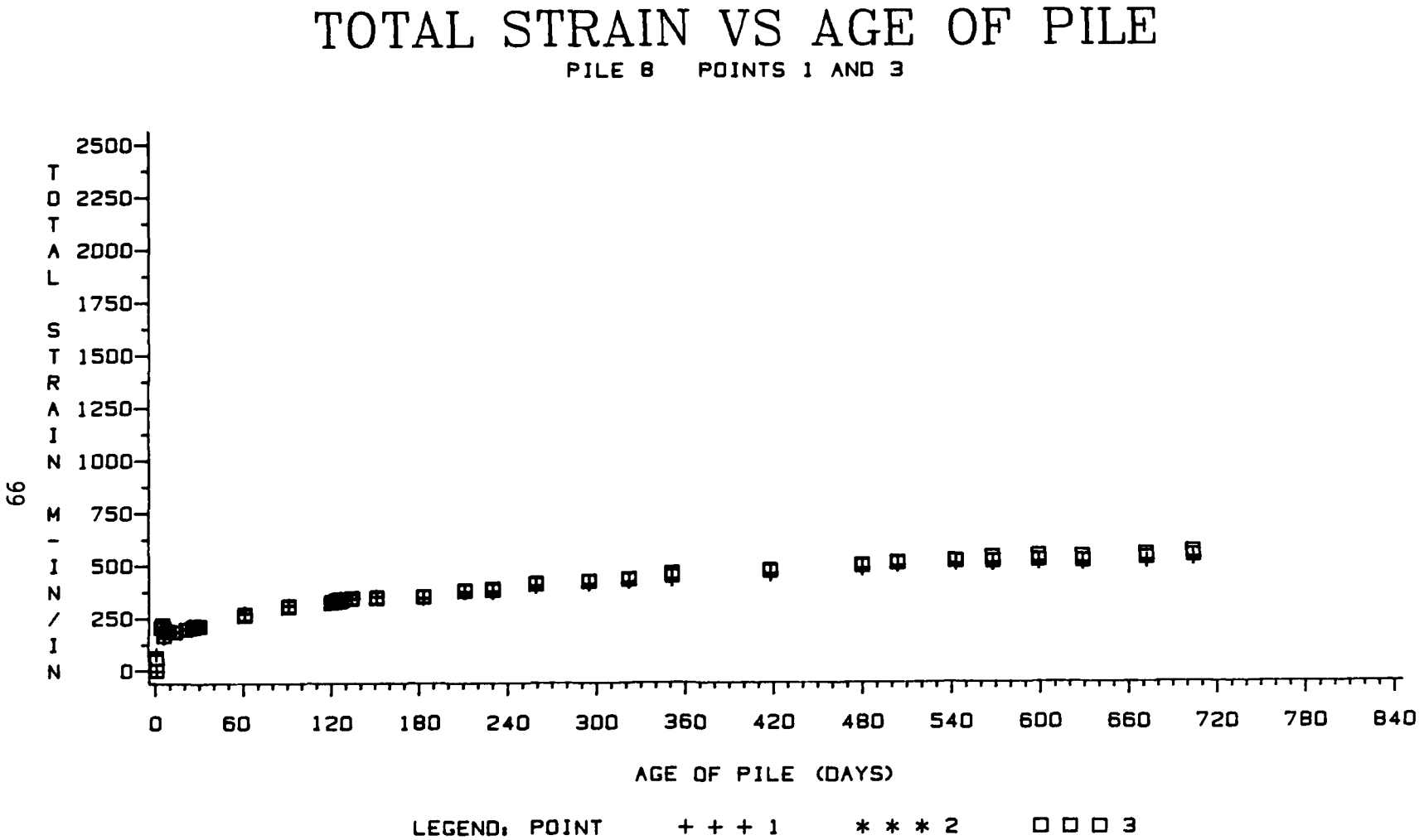

Figure 8 Total Strain versus Age of Pile Pile 8 Points 1 and 3

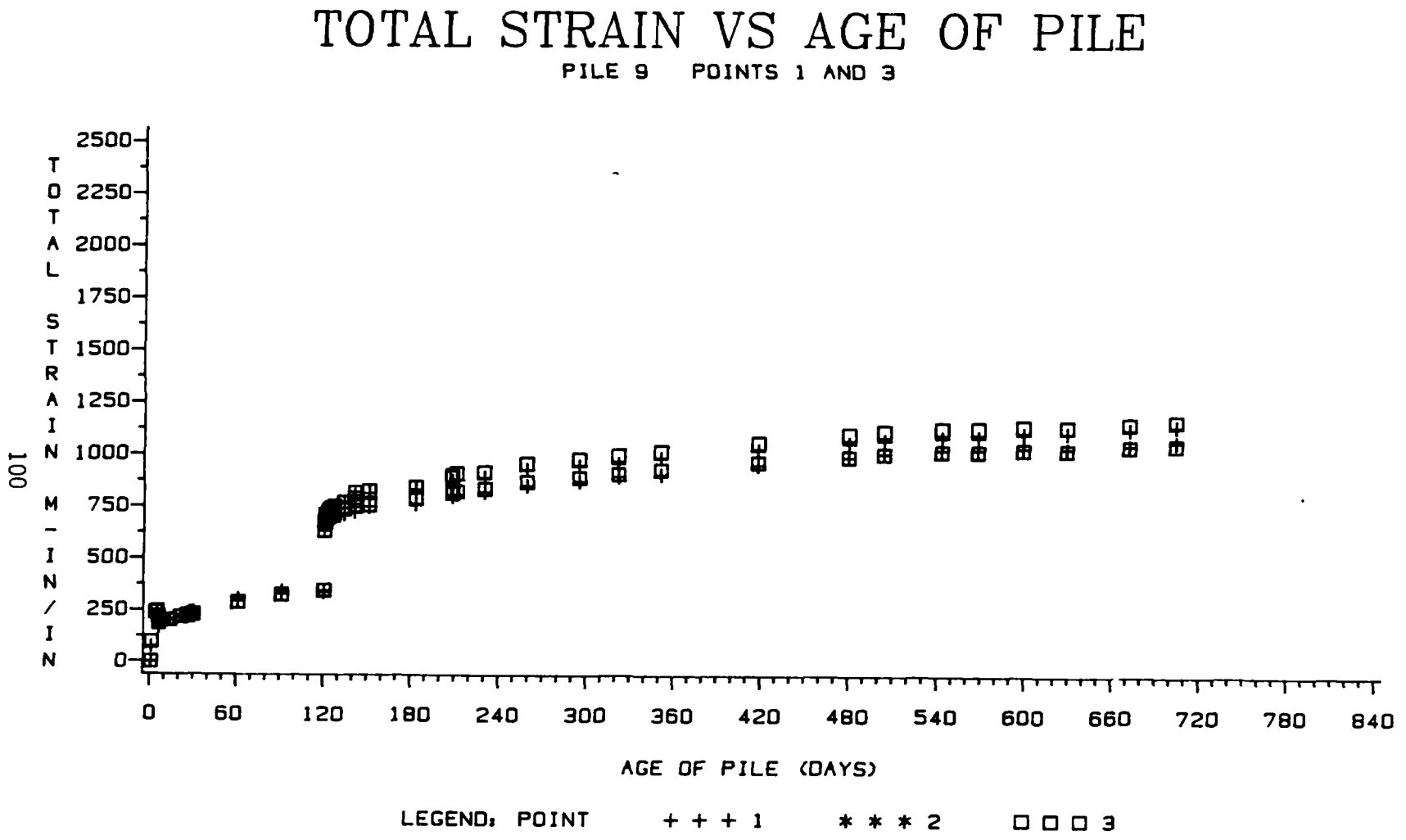

Figure 9 Total Strain versus Age of Pile Pile 9 Points 1 and 3

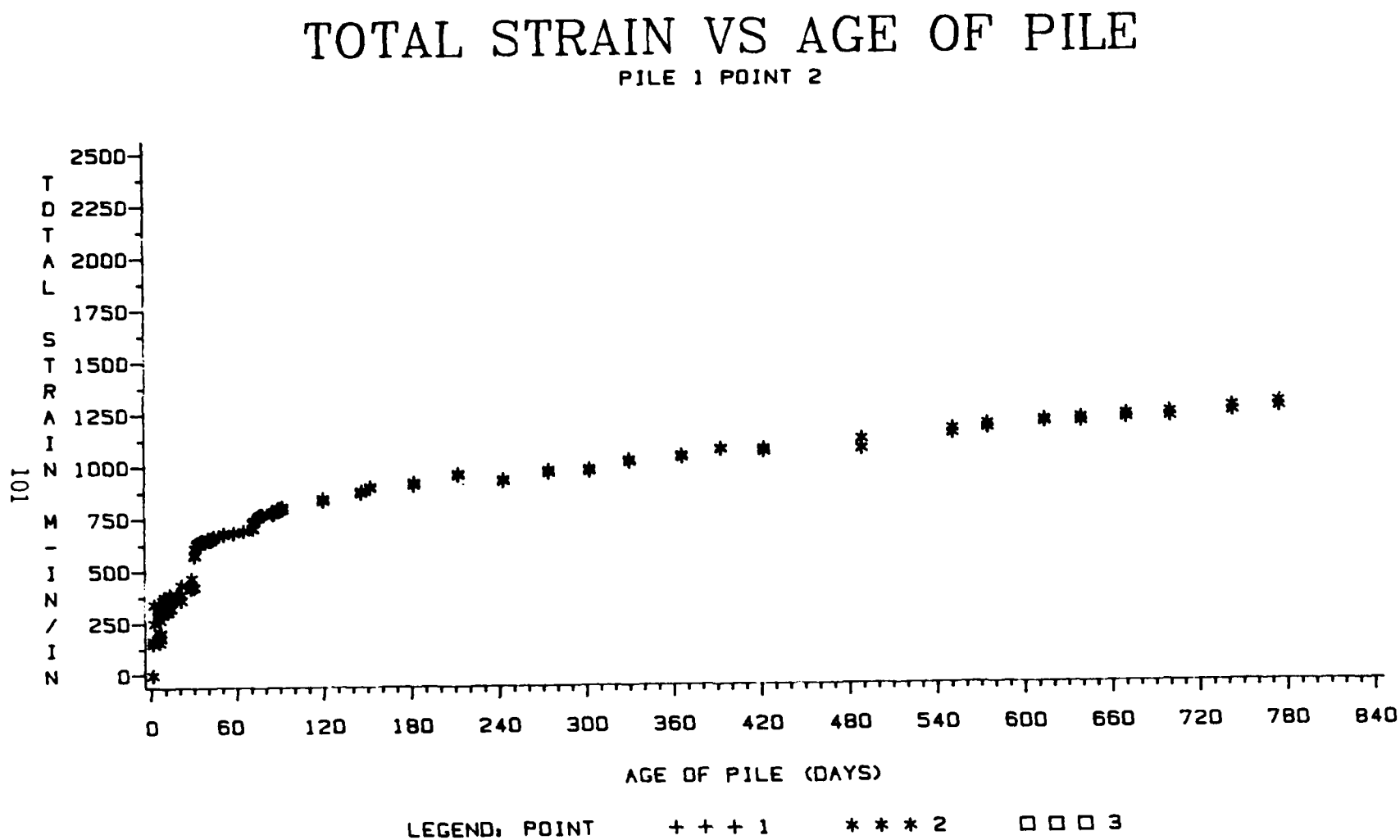

Figure 10 Total Strain versus Age of Pile Pile 1 Point 2

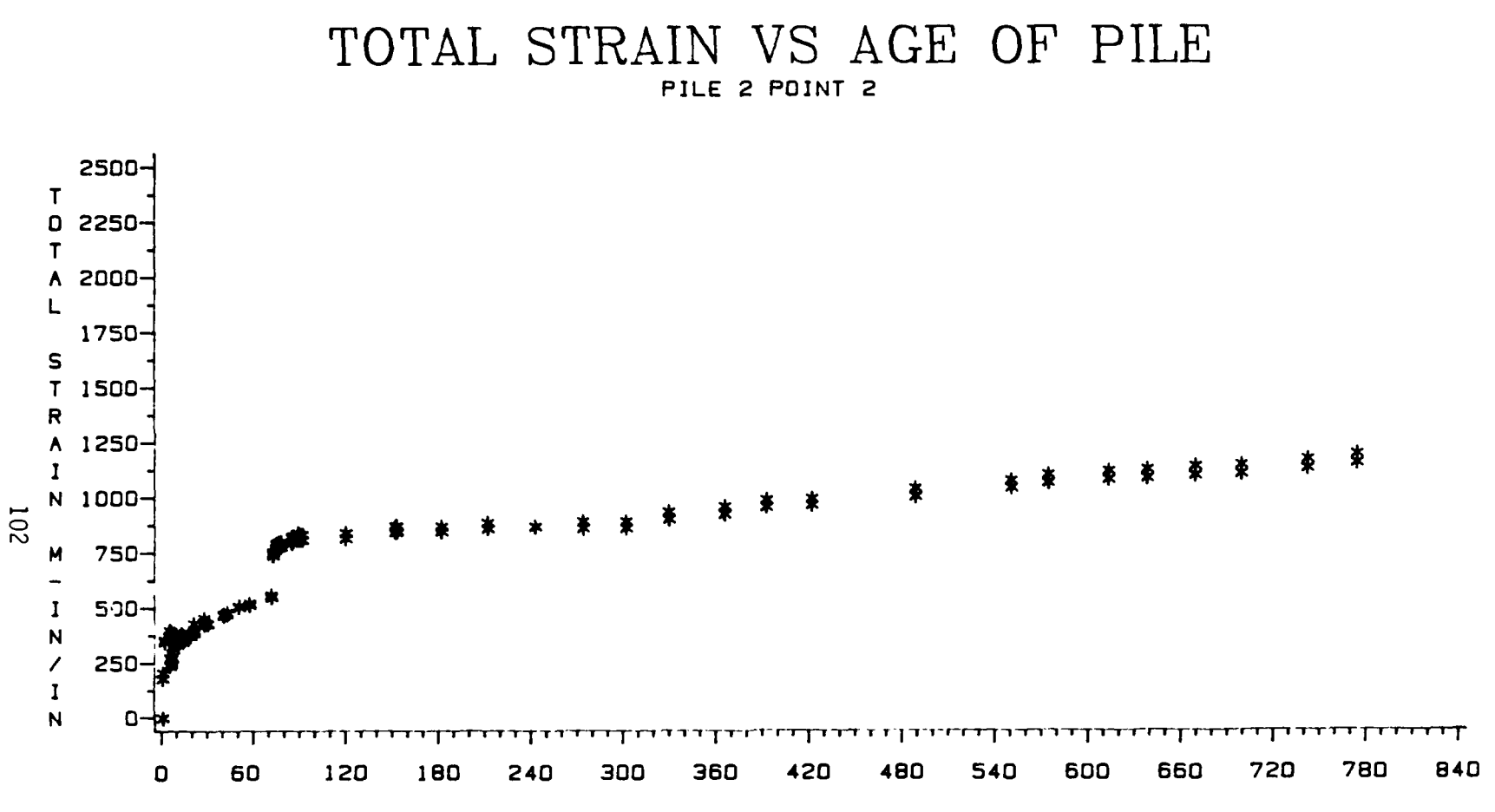

Figure 11 Total Strain versus Age of Pile Pile 2 Point 2

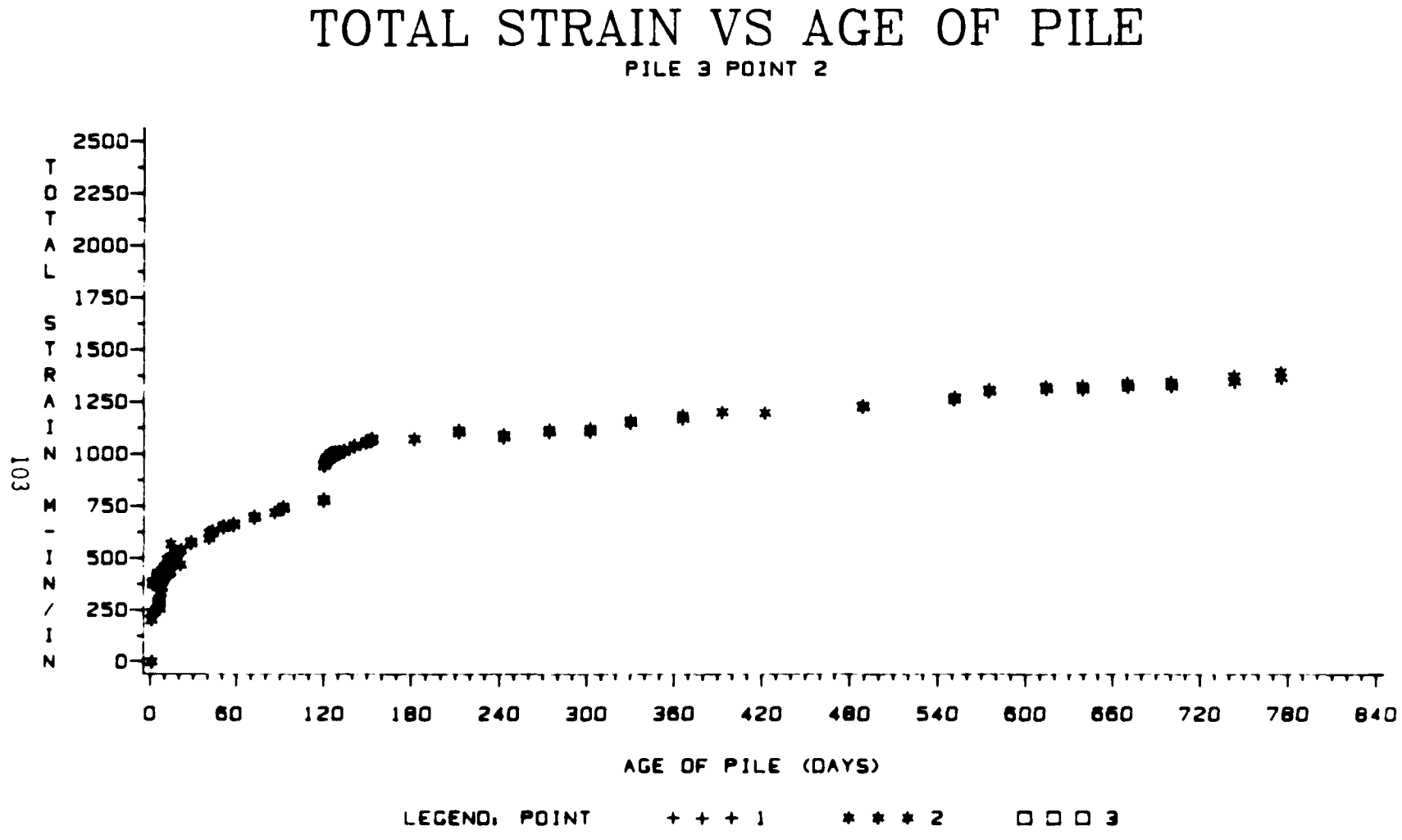

Figure 12 Total Strain versus Age of Pile Pile 3 Point 2

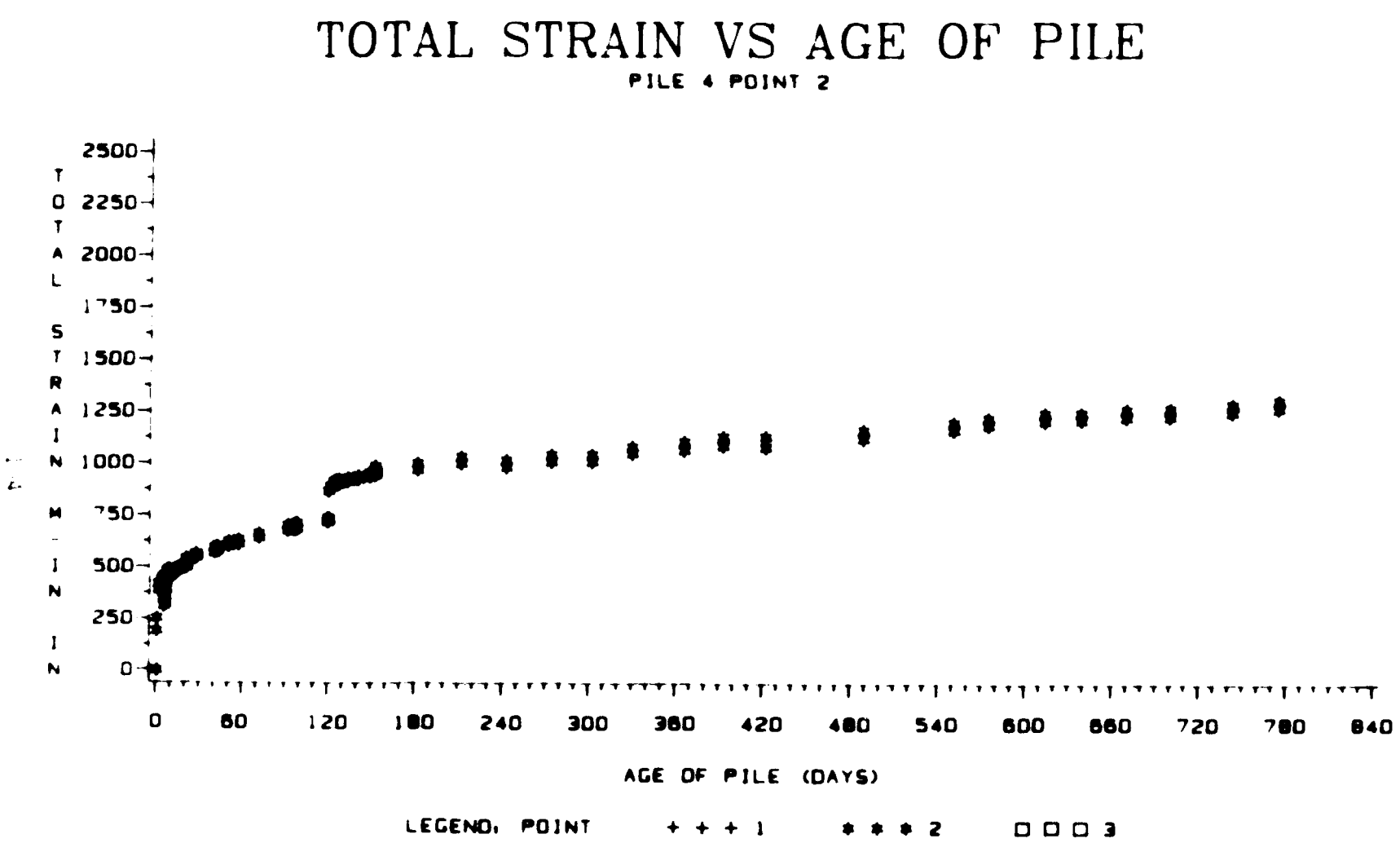

Figure 15. Total Strain versus Age of Pile, Pile 4 Point 2

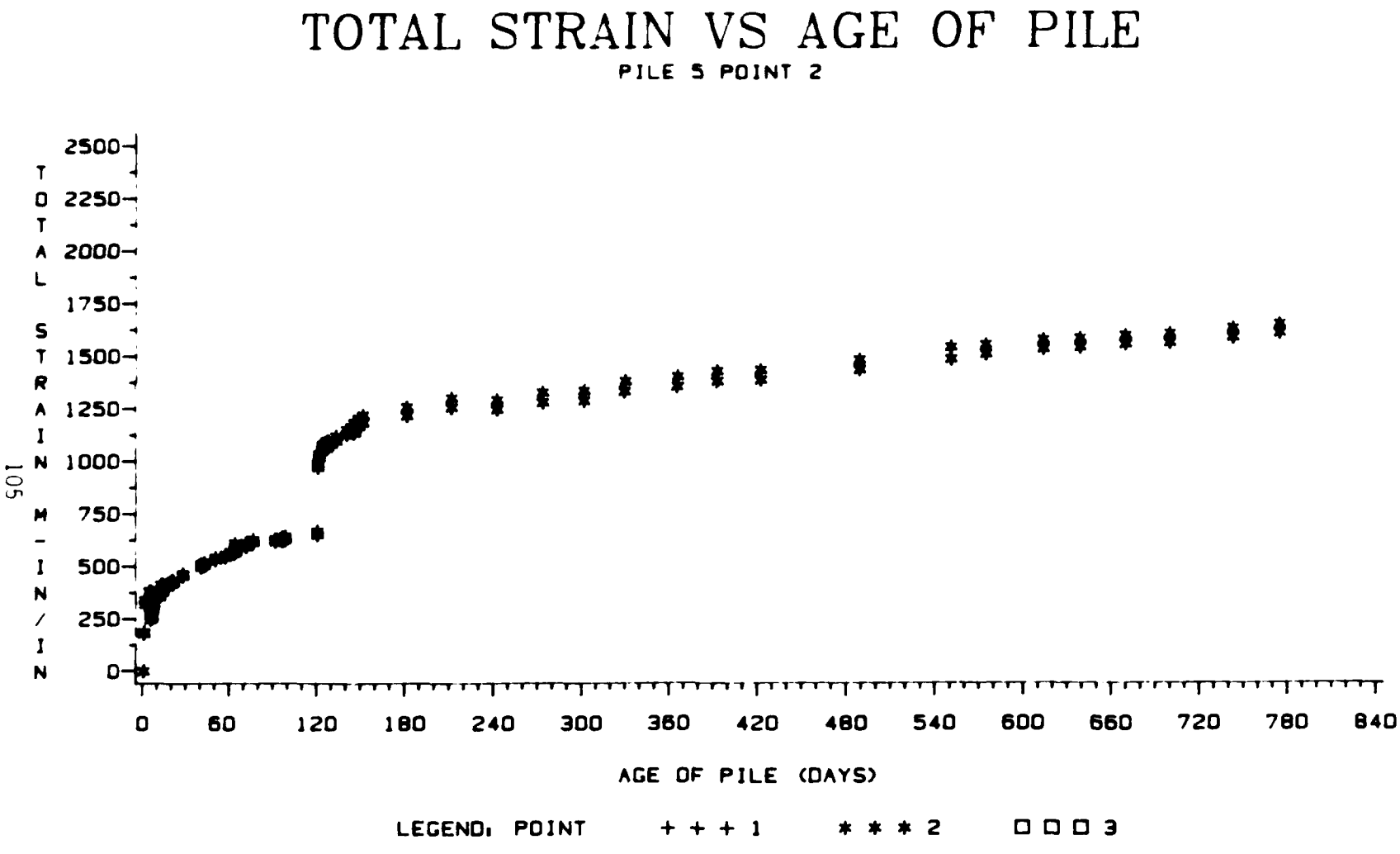

Figure 14 Total Strain versus Age of Pile Pile 5 Point 2

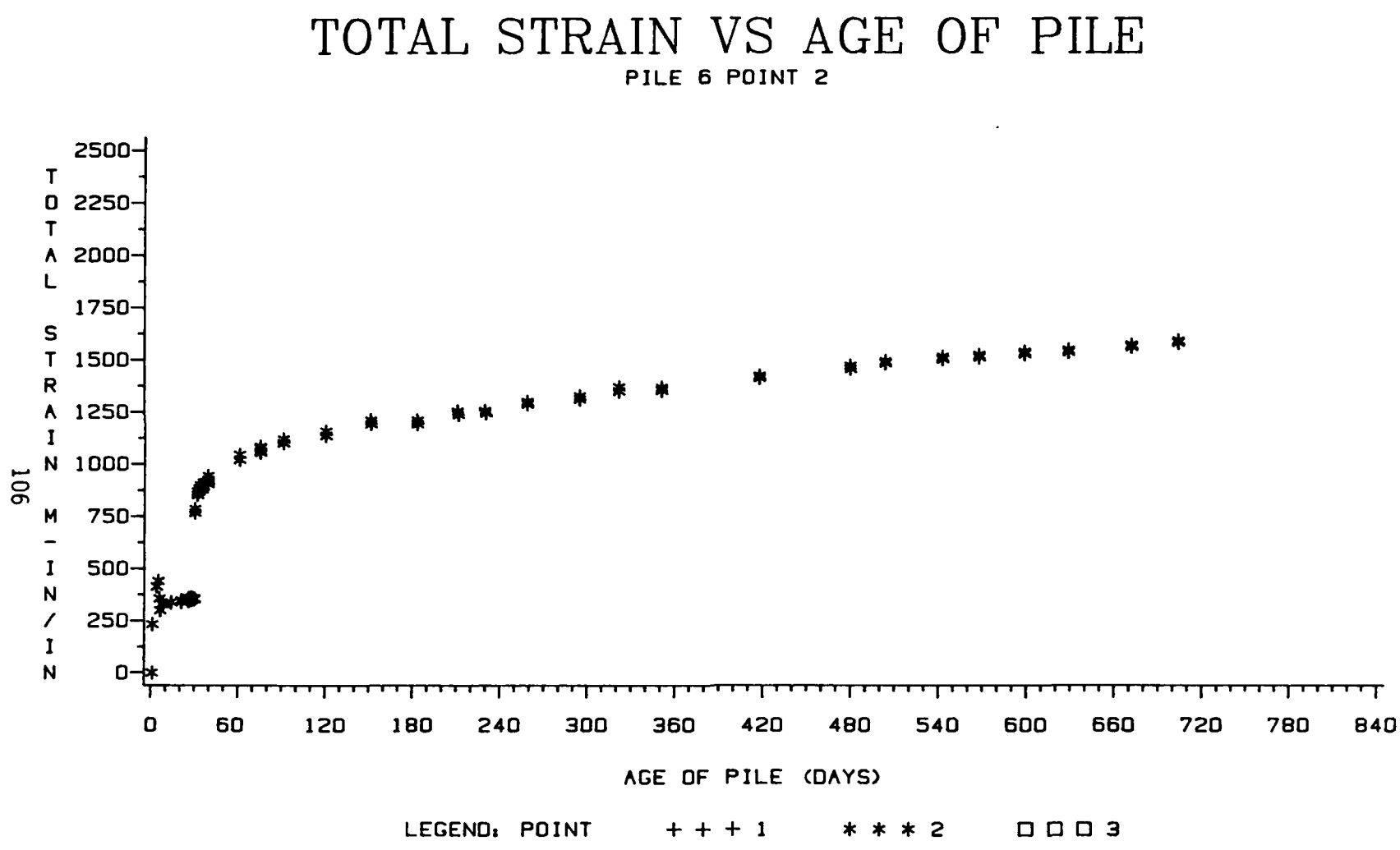

Figure 15 Total Strain versus Age of Pile Pile 6 Point 2

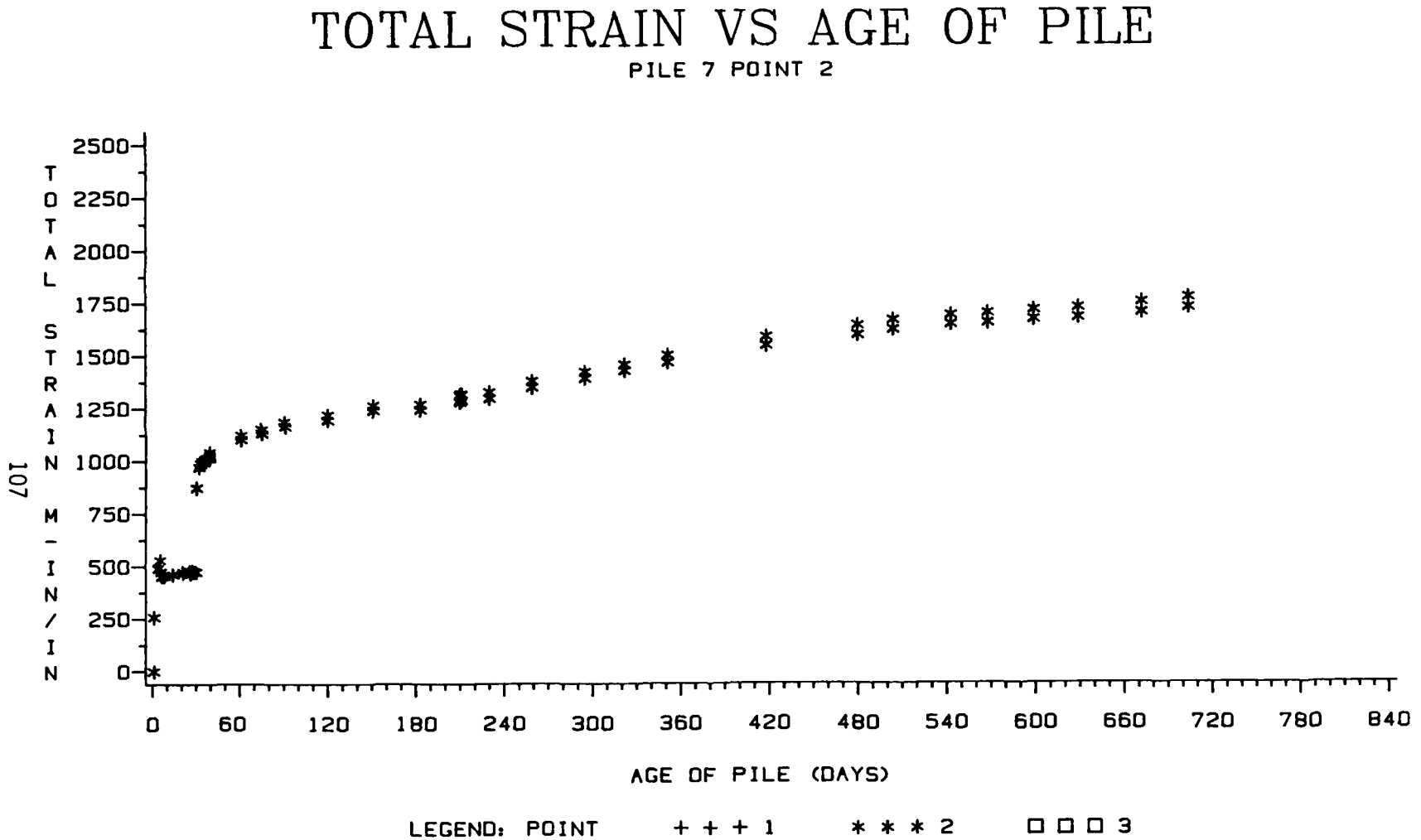

Figure 16 Total Strain versus Age of Pile Pile 7 Point 2

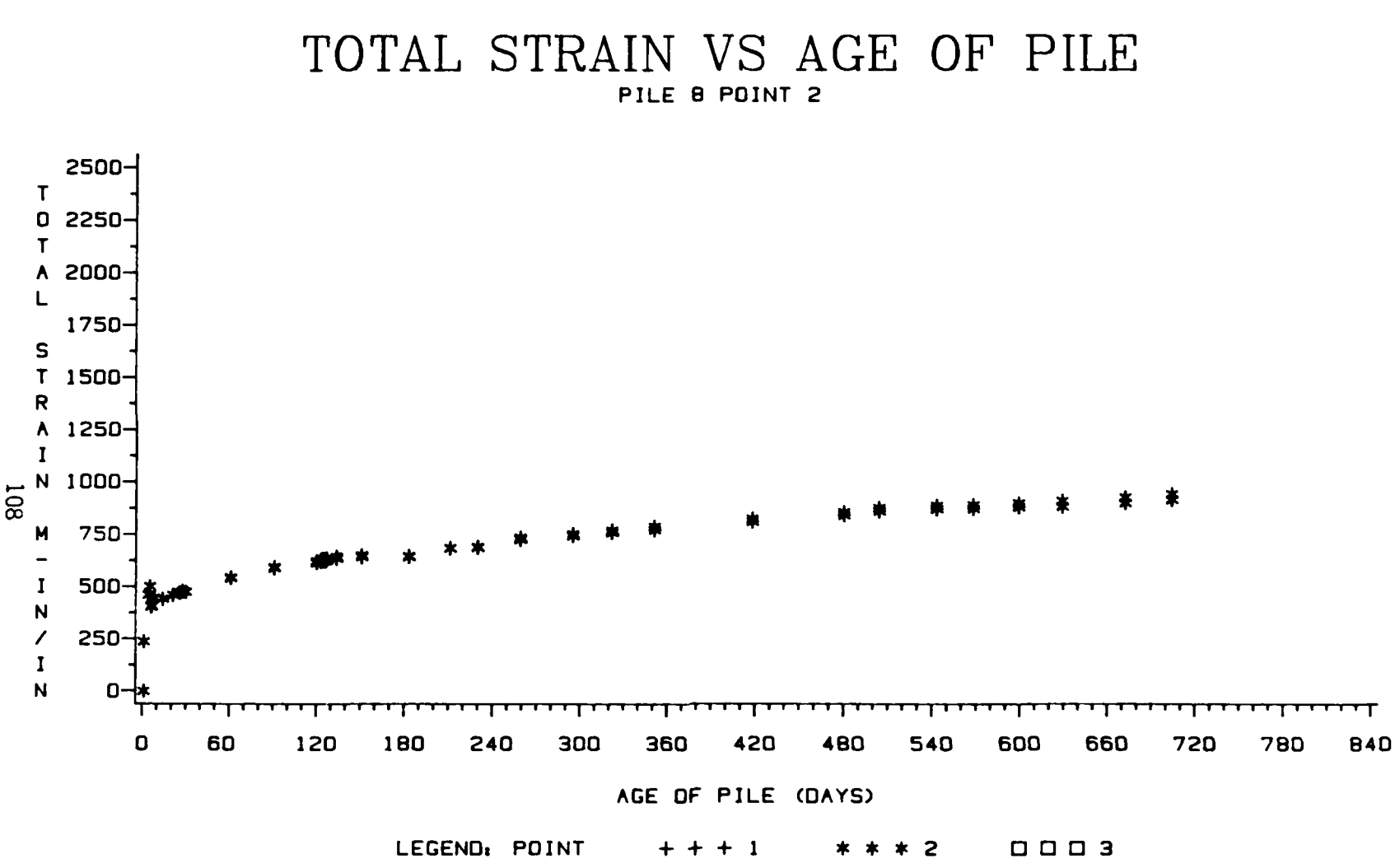

Figure 17 Total Strain versus Age of Pile Pile 8 Point 2

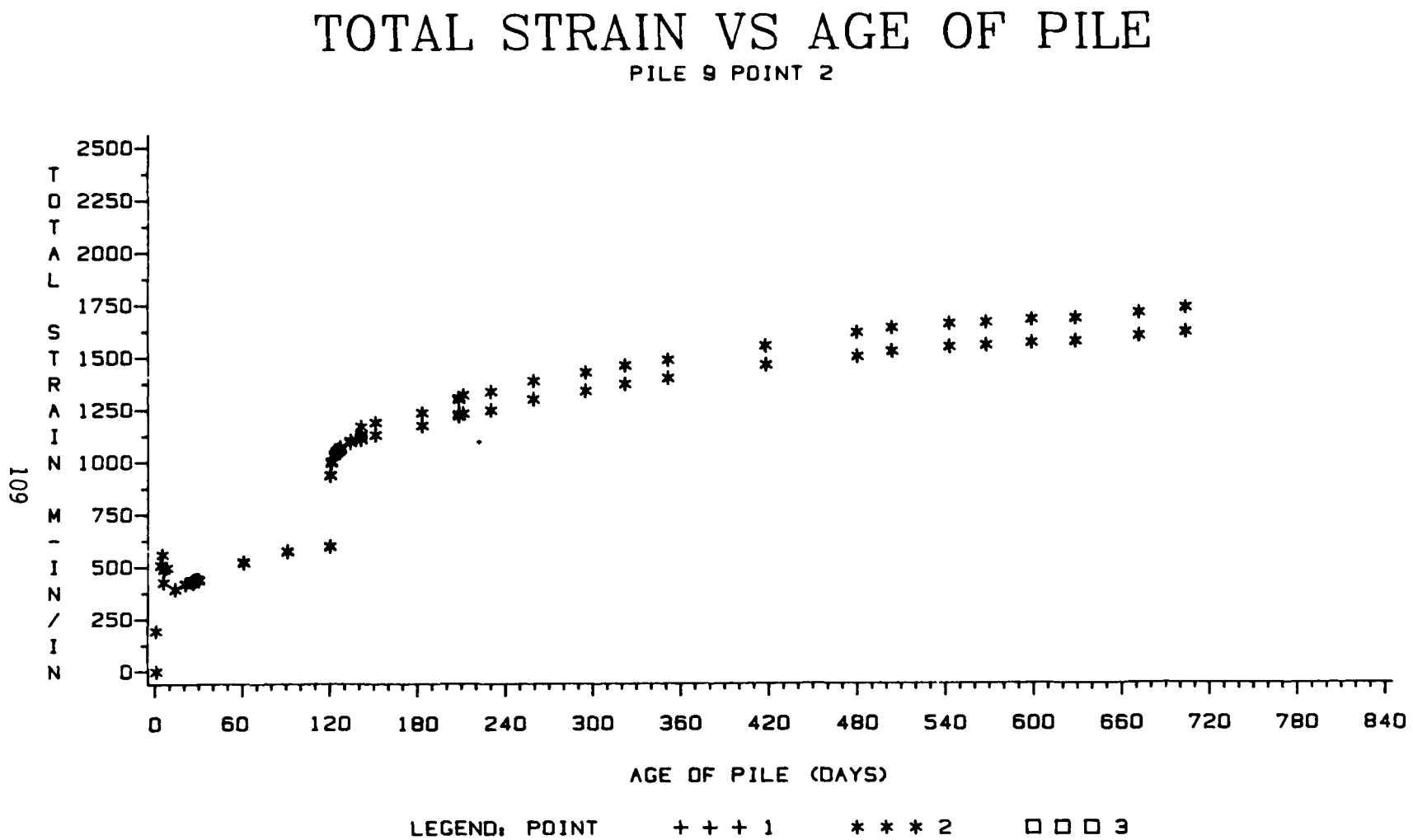

Figure 18 Total Strain versus Age of Pile Pile 9 Point 2

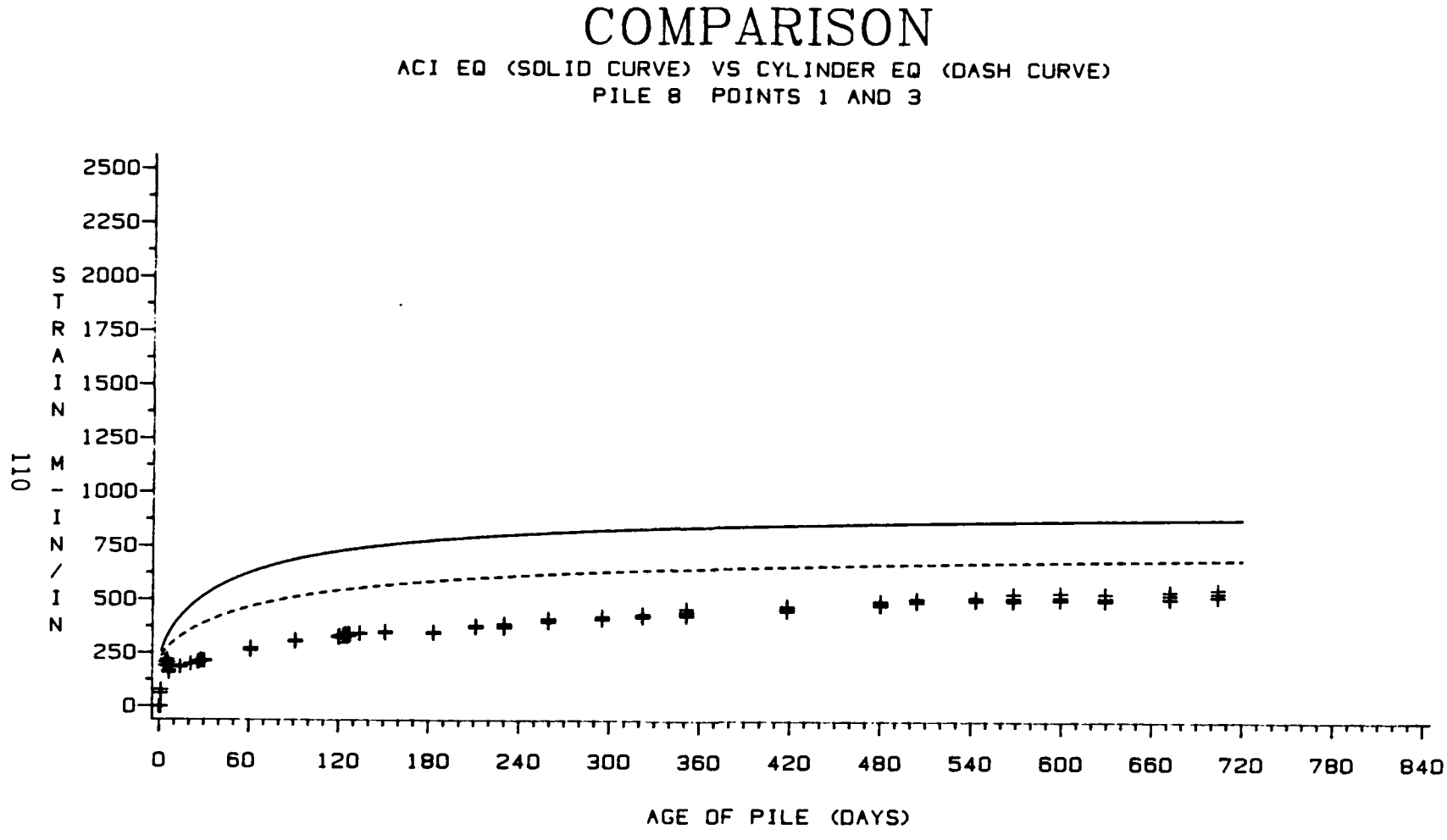

Figure 19 Comparison of Total Strain, Direct Solution Method Using the ACI Equations and Cylinder Equations Against Pile 8 Points 1 and 3 Observed Data

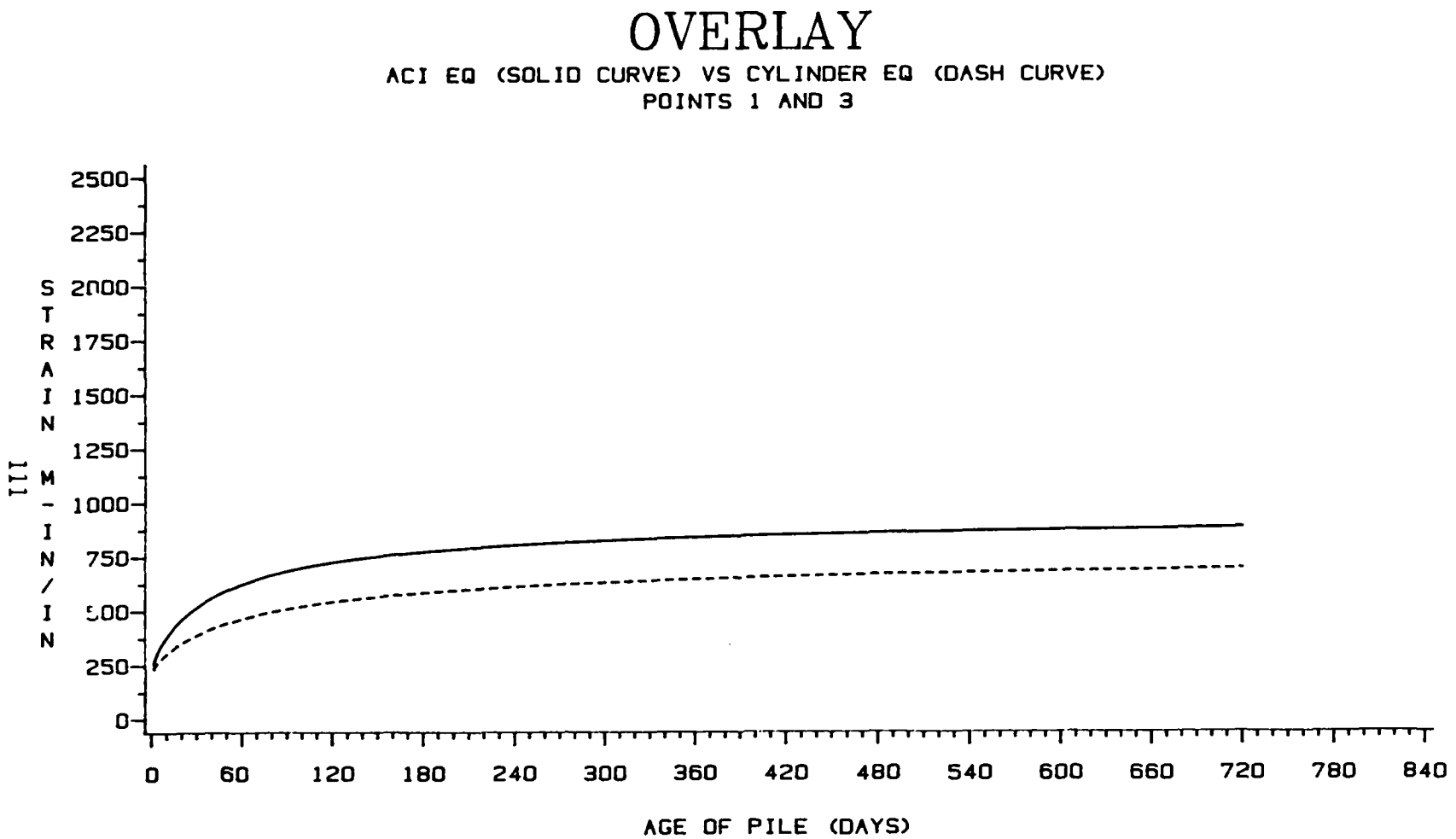

Figure 20 Overlay of Total Strains, Direct Solution Method Using the ACI Equations and Cylinder Equations for Points 1 and 3

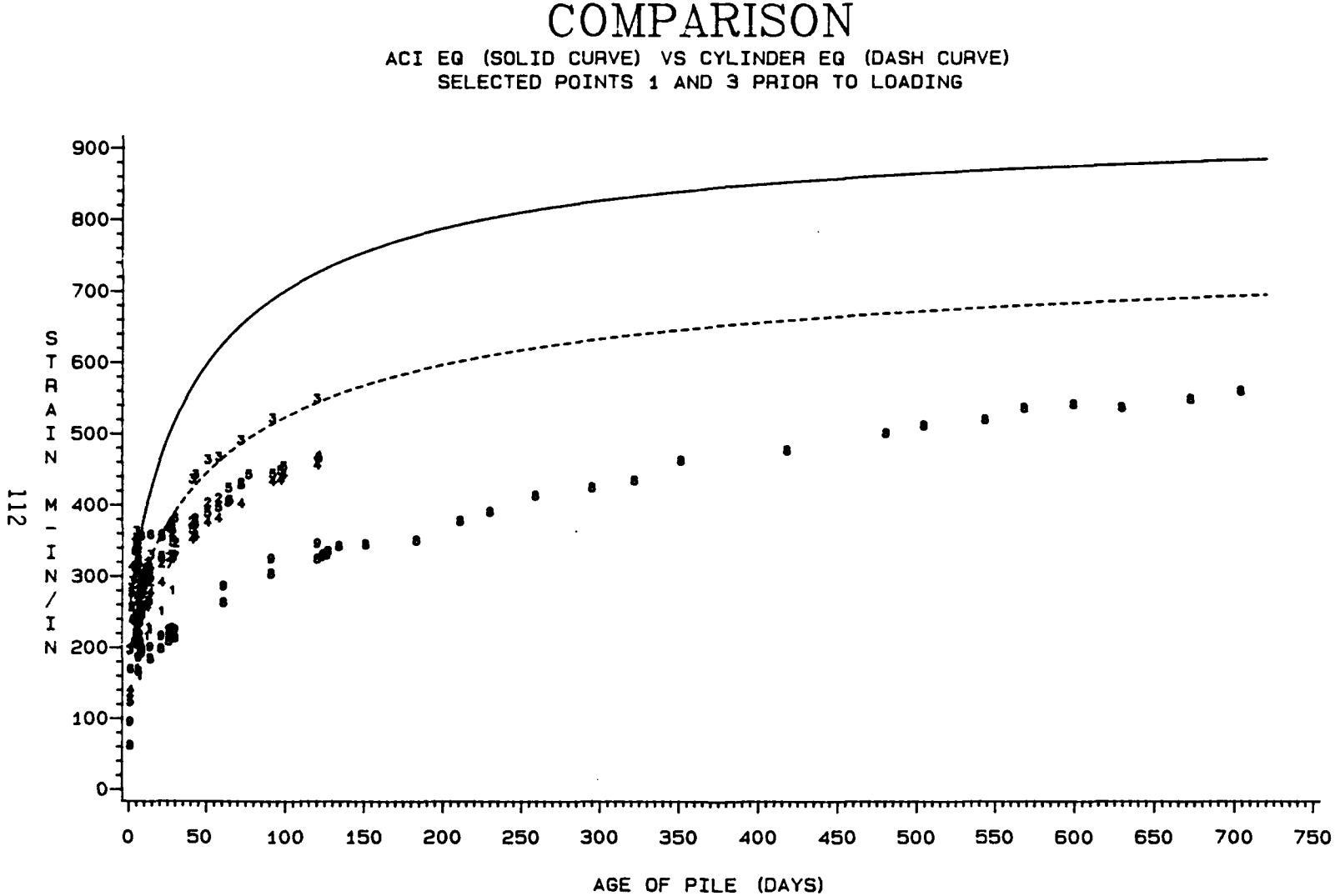

Figure 21 Comparison of Total Strains of Points 1 and 3 Prior to Loading, All Piles, Direct Solution Method Using ACI Equations and Cylinder Equations

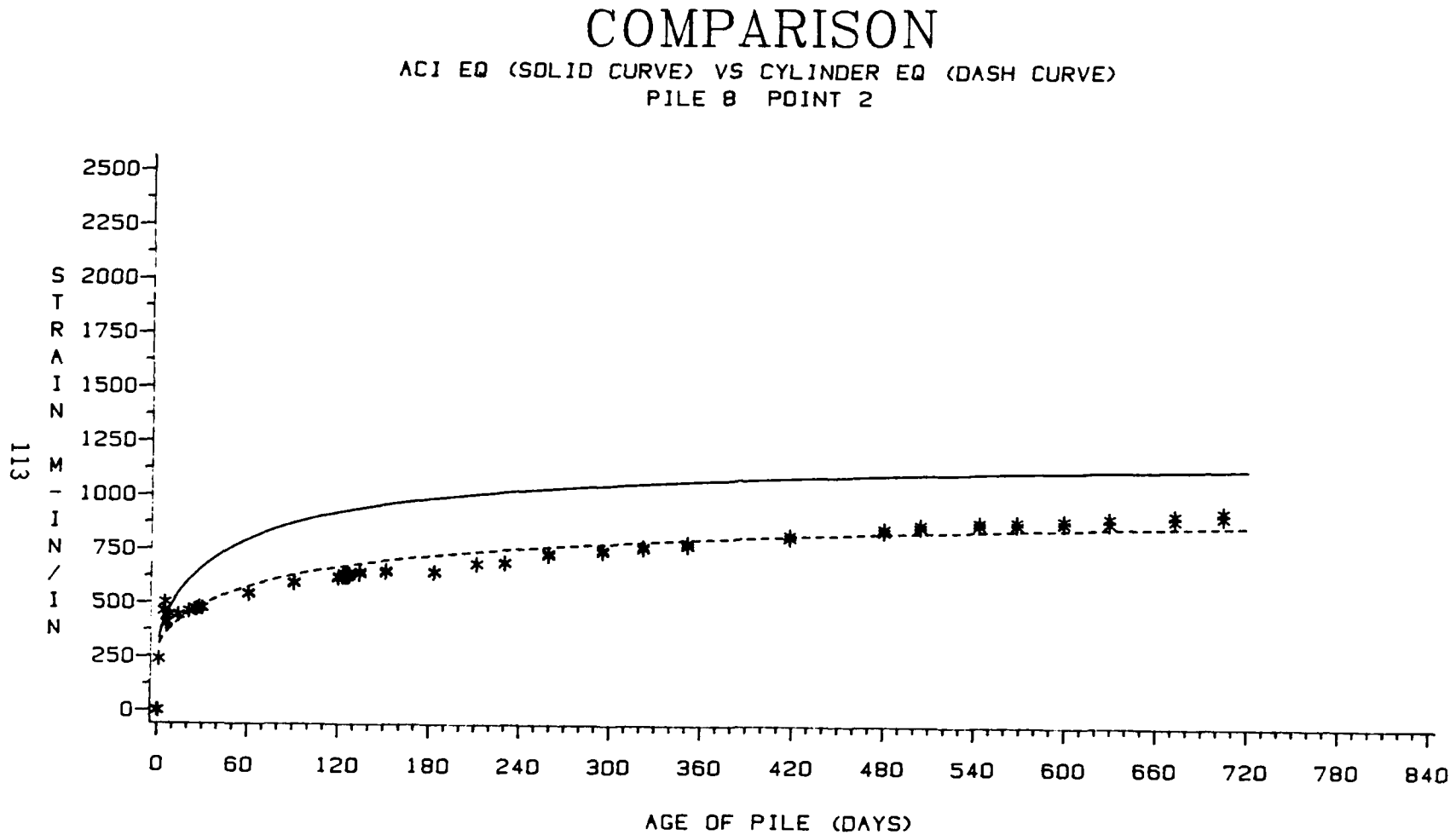

Figure 22 Comparison of Total Strain, Direct Solution Method Using the ACI Equations and Cylinder Equations Against Pile 8 Point 2 Observed Data

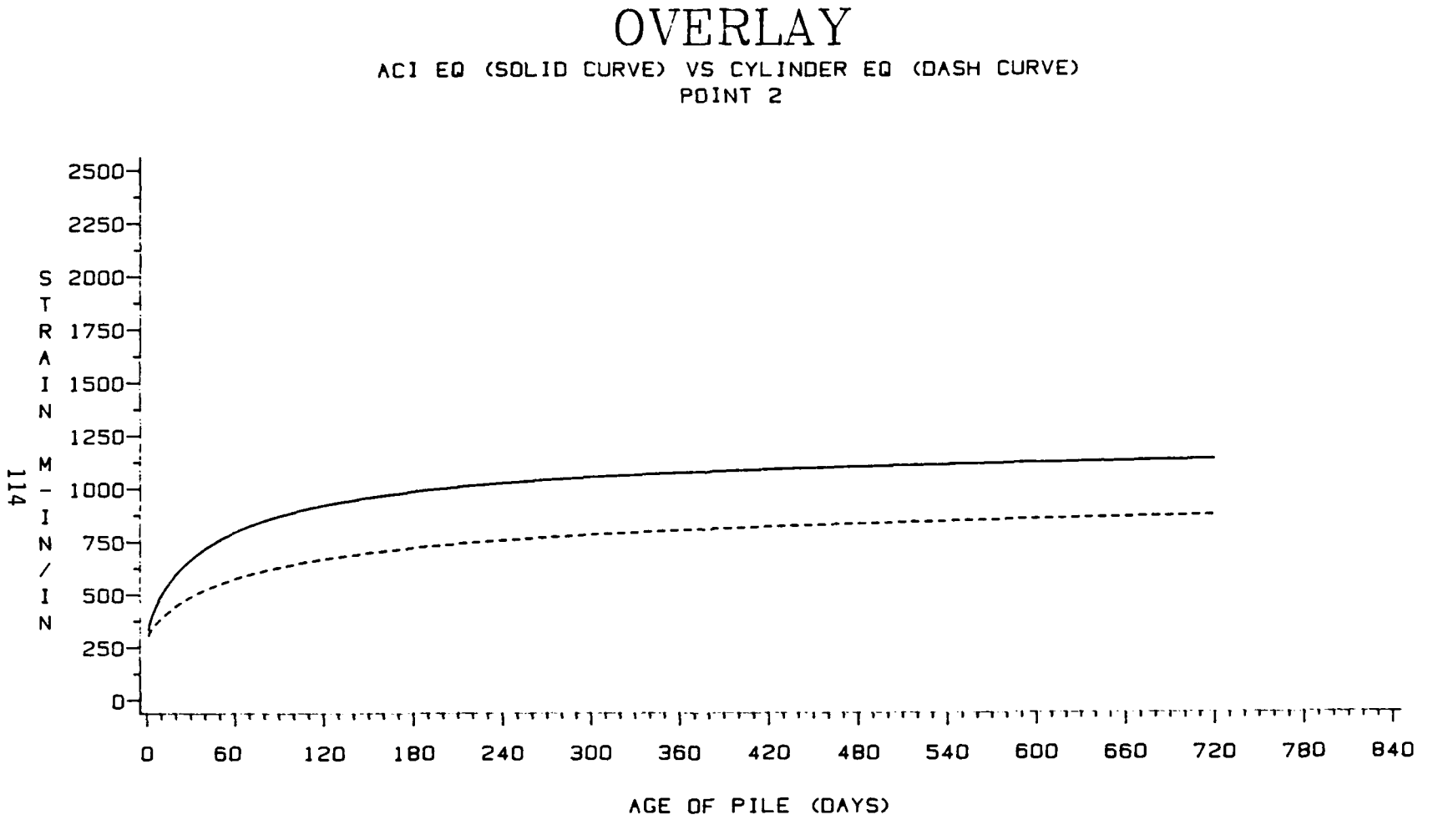

Figure 23 Overlay of Total Strains, Direct Solution Method Using the ACI Equations and Cylinder Equations for Point 2

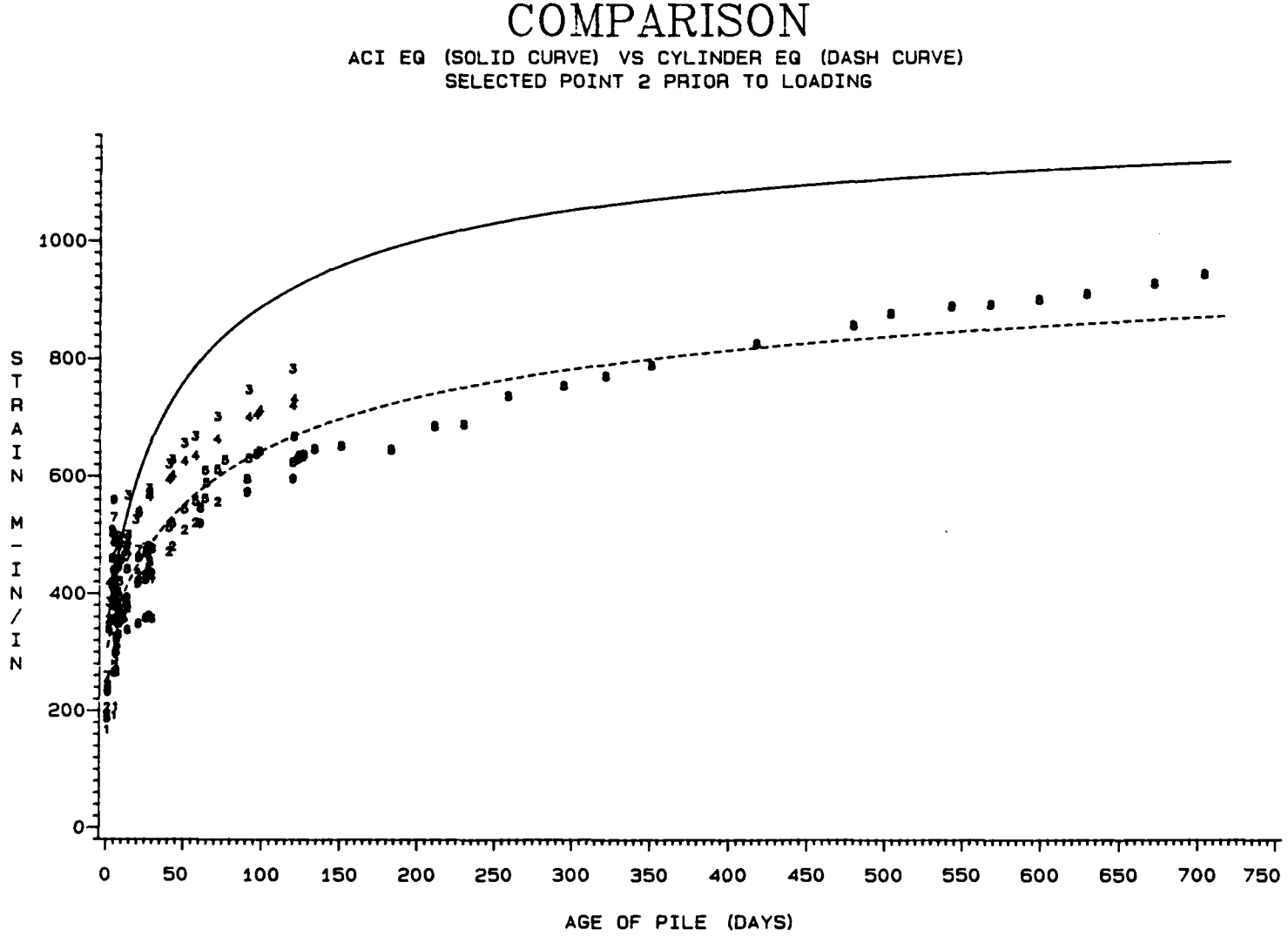

Figure 24 Comparison of Total Strains of Point 2 Prior to Loading, All Piles, Direct Solution Method Using ACI Equations and Cylinder Equations

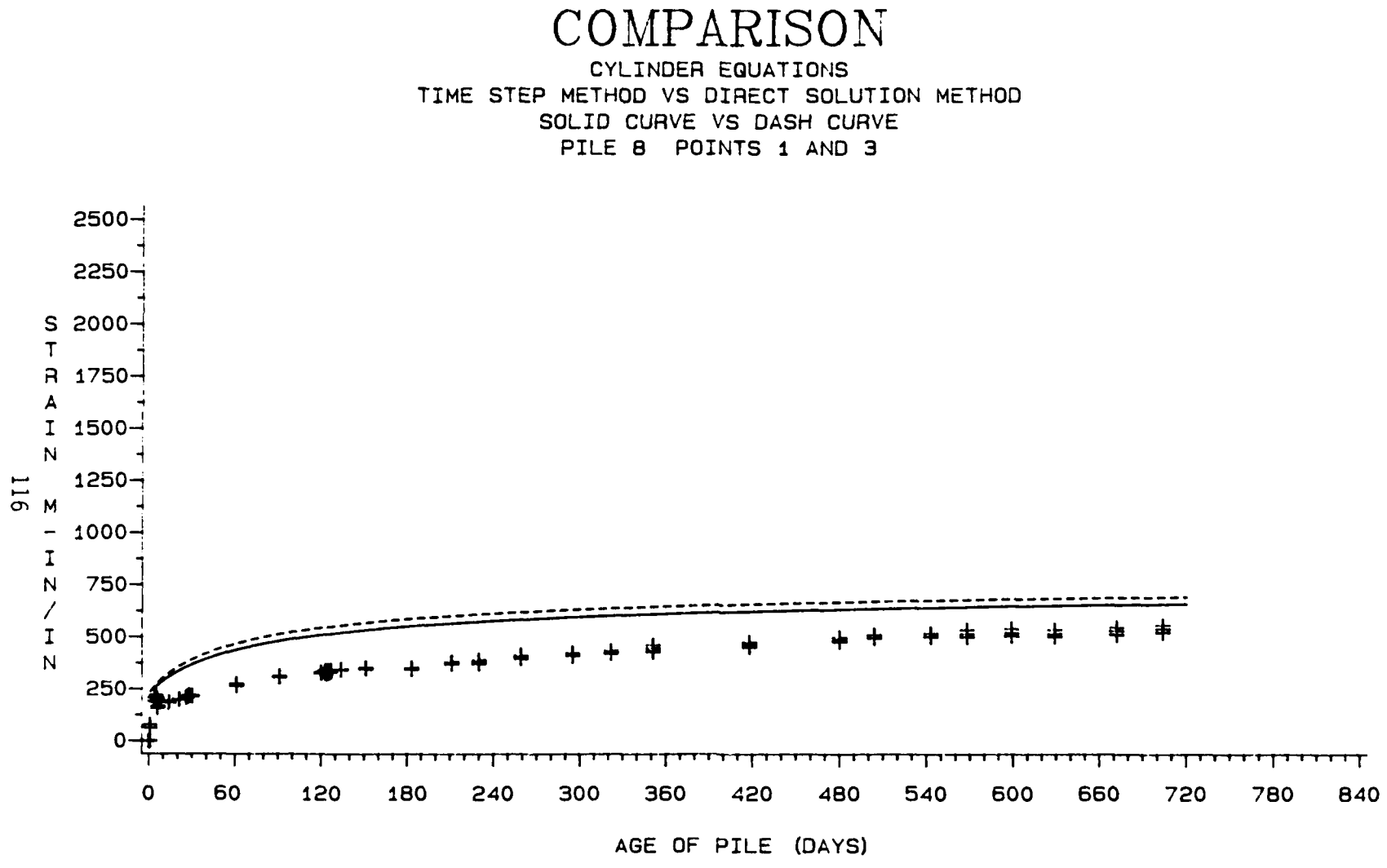

Figure 25 Comparison of Total Strain, Cylinder Equations, Incremental Time Step Method versus Direct Solution Method Against Pile 8 Points 1 and 3 Observed Data

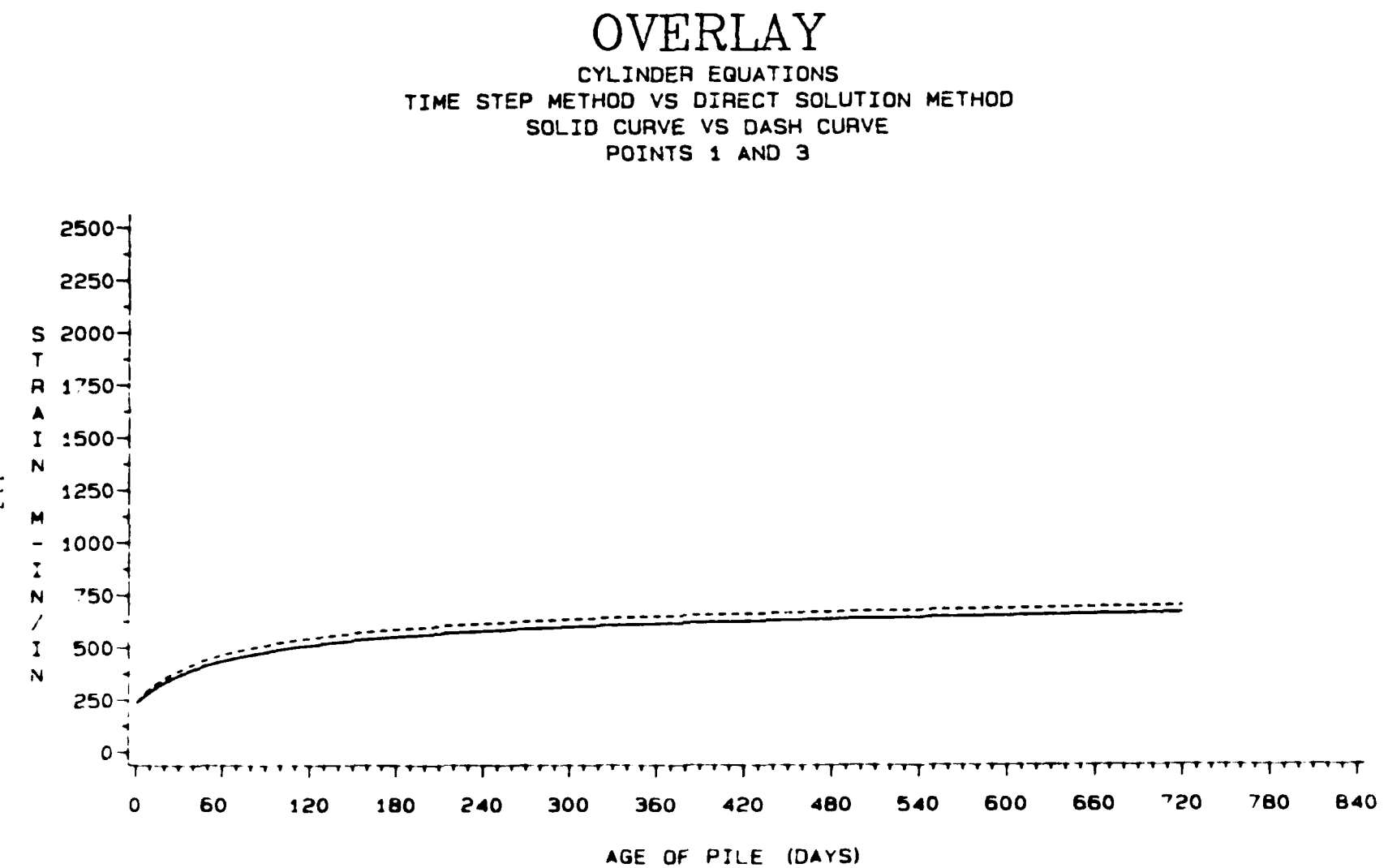

Figure 26 Overlay of Total Strain, Cylinder Equations, Incremental Time Step Method versus Direct Solution Method for Points 1 and 3

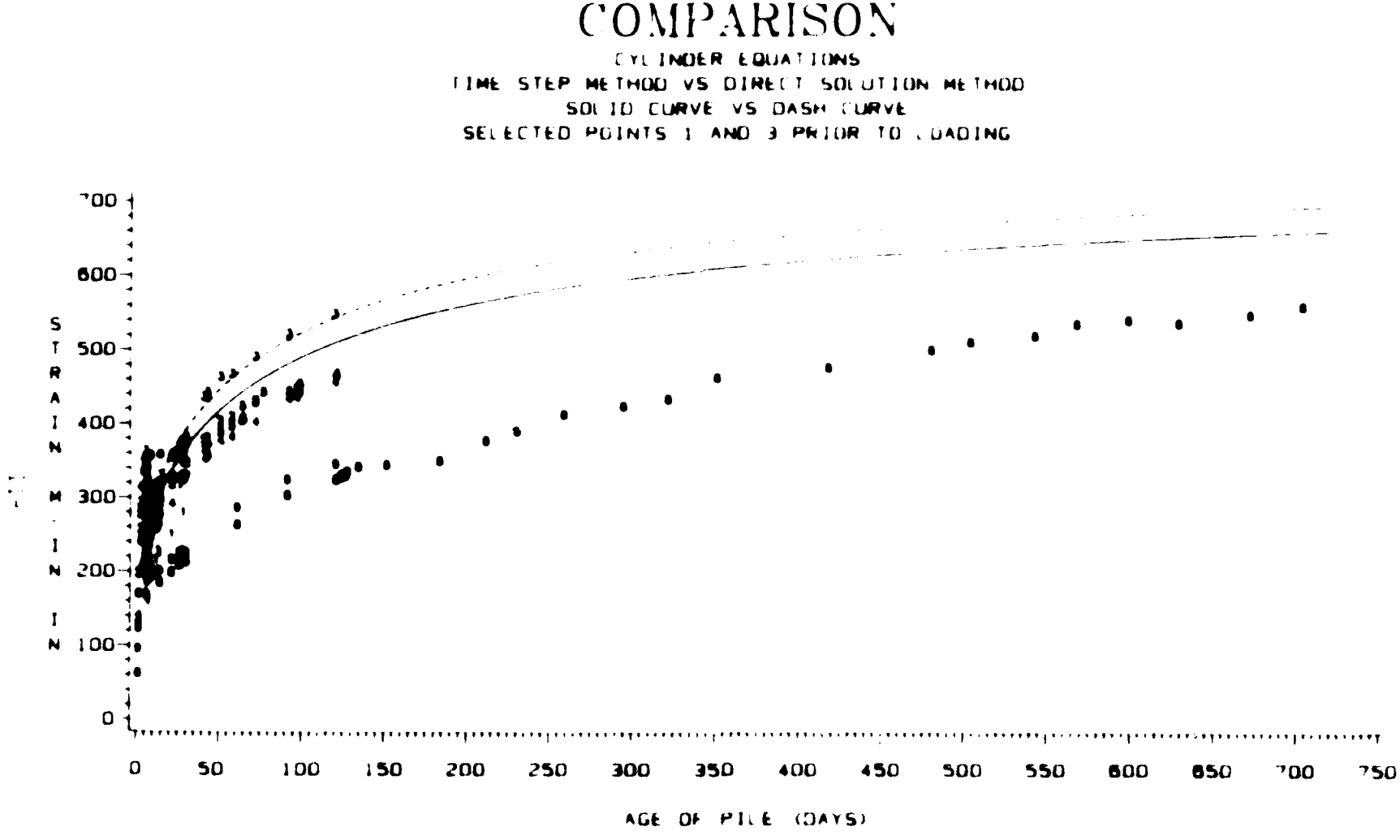

Figure 2. Comparison of Total Strains at Points 1 and 3 Prior to Loading, All Piles, Cylinder Equations, Incremental Time Step Method versus Direct Solution Method

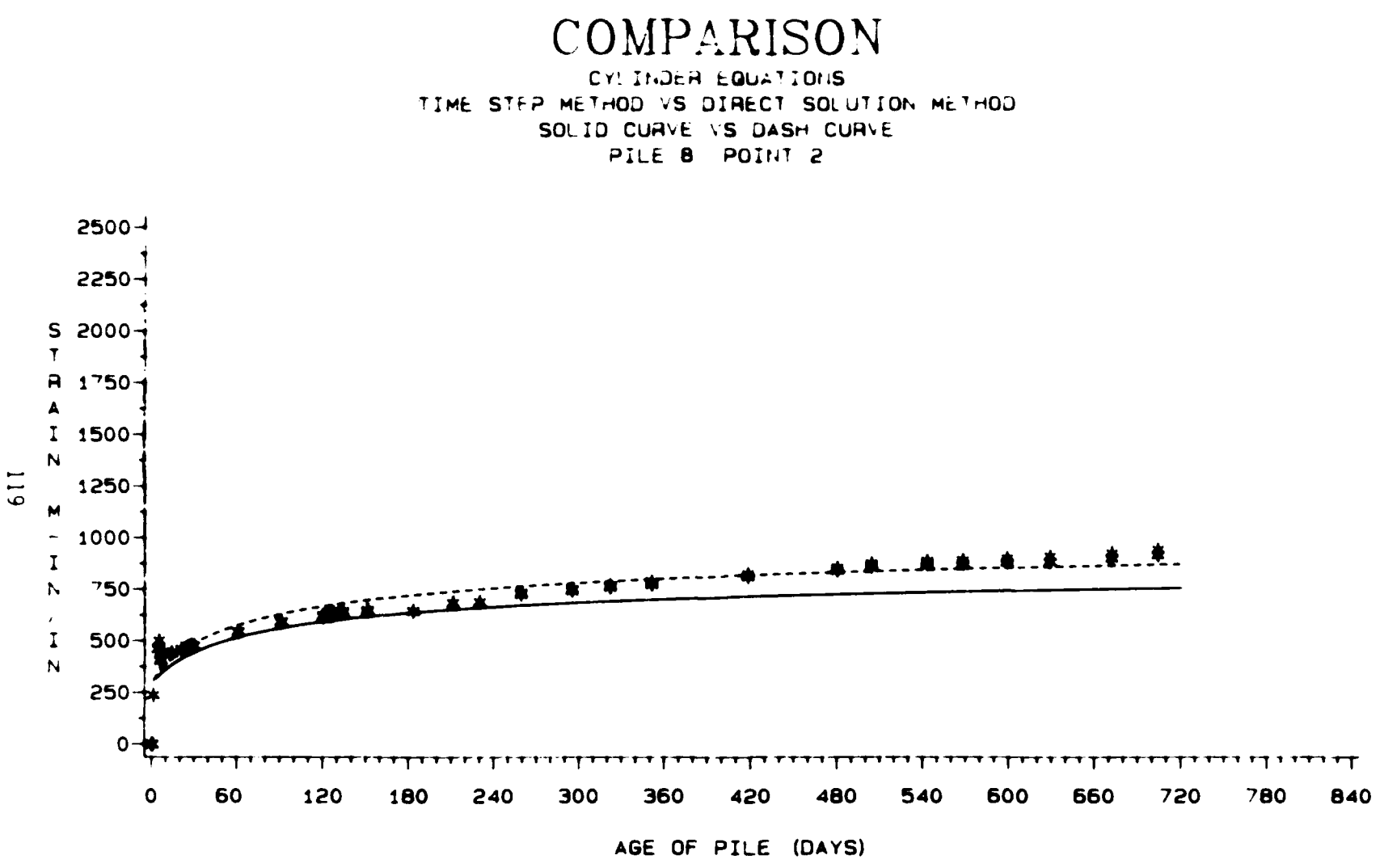

Figure 28 Comparison of Total Strain, Cylinder Equations, Incremental Time Step Method versus Direct Solution Method Against Pile 8 Point 2 Observed Data

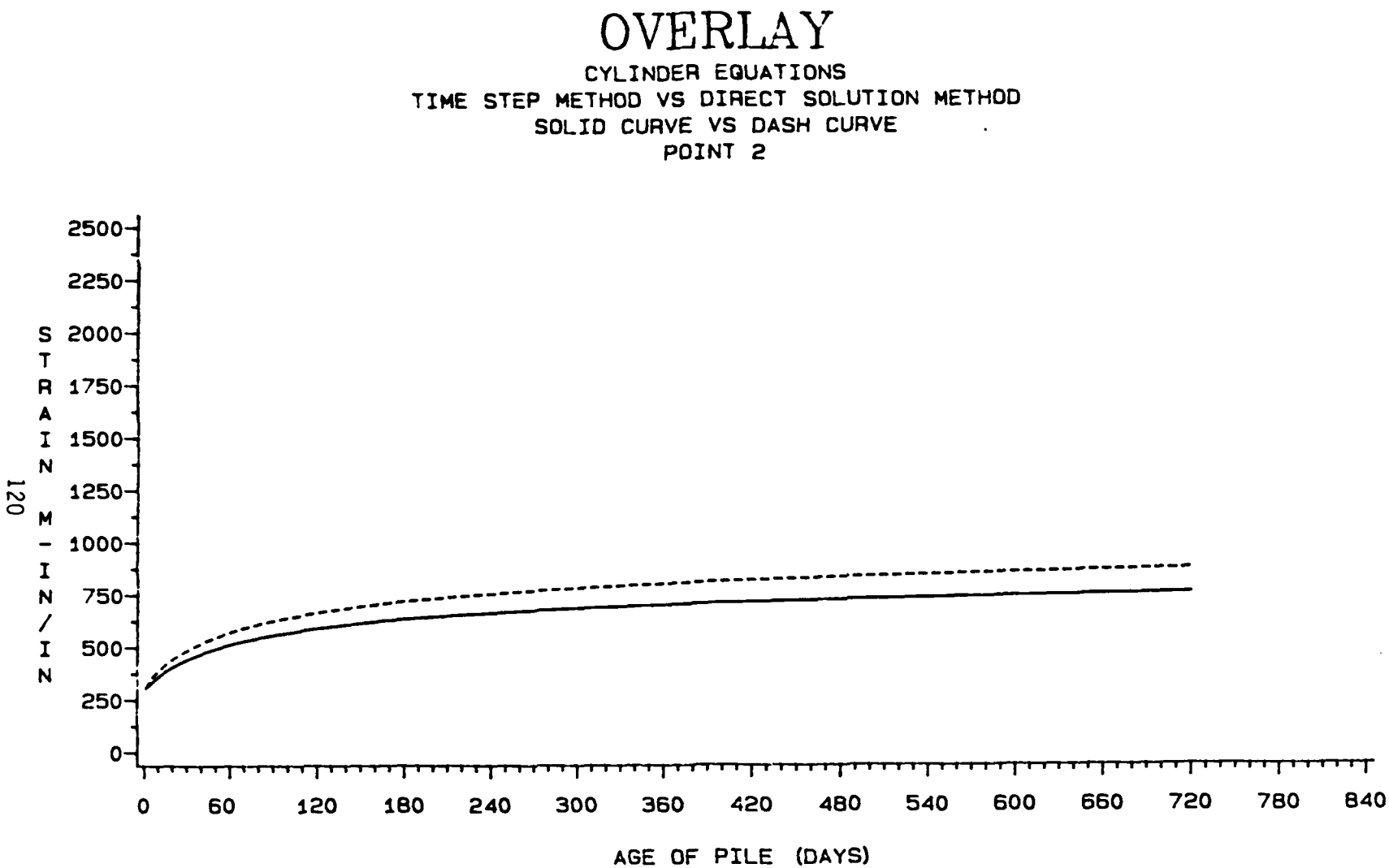

Figure 29 Overlay of Total Strain, Cylinder Equations, Incremental Time Step Method versus Direct Solution Method for Point 2

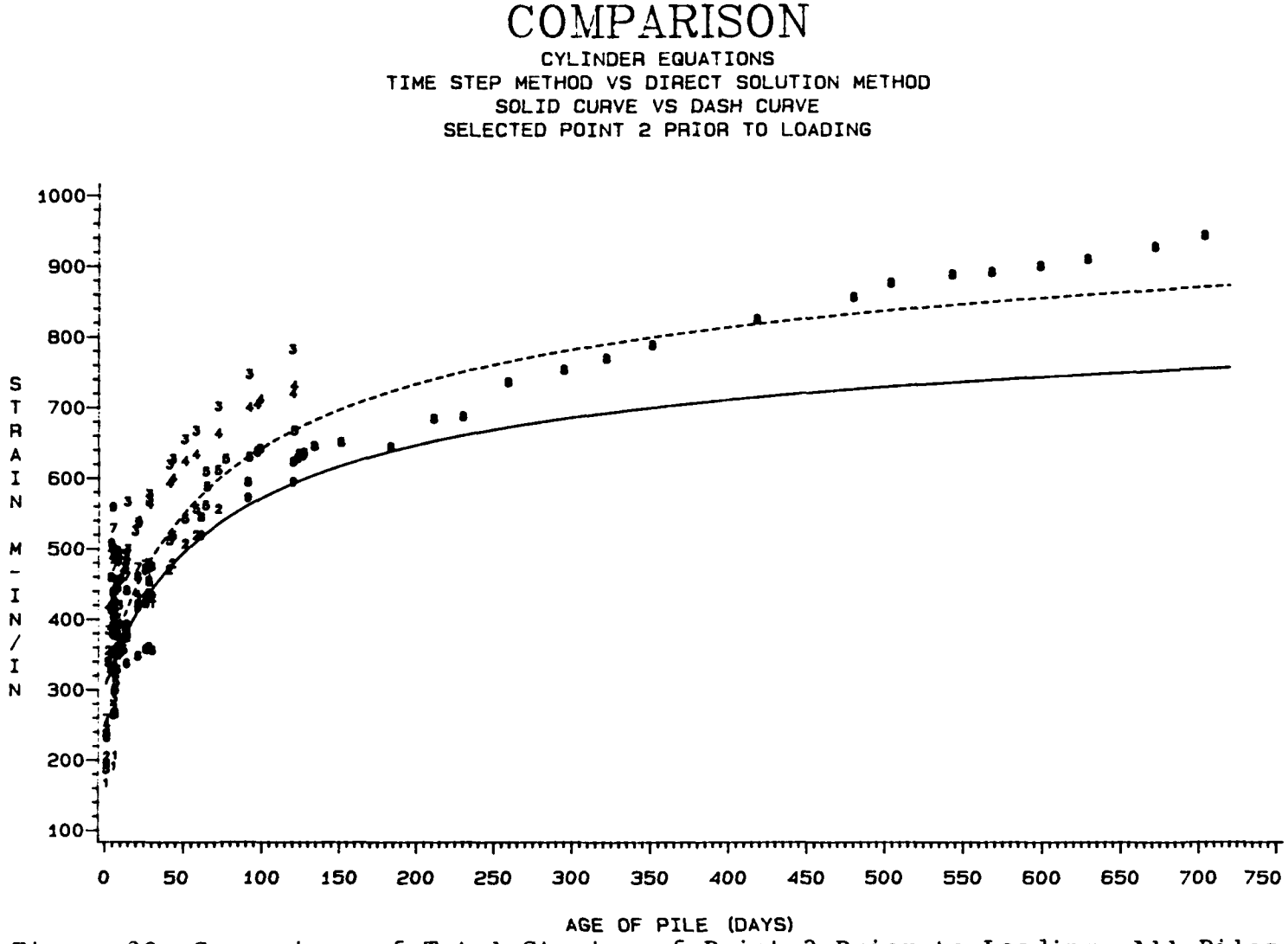

Figure 30 Comparison of Total Strains of Point 2 Prior to Loading, All Piles, Cylinder Equations, Incremental Time Step Method versus Direct Solution Method

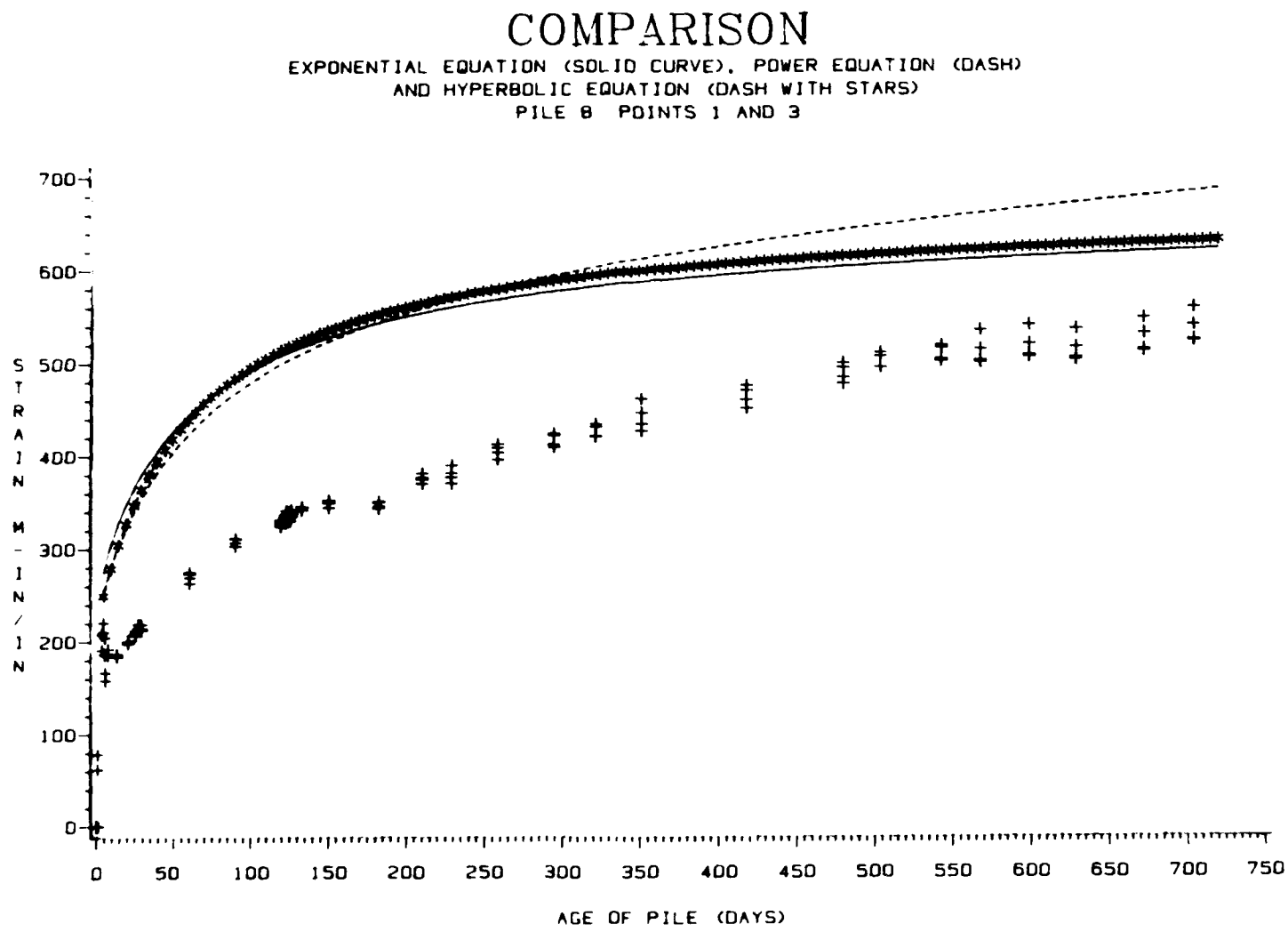

Figure 31 Comparison of Total Strain, Curve Fitted Equations Against Pile 8 Points 1 and 3

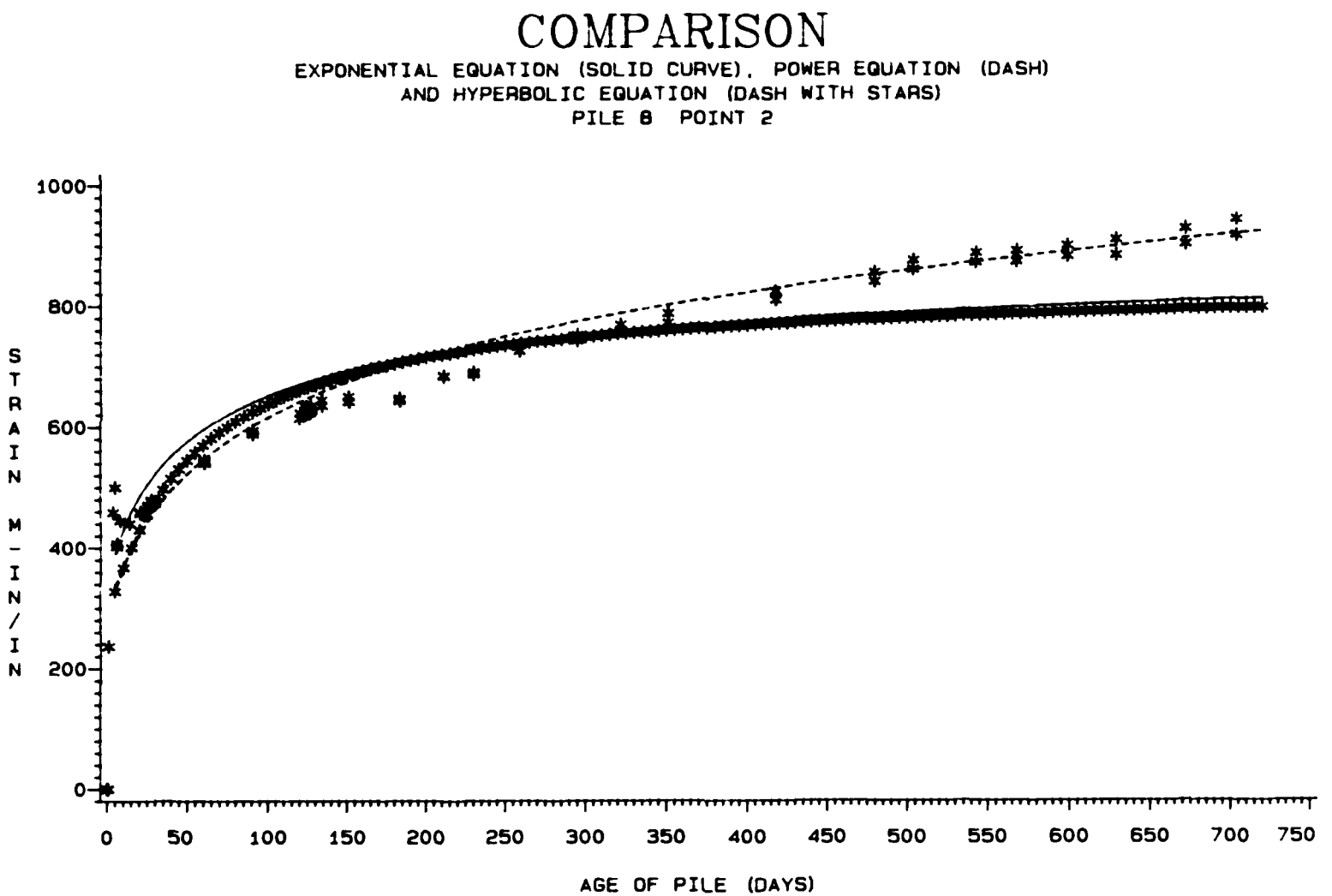

Figure 32 Comparison of Total Strain, Curve Fitted Equations Against Pile 8 Point 2

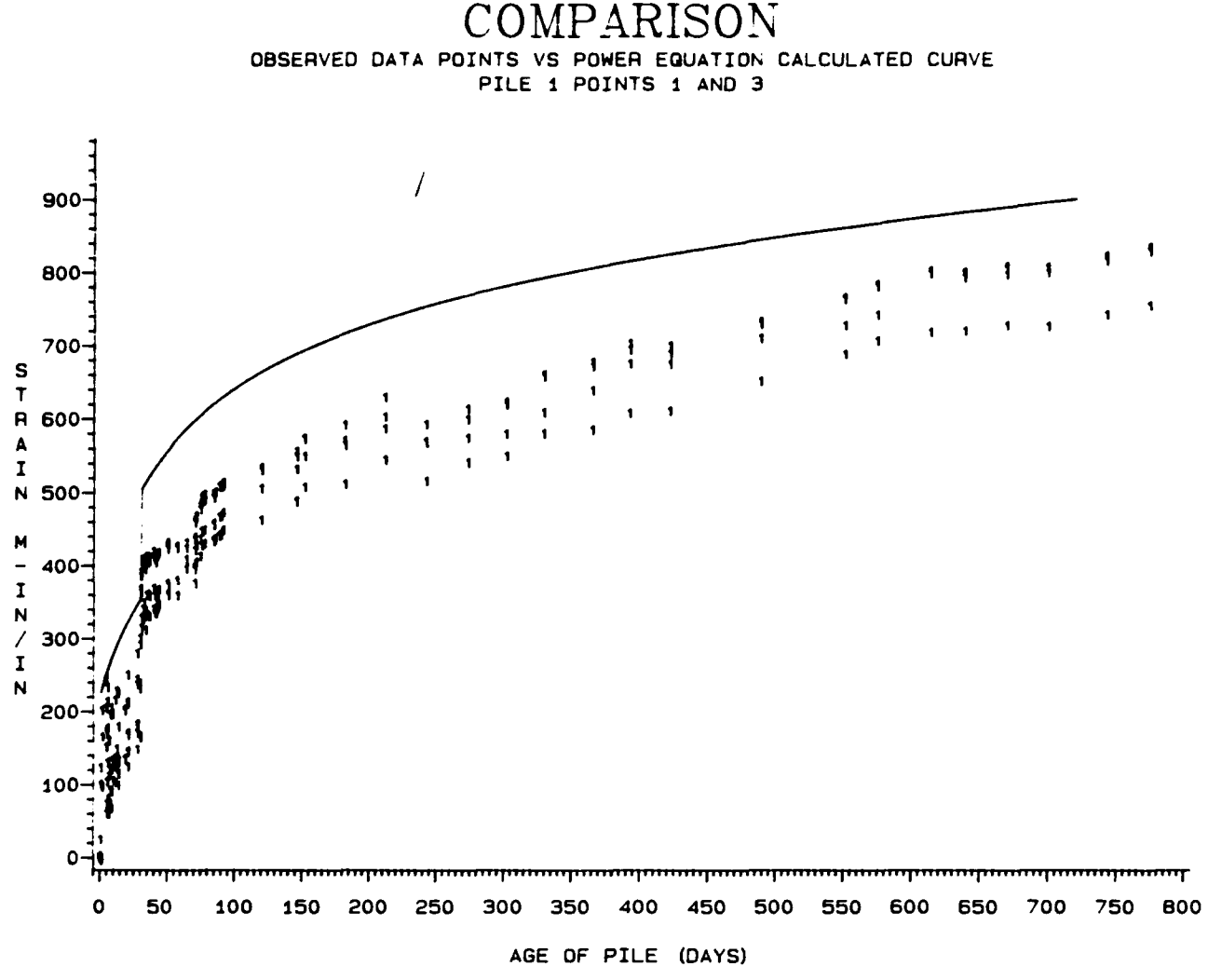

Figure 33 Comparison of Total Strain versus Calculated Curve Using Creep Power Equation, Cylinder Shrinkage Equation, and Observed Initial Elastic Strain Pile 1 Points 1 and 3

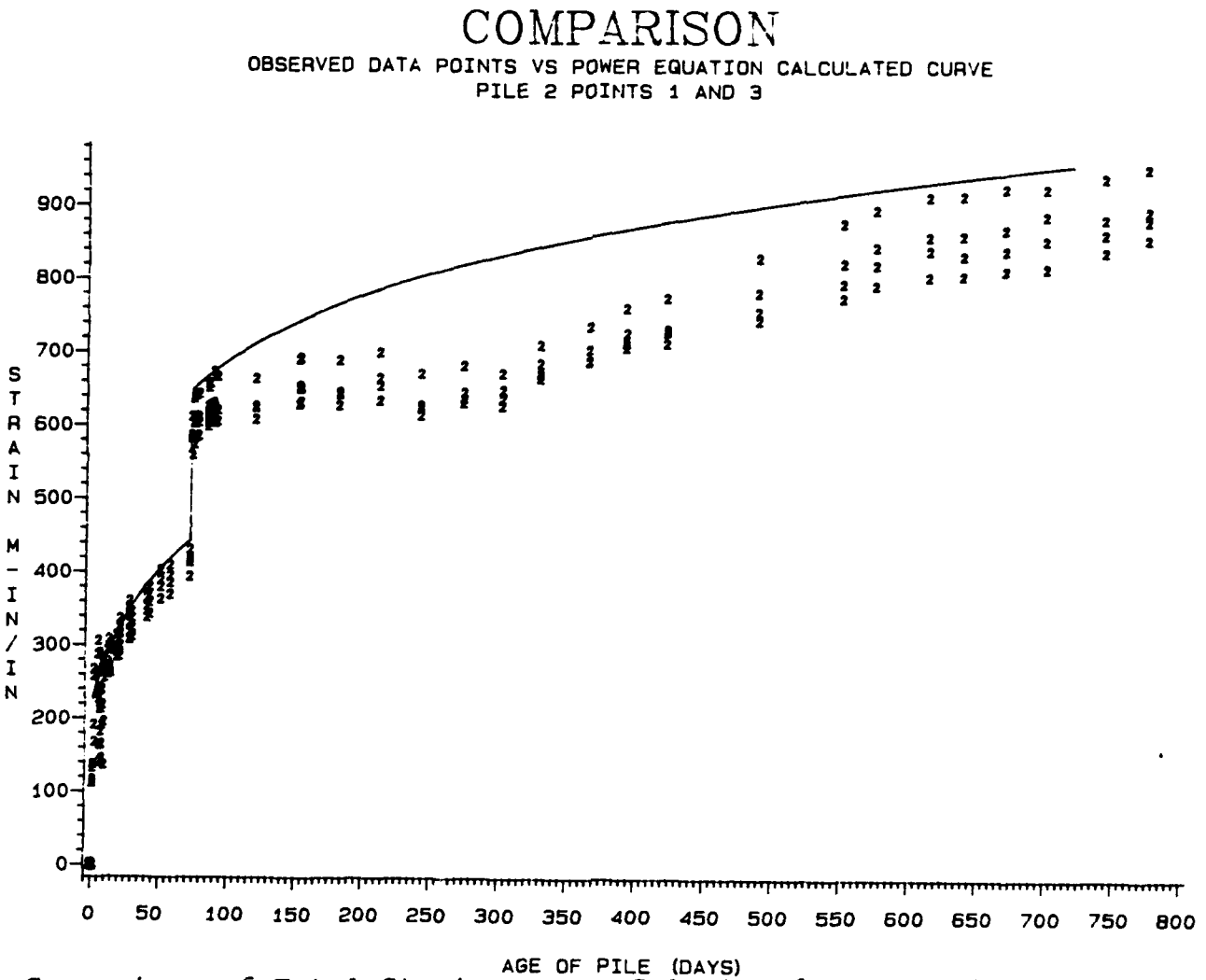

Figure 34 Comparison of Total Strain versus Calculated Curve Using Creep Power Equation, Cylinder Shrinkage Equation, and Observed Initial Elastic Strain Pile 2 Points 1 and 3

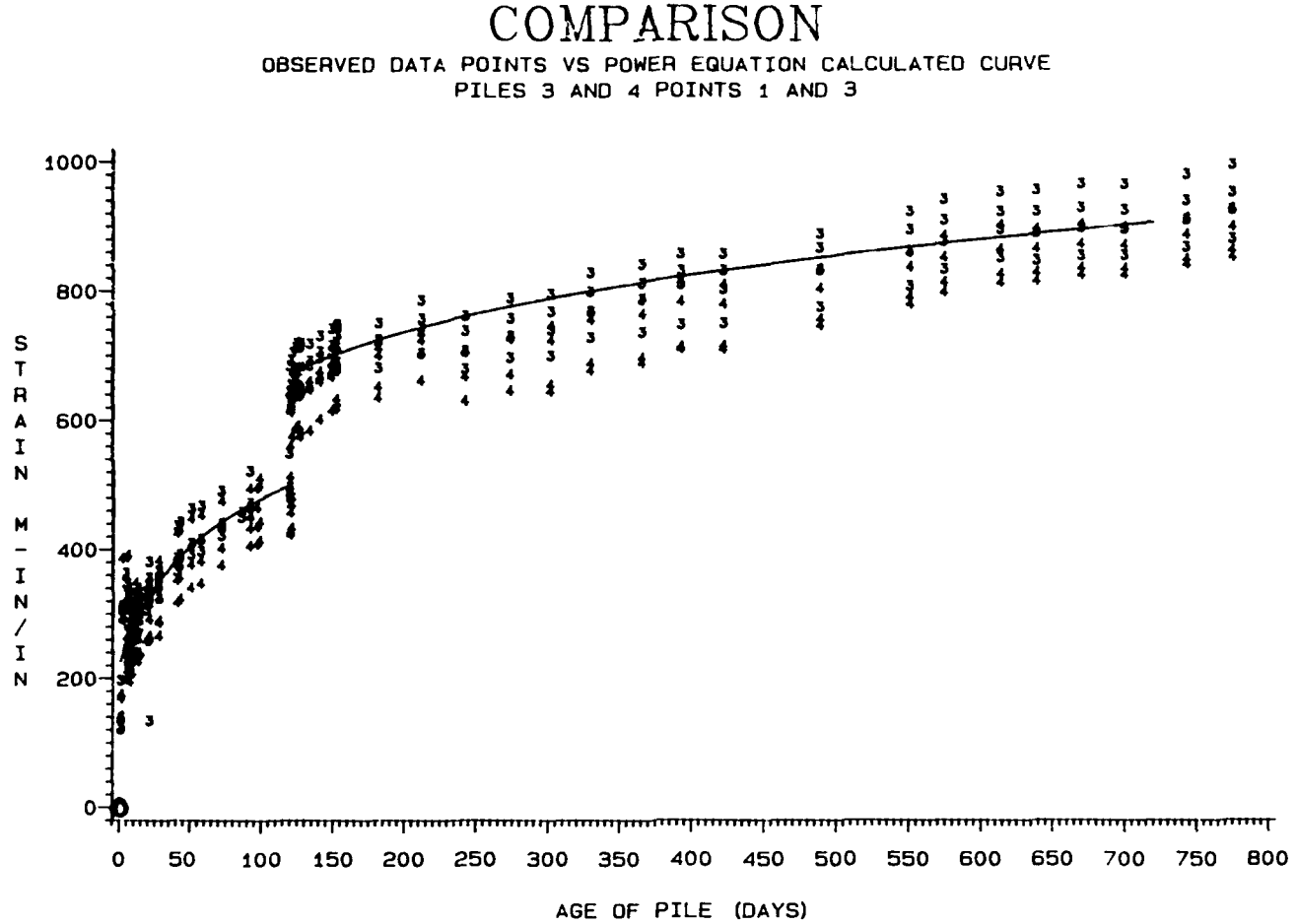

Figure 35 Comparison of Total Strain versus Calculated Curve Using Creep Power Equation, Cylinder Shrinkage Equation, and Observed Initial Elastic Strain Piles 3 and 4 Points 1 and 3

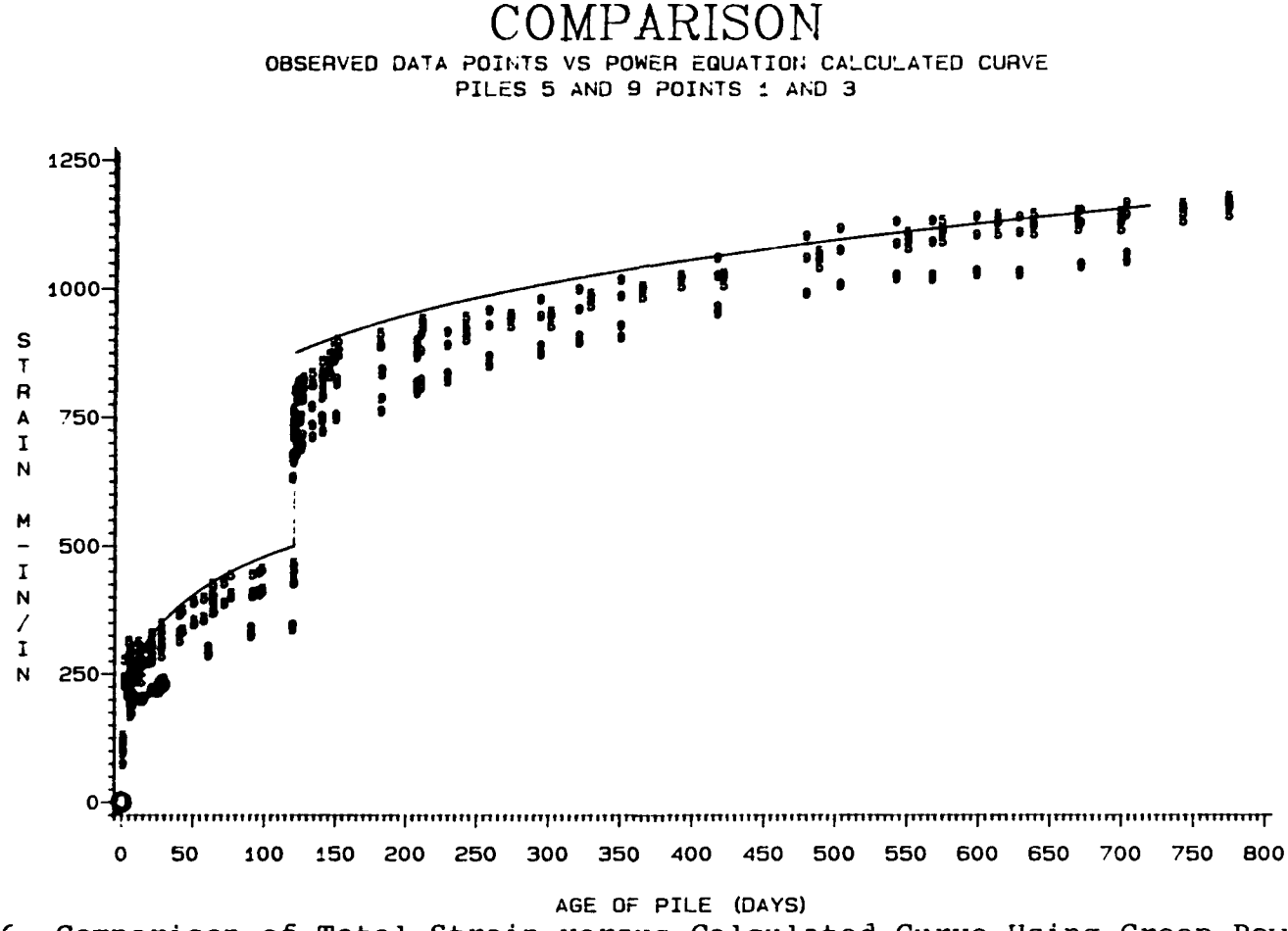

Figure 36 Comparison of Total Strain versus Calculated Curve Using Creep Power Equation, Cylinder Shrinkage Equation, and Observed Initial Elastic Strain Piles 5 and 9 Points 1 and 3

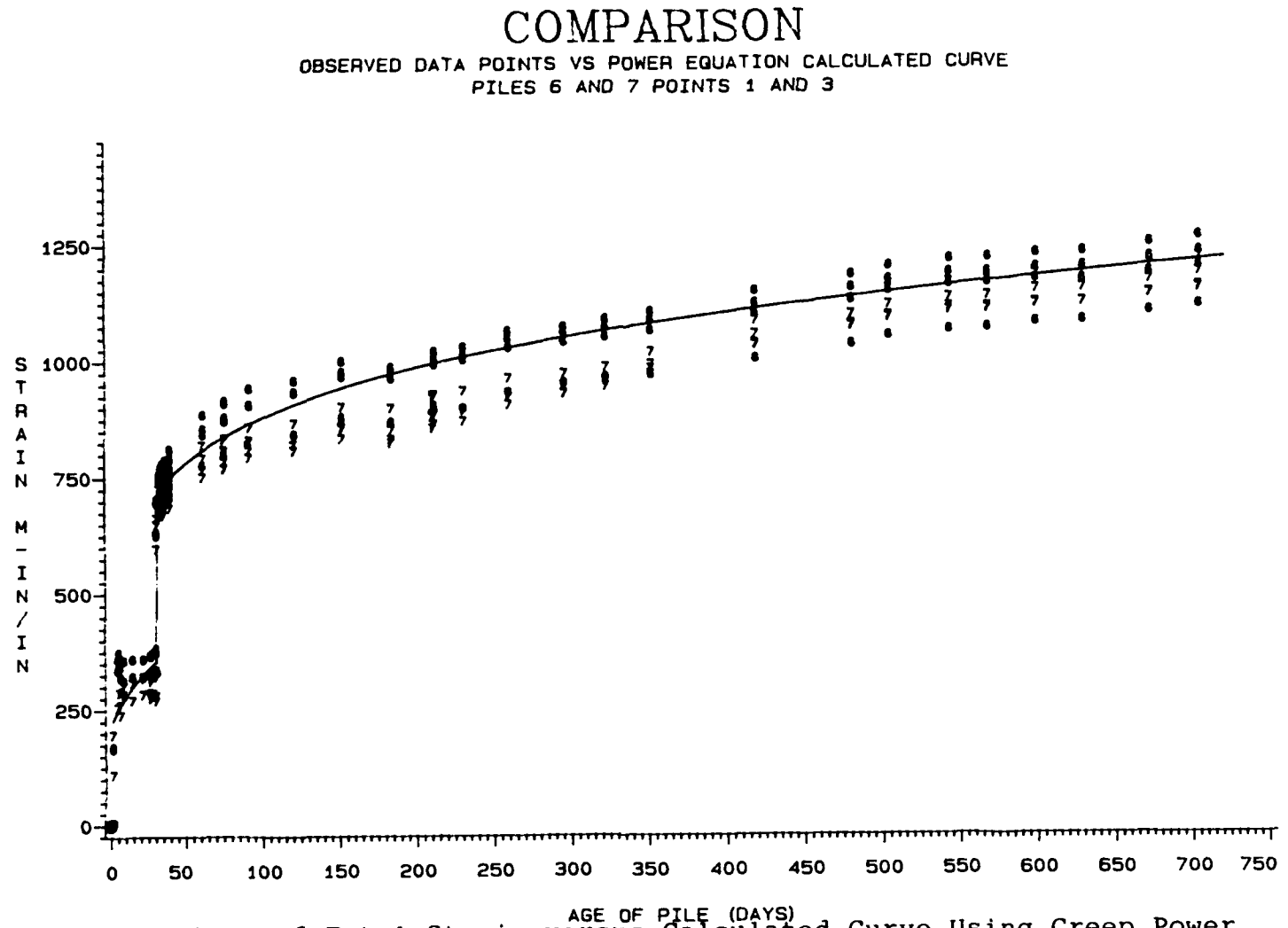

Figure 37 Comparison of Total Strain versus Calculated Curve Using Creep Power Equation, Cylinder Shrinkage Equation, and Observed Initial Elastic Strain Piles 6 and 7 Points 1 and 3

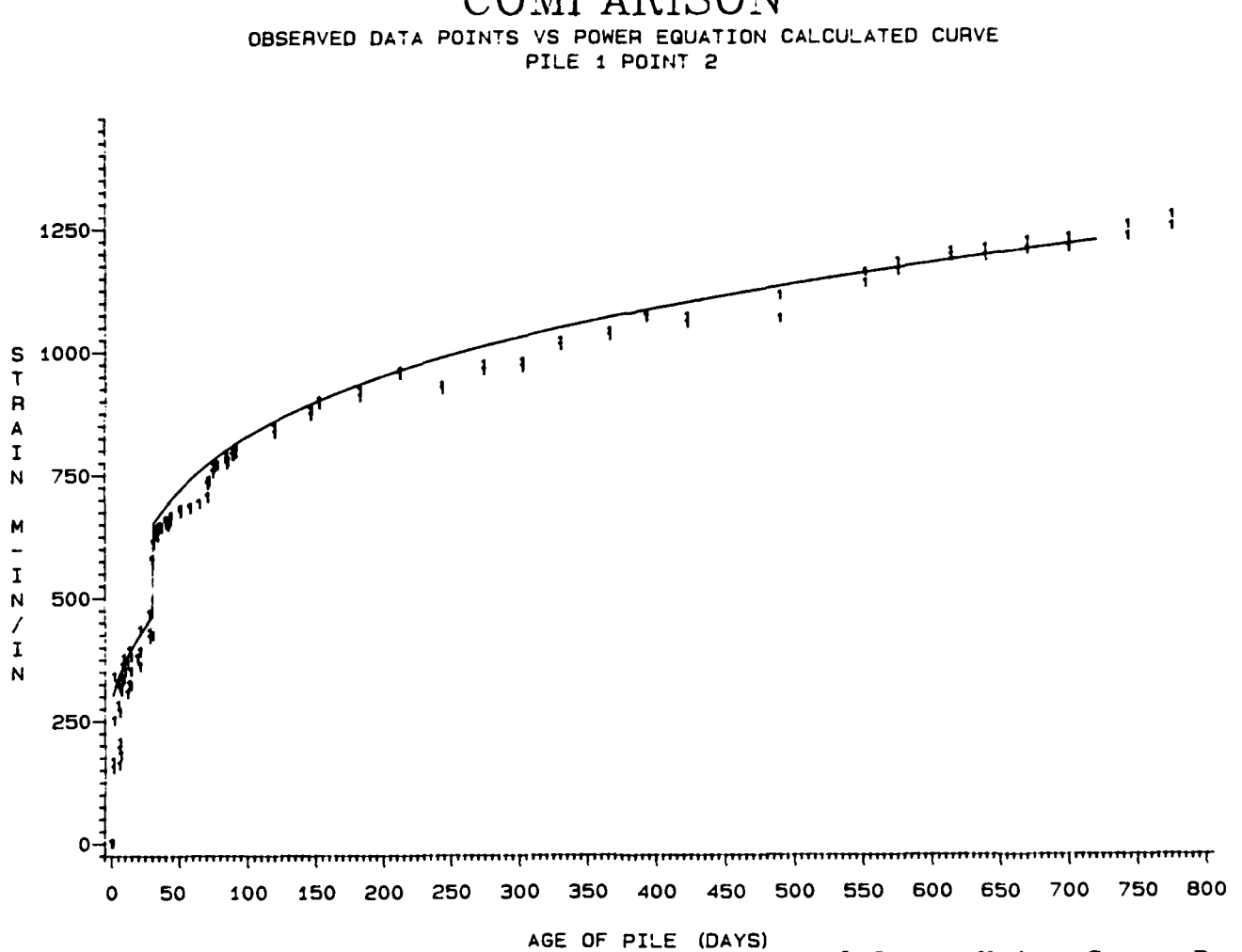

Figure 38 Comparison of Total Strain versus Calculated Curve Using Creep Power Equation, Cylinder Shrinkage Equation, and Observed Initial Elastic Strain Pile 1 Point 2

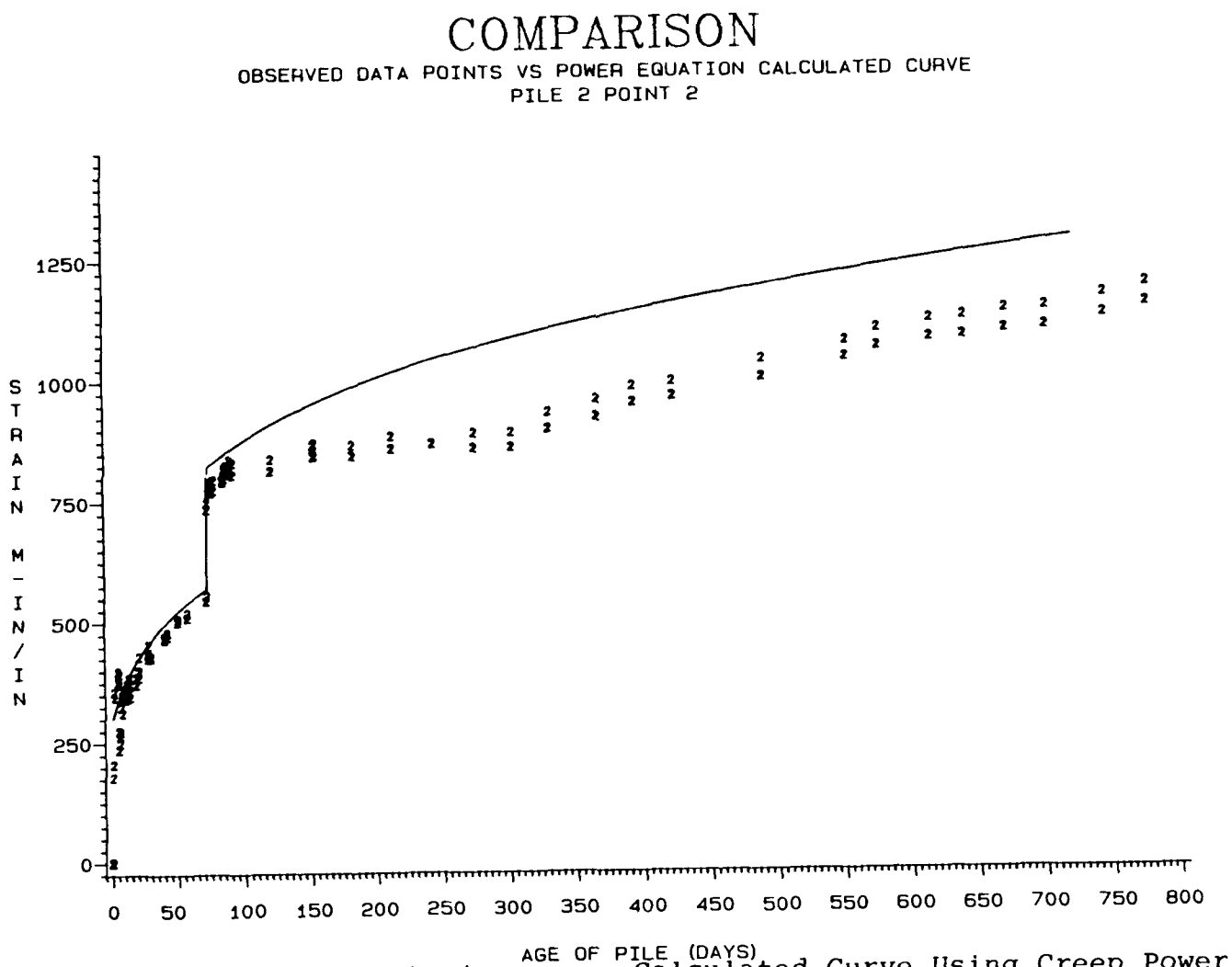

Figure 39 Comparison of Total Strain versus Calculated Curve Using Creep Power Equation, Cylinder Shrinkage Equation, and Observed Initial Elastic Strain Pile 2 Point 2

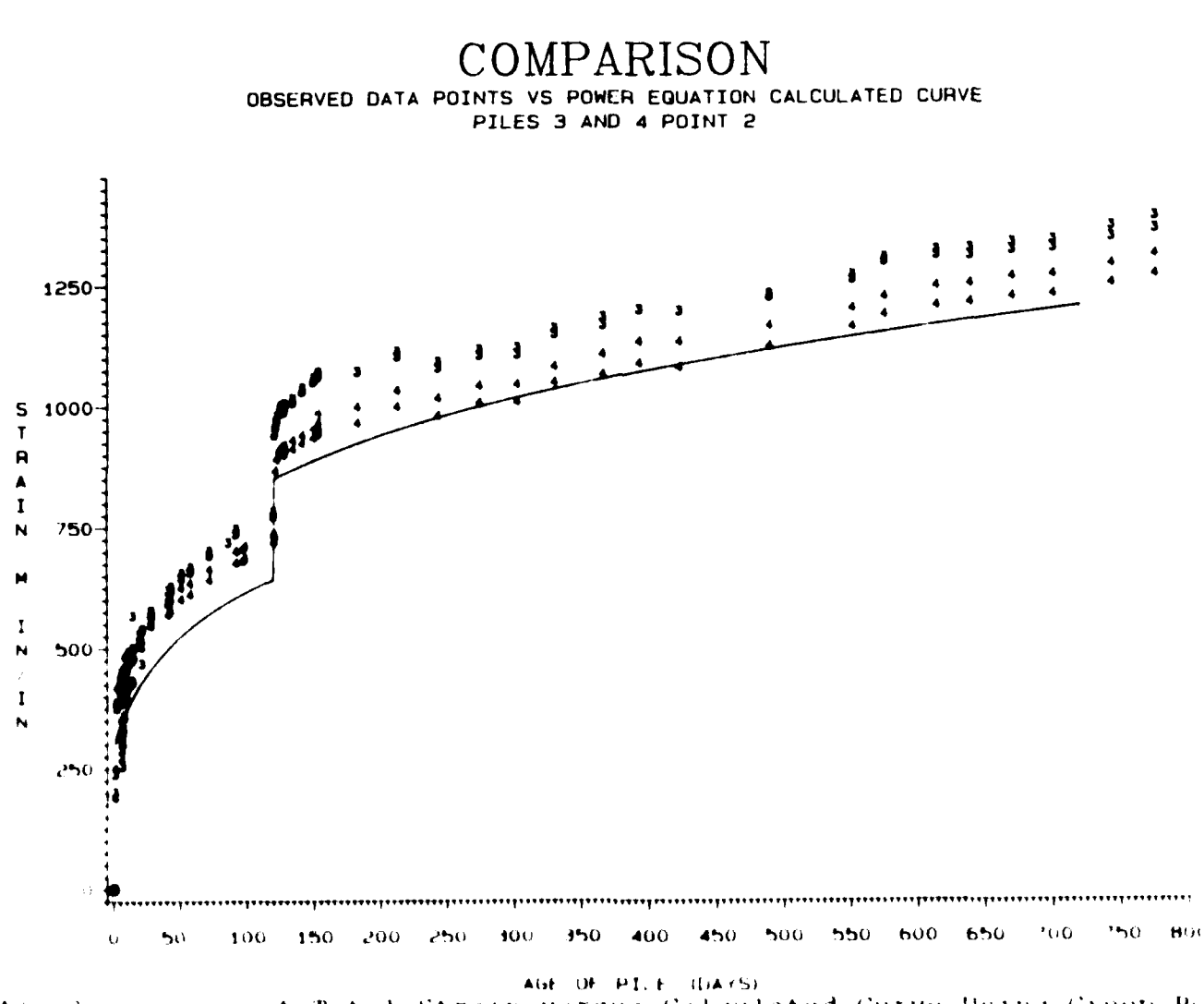

Figure 40 Comparison of Total Strain versus Calculated Curve Using Creep Power Equation, Cylinder Shrinkage Equation, and Observed Initial Elastic Strain Piles 3 and 4 Point 2

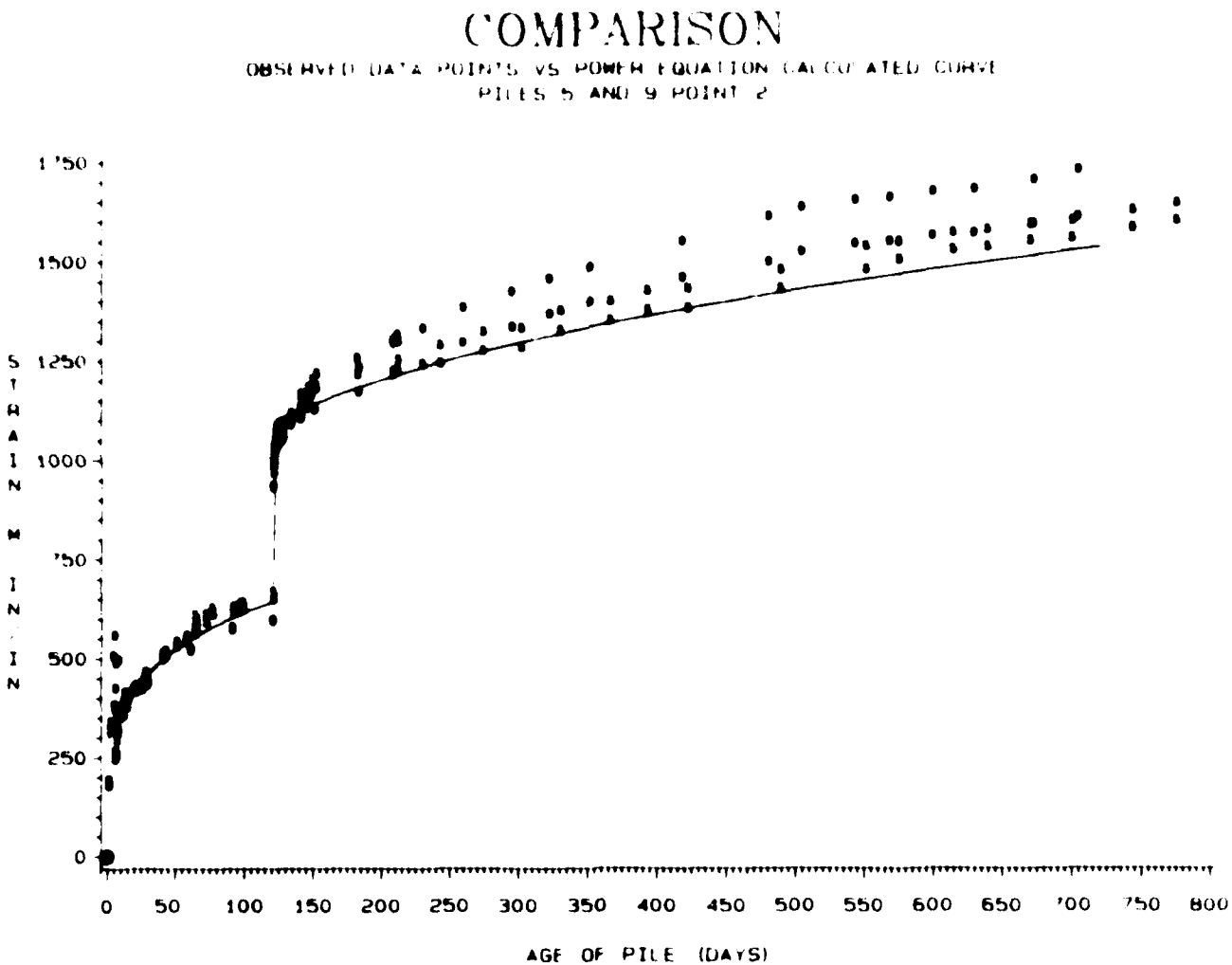

Figure 41 Comparison of Total Strain versus Calculated Curve Using Creep Power Equation, Cylinder Shrinkage Equation, and Observed Initial Elastic Strain Piles 5 and 9 Point 2

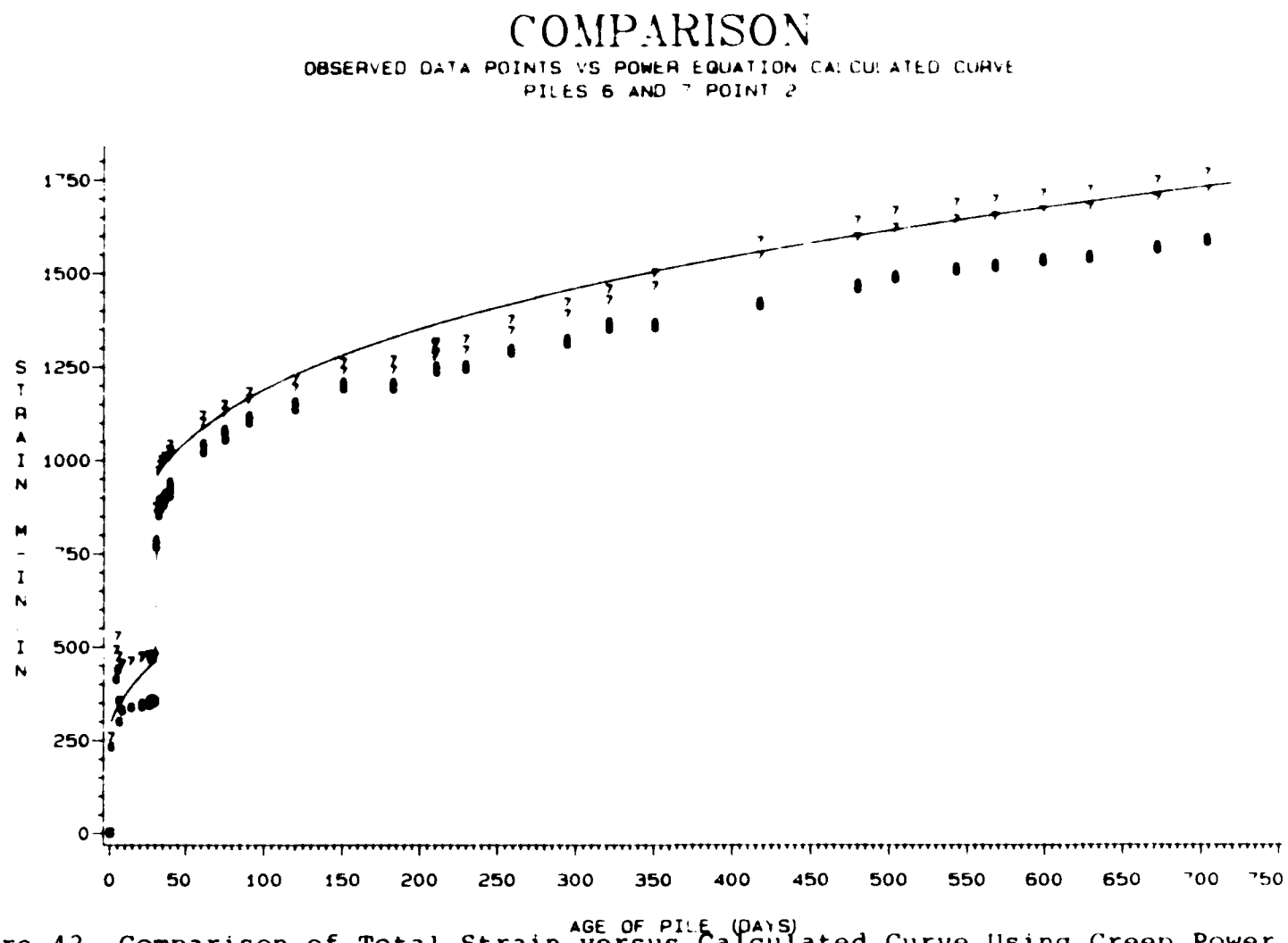

Figure 42 Comparison of Total Strain versus Calculated Curve Using Creep Power Equation, Cylinder Shrinkage Equation, and Observed Initial Elastic Strain Piles 6 and 7 Point 2

LIST OF REFERENCES

1. Clemente, Frank M., Jr. Downdrag, Negative Skin Friction and Bitumen Coatings on Prestressed Concrete Piles. Tulane University, 1984.

2. Kalani, Keith K. and Harold S. Hamada. Creep and Shrinkage of Hawaiian Aggregate Conrete. Department of Civil Engineering, University of Hawaii at Manoa, 1985.

3. Mukai, David J. and Harold S. Hamada. Creep in Prestressed Concrete Piles. Department of Civil Engineering, University of Hawaii at Manoa, 1985.

4. Neville, A. M. Creep of Concrete: Plain, Reinforced and Prestressed. Amsterdam: North Holland Publishing Company, 1970.

5. Hanson, J.A. "Prestress Loss as Affected by Type of Curing". Prestress Concrete Institute Journal, 9(April 1964), 69-93.

6. Marechal, J.C. "Le Flunge du Beton in Function de la Temperature". Materials and Structures, 2(March-April 1969), 111-115.

7. American Concrete Institute. Creep, Shrinkage and Temperature, SP-27. Detroit: ACI, 1971.

8. Hanson, Torben C. and Alan H. Mattock. "Influence of Size and Shape of Member on the Shrinkage and Creep of Concrete". Journal of the American Concrete Institute, 63(February 1966), 267-289.

9. Nilson, Arthur H. Design of Prestressed Concrete. New York: John Wiley and Sons, 1973.

10. American Concrete Institute. Design for Creep and Shrinkage in Concrete Structures, SP-76. Detroit: ACI, 1982.

11. Prestressed Concrete Institute Committee on Prestress Losses. "Recommendation for Estimating Prestress Losses". Prestress Concrete Institute Journal, 20(July-August 1975) 43-75.

12. Hann, Charles T. Statistical Methods in Hydrology. Ames: The Iowa State University Press, 1977.

13. Snedecor, George W. and William G. Cochran. Statistical Methods. Ames: The Iowa State University Press, 1982.

END

7-87

DTIC